SINGLE MOLECULE FLUORESCENCE IMAGING OF PROTEIN-SURFACE AND PROTEIN-PROTEIN INTERACTIONS AT A GLASS-WATER INTERFACE

by

Douglas Michael Kriech

A dissertation submitted to the faculty of
The University of Utah
in partial fulfillment of the requirements for the degree of

Doctor of Philosophy

Department of Chemistry

The University of Utah

May 2015

The University of Utah Graduate School

STATEMENT OF DISSERTATION APPROVAL

The dissertation of **Douglas Michael Kriech**

has been approved by the following supervisory committee members:

Joel M. Harris	, Chair	**12/11/2014** Date Approved
Peter F. Flynn	, Member	**12/11/2014** Date Approved
Erik M. Jorgensen	, Member	**12/11/2014** Date Approved
Michael D. Morse	, Member	**12/11/2014** Date Approved
Marc D. Porter	, Member	**12/11/2014** Date Approved

and by **Cynthia J. Burrows** , Chair/Dean of

the Department/College/School of **Chemistry**

and by David B. Kieda, Dean of The Graduate School.

ABSTRACT

Solid-phase immunoassays (SPIs) have become an indispensible tool for research, diagnostics, and therapeutics. Understanding the antibody-antigen interaction occurring at a solid-liquid interface is needed in order to develop more sensitive and selective sensors with lower limits of detection. In turn, this will provide a better understanding of the immune system, and lead to the discovery of more effective immunotherapy treatments. In this work, total internal reflection fluorescence (TIRF) microscopy is employed to investigate individual ligand-receptor interactions at a glass-water interface. The extreme sensitivity of TIRF imaging requires the measurement surfaces to resist the nonspecific adsorption of proteins in order to minimize backgrounds, while containing low density of optically resolvable capture sites. The nonspecific adsorption of antibodies to poly(ethylene glycol) (PEG) monolayers covalently bound to glass surfaces was characterized for two different PEG immobilization procedures. First, N-hydroxysuccinimide (NHS) active esters of 2000 g/mol PEG were reacted to the amine functionality of (3-aminopropyl)triethoxysilane (APTES) derivatized glass slides; secondly, in addition, 750 g/mol and 2000 g/mol PEG-amines were reacted to the epoxide functionality of (3-Glycidyloxypropyl)trimethoxysilane (GOPTS) modified glass slides. The protein resistant property of each PEG-modified surface was characterized by monitoring the adsorption of monoclonal mouse derived antibiotin using single-molecule

fluorescence imaging. The protein resistant coating produced using epoxide-amine PEG chemistry was adapted to produce a glass modified surface containing a low density of biotin conjugation sites by reacting a mixture containing a lower concentration of biotin-labeled 2000 g/mol PEG-amine and a higher concentration of 750 g/mol PEG-amine to GOPTS modified glass slides. The density of biotin conjugation sites within the diluent PEG layer was characterized using fluorescently-labeled streptavidin, where the surface concentration of biotin increased linearly with biotin-PEG concentration in the reaction solution. Using the low density biotin capture surfaces, the activity of a surface immobilized rabbit-antigoat IgG receptor was investigated using TIRF imaging for four different antibody immobilization strategies: (i) passive adsorption to the mPEG surface, (ii) active bioaffinity immobilization directly to streptavidin capture sites, (iii) two-step sequential immobilization of streptavidin and protein A intermediate, and (iv) a one-step immobilization to a preassociated chimeric streptavidin-protein A complex.

“I prefer to be true to myself, even at the hazard of incurring the ridicule of others, rather than to be false, and to incur my own abhorrence.”

— Frederick Douglass

TABLE OF CONTENTS

LIST OF TABLES

LIST OF FIGURES

CHAPTER 1

INTRODUCTION

1.1 Overview

Antibodies consist of a variety of globular proteins referred to as immunoglobulins that are contained within the plasma and extracellular fluids of vertebrates. Incredibly diverse in their ability to selectively recognize and bind specific epitopes of proteins, antibodies aid in the recognition and destruction of foreign invaders such as bacteria and viruses, known as antigens.[1] Besides serving as one of the principal effectors of the adaptive immune system, antibodies have also been extensively used in science and medicine for research,[2] diagnostics,[3,4] and therapeutic purposes.[5] The goal of this dissertation is to develop tools to characterize individual antibody-antigen interactions at the single-molecule level. This technology could eventually produce more sensitive and selective immunosensors, provide a better understanding of the immune system, and lead to the discovery of more effective immunotherapy treatments.

Biological science has long since been confronted with numerous challenges to develop *in vitro* models that accurately depict *in vivo* processes. The majority of the active antibodies within living organisms act in concert with cell membranes, carrying out their molecular recognition functions at membrane interfaces.[1] As a result, interfacial

reaction conditions have commonly been employed to measure a host of antibody-antigen interactions *in vitro*. In fact, it has been documented that the kinetics of cell surface-antibody interactions are more accurately represented by solid-phase antibody-antigen measurements than those observed in free solution;[6,7] however, the direct comparison of *in vivo* cell-membrane receptor-ligand interactions with *in vitro* solid-phase receptor-ligand interactions neglects to account for significant differences between the properties of the two interfaces. Solid-phase surfaces are rigid and chemically fixed unlike the dynamic fluidity exhibited by living membranes, a property that has been shown to contribute to membrane-associated protein-protein interactions.[8,9] As a result, *in vitro* solid-phase receptor-ligand interactions are often times perturbed by intrinsic surface properties associated with the measurement platform, including transport limitations, restricted reaction volumes, steric interactions between densely packed receptor molecules, structural changes within surface immobilized protein-receptor molecules, and the orientation of surface-immobilized receptor molecules.[10-14]

Interfacial antibody-antigen interactions have been characterized using a variety of techniques including radiometry,[15-18] ellipsometry,[19] surface plasmon resonance (SPR),[20,21] colorimetry,[22-24] and quartz crystal microbalance (QCM).[25-27] Each of these techniques measures average signals that reveal little information about the heterogeneity, for multistep capture assays, and the molecular history of individual receptor sites. In addition, such methods often require a high density of receptor surface sites in order to achieve detectable signals, which results in transport limitations and crowding effects that perturb reaction kinetics.[28] In order to minimize such effects, the density of receptor sites needs to be reduced to very low fractions ($<10^{-4}$) of a protein

(~50 kDa) monolayer; however, this requires an extremely sensitive measurement technique capable of resolving single-molecules at an interface.

In order to image single receptor sites, it is necessary to probe small volumes near the measurement interface, while rejecting background signal from the bulk solution. Total internal reflection fluorescence (TIRF) imaging accomplishes these requirements by producing a nonpropagating evanescent wave that only excites fluorescently labeled ligand-molecules contained within the first ~150 nm from a glass/water interface. Although background fluorescence from solution is reduced using this technique, the sensitivity of such measurements requires that the surface resist the nonspecific adsorption of proteins, while containing a low density of receptor sites in order to resolve specific single-molecule events. When combined with TIRF imaging, such surfaces would allow individual interfacial ligand-receptor interactions to be investigated, where the heterogeneity from site-to-site and the capture history of individual sites for multi-step capture assays could be characterized.

1.2 Immunoglobulin G Structure

Secreted by B lymphocytes (plasma cells), antibodies are glycoproteins belonging to a family of globular proteins known as immunoglobulins (Ig), which aid in the immune response against antigens within living vertabrates. Gamma-globulins (IgG), commonly used in solid-phase immunoassays, are composed of two identical halves, both of which contain a heavy (~55 kDa) and light (~25 kDa) polypeptide chain held together by disulfide linkages and electrostatic interactions. The resulting tetrameric-quaternary structure of the IgG antibody, as illustrated in Figure 1.1, adopts the well-known Y-

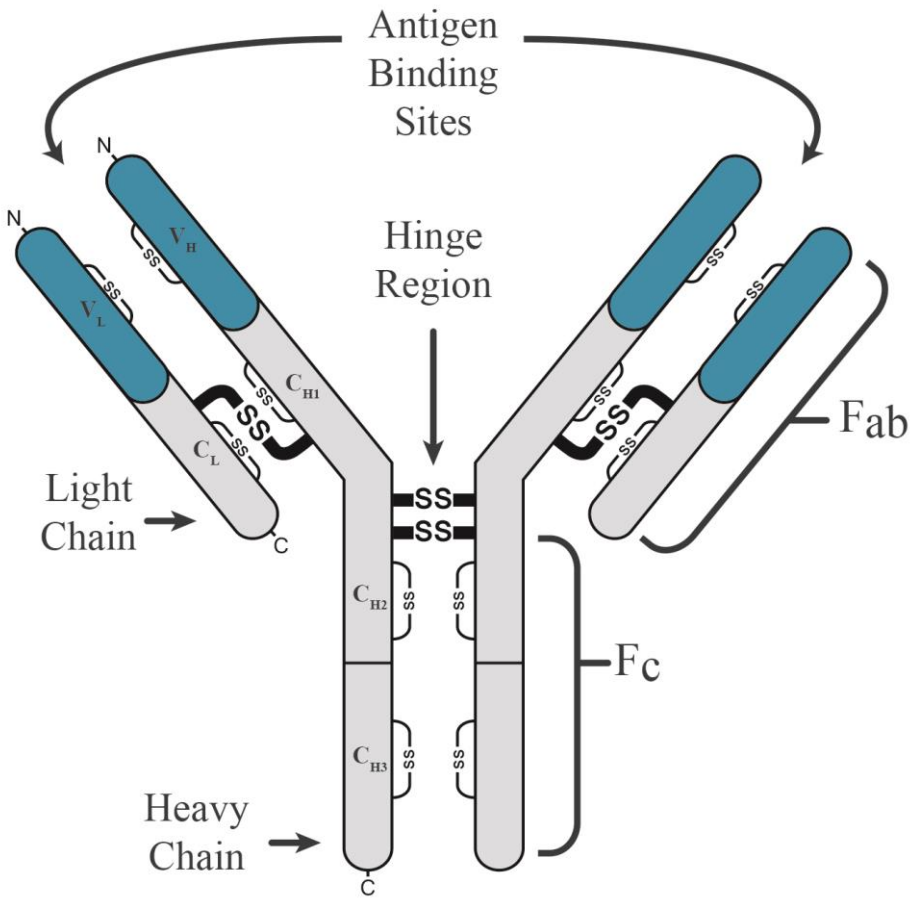

Figure 1.1: Structure of the immunoglobulin G (IgG) antibody molecule. Composed of two identical halves, both of which contain a light polypeptide chain (~25 kDa) and the heavy polypetide chain (~55 kDa) held together by disulfide linkages and electrostatic interactions. Each of the identical Fab (varible) domains can independently bind an individual antigen. The Fc (constant) region aids in effector functions.

shape. The IgG molecule is composed of three fragments all connected, through multiple disulfide linkages, at the center of the "Y," known as the hinge region, giving the antibody dynamic flexibility. Having two identical fragments, known as the variable domains (Fab), that are responsible for the binding antigens, the IgG is bivalent, capable of binding two antigens at once. The amino acid sequences that compose the two identical Fab domains vary from IgG-to-IgG, giving each clone of IgG molecules the ability to bind specific, yet different antigens. The third fragment of the IgG molecule, referred to as the constant region (Fc), is nearly conserved from clone-to-clone of IgG molecules, and the primary function of the Fc region is to aid in effector functions.[1,29]

1.3 Solid Phase Immunoassays and Interfacial Protein Activity

Landsteiner first presented the concept of the immunoassay in 1945 by demonstrating small molecules (haptens) could illicit an immune response when conjugated to larger carrier molecules;[30] however, it was not utilized until the late 1950s when Yalow and Berson reported on the first radioimmunoassay (RIA). Using ^{131}I-labeled insulin, Yalow and Berson were able to measure the concentration of insulin in human serum establishing the first competitive immunoassay.[31] In such assays, the analyte-antigen competes with a known concentration of ^{131}I-labeled antigen for homologous antibodies. At equilibrium, the ratio of free-to-bound ^{131}I-labeled antigen is directly proportional to the concentration of total antigen in solution; however, measuring this ratio requires that the free antigen be separated from the bound antigen-antibody complex, which is a slow and cumbersome process.

In order to make the separation of free antigen more efficient and cost effective,

Catt and Tregear developed the solid-phase immunoassay (SPI) in the late 1960s.[32] The fundamental principle behind the SPI utilizes surface-immobilized capture antibodies (receptor) to selectively bind antigens from free solution (ligand). After equilibrium has been established, the unbound antigen is simply rinsed from the surface, leaving only those antigens captured by interfacially immobilized antibodies. Since their introduction, SPIs have undergone a variety of permutations and improvements, while maintaining the original fundamental principles. Today, SPIs have been interfaced with a variety of analytical techniques, including electrochemical,[33-35] quartz crystal microbalance (QCM),[25,36] surface plasmon resonance (SPR),[37,38] and fiber-optic-fluorescence[39-42] for use in clinical,[3,43] environmental,[44] and agricultural diagnostics.[4,45]

The specific binding of ligands to surface-immobilized receptor sites commonly exhibits reactivities that differ greatly from the equivalent interaction observed in free solution. The measured reaction rates for ligand-receptor complexation at a solid-liquid interface are often times convoluted with mass transport effects resulting from diffusion to the surface, restricted reaction volumes,[8,46] and the surface density of the receptor sites.[7] Because the receptor molecule is directly immobilized to the interface in heterogeneous assays, the true reaction volume is confined within the attractive distance of the strongest electrostatic, Van der Waals, or hydrophobic interactions occurring between free-solution ligand and immobilized receptor. This is confined to ~10-100 Å from the receptor.[8,14] The time required for diffusion to bring ligands into these reaction volumes in sufficient numbers to satisfy a significant fraction of the receptors on the surface can cause the measured binding rates to be transport limited,[46-48] as is discussed in the following section.

In addition to the observed forward reaction rate often being mass transport limited, the antibody-antigen reactions at a solid-liquid interface often generally do not exhibit reversible kinetics. It has been demonstrated both theoretically and experimentally that once bound, antibody-antigen complexes at surfaces are stabilized and rarely dissociate.[7,49,50] It has been reported that the Langmuir-like kinetics observed for an interfacial antibody-antigen binding isotherm are the result of concentration-dependent saturation levels and not dynamic equilibria.[19] Currently there are two possible explanations as to why the interfacial antibody-antigen complex appears to be irreversible (see Figure 1.2). First, at a high surface concentration of an immobilized antigen or hapten receptor, it may be possible that the bivalency of an antibody-ligand interaction allows both antigen-binding sites to be simultaneously bound to multiple, closely spaced receptor molecules. This could also be true for a multivalent receptor site binding multiple epitopes of a single antigen. As a result, the probability of both binding sites dissociating is vanishingly small, so that the ligand cannot escape the surface. Secondly, if dissociation does occur, diffusion must carry the ligand away from the surface. For a high density of receptor sites, it has been hypothesized that transport away from a surface may not compete efficiently with the recapture by surface receptors, so that unbound ligands are unable to reach the stirred boundary layer, where flowing solution actively carries them downstream from the area of observation.[19,49] It has been well documented that the unbinding of a ligands from a capture surface can be an extremely slow process; however, the mechanisms explaining the slow off rates observed in SPIs are only hypothesized and have not verified by direct observations.

In addition to the unique reaction kinetics associated with interfacial antibody-

Figure 1.2: Hypothesized source of irreversible kinetics associated with the interaction of a ligand with a specific surface receptor site, while this figure specifically demonstrates the binding of an antibody-ligand to an antigen-receptor, the situation is also applicable to closely spaced multivalent receptor sites capturing multiple epitopes of an antigen-ligand. (a) Bivalent interactions with closely spaced receptor sites prevent dissociation. (b) Transport away from the surface may not efficiently compete with the recapture of ligand to receptor so that unbound ligands are unable to reach the unstirred boundary layer (gray dotted line), where flowing solution actively carries them downstream from the area of observation.

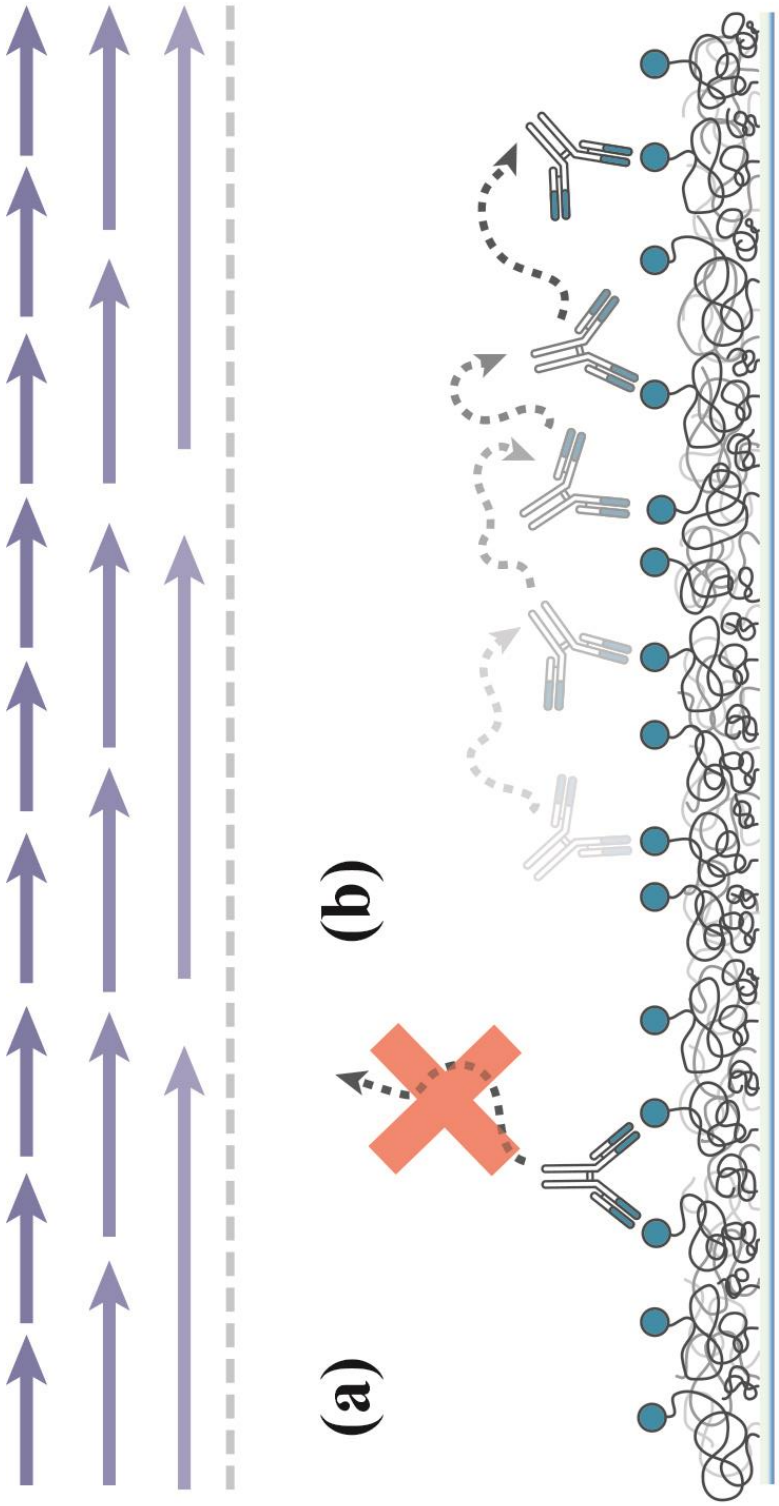
(a)
(b)

antigen interactions, it is also well known that capture antibodies immobilized to solid surfaces exhibit decreased bioactivities compared to those measured in free solution.[16,51] Butler and coworkers reported that >90% of monoclonal antibodies immobilized to a polystyrene interface are rendered inactive and incapable of capturing solution-phase ligand molecules.[52] It is believed that the orientation and configuration of the immobilized capture antibodies with respect to the interface are responsible for the decreased activity.[27,52-54] There have been many attempts to increase the surface activity of capture antibodies by immobilizing them in specific orientations that promote access to the Fab domains to solution. Strategies for oriented immobilization of antibodies include the use of intermediate immunoglobulins,[55] Fc binding proteins such as protein A and protein G,[56-60] and disulfide linkages.[61-63] In many cases, capture antibodies immobilized to solid surfaces in an orientation that promotes the accessibility of the binding domain(s) have shown a significant increase in bioactivity; however, these methods commonly fail to achieve free solution-like activity or reversibility.[21]

From these observations, it is clear that interfacial measurements of antigen-antibody activity are quite complex. In order to achieve an SPI that accurately represents *in vivo* interactions, the processes that govern the unique kinetics and decreased activities associated with *in vitro* interfacial interactions must be better understood. This goal could be advanced by querying interfacial-receptor activities at an individual receptor-ligand level. To our knowledge, nothing has been reported on characterizing and understanding the activities of individual ligand-receptor interactions commonly associated with SPIs at the single-molecule level. By using single-molecule imaging, the sources of interference or inefficiency can be isolated and measured in order to better und

understand interfacial ligand-receptor interactions.

1.4 Mass Transport

As illustrated in Figure 1.3, transport limitations in surface-binding reactions are the result of the interfacial-ligand concentration gradient that develops upon depletion of ligand molecules captured by receptor sites. The depletion layer (l_s) is the distance into solution that contains the number of ligand molecules needed to provide half of the immobilized receptor sites with a ligand molecule. For a surface concentration of receptor sites, R in cm^{-2}, which would be, for example, half-occupied by ligands upon reaction from a solution of concentration, $[L]$ in $mols/cm^3$, the depletion layer thickness is given by:

$$l_s = \frac{R}{2N_a[L]} \tag{1.1}$$

where N_a is Avogadro's number. The time, τ_s, required to relax this concentration gradient, through diffusion to the surface, is given by:

$$\tau_s = \frac{l_s^2}{2D} \tag{1.2}$$

The diffusion coefficient, D, for a small protein is ~3×10^{-7} cm^2s^{-1}.[64] For a ligand concentration in solution of $[L] = 1 \times 10^{-9}$ M, and for a typical capture surface used in ensemble measurements, where the density of receptor sites is $R \sim 1 \times 10^{13}$ cm^{-2},[65] the

Figure 1.3: Transport limitations in the surface-binding reaction for a high density (left) and low density (right) of receptor surface sites (blue circles) to 0.5 coverage of ligand (purple semicircles). The red dotted line represents the depletion layer, l_s, the distance into solution that contains the number of ligands to provide 0.5 of the receptor sites with a ligand molecule.

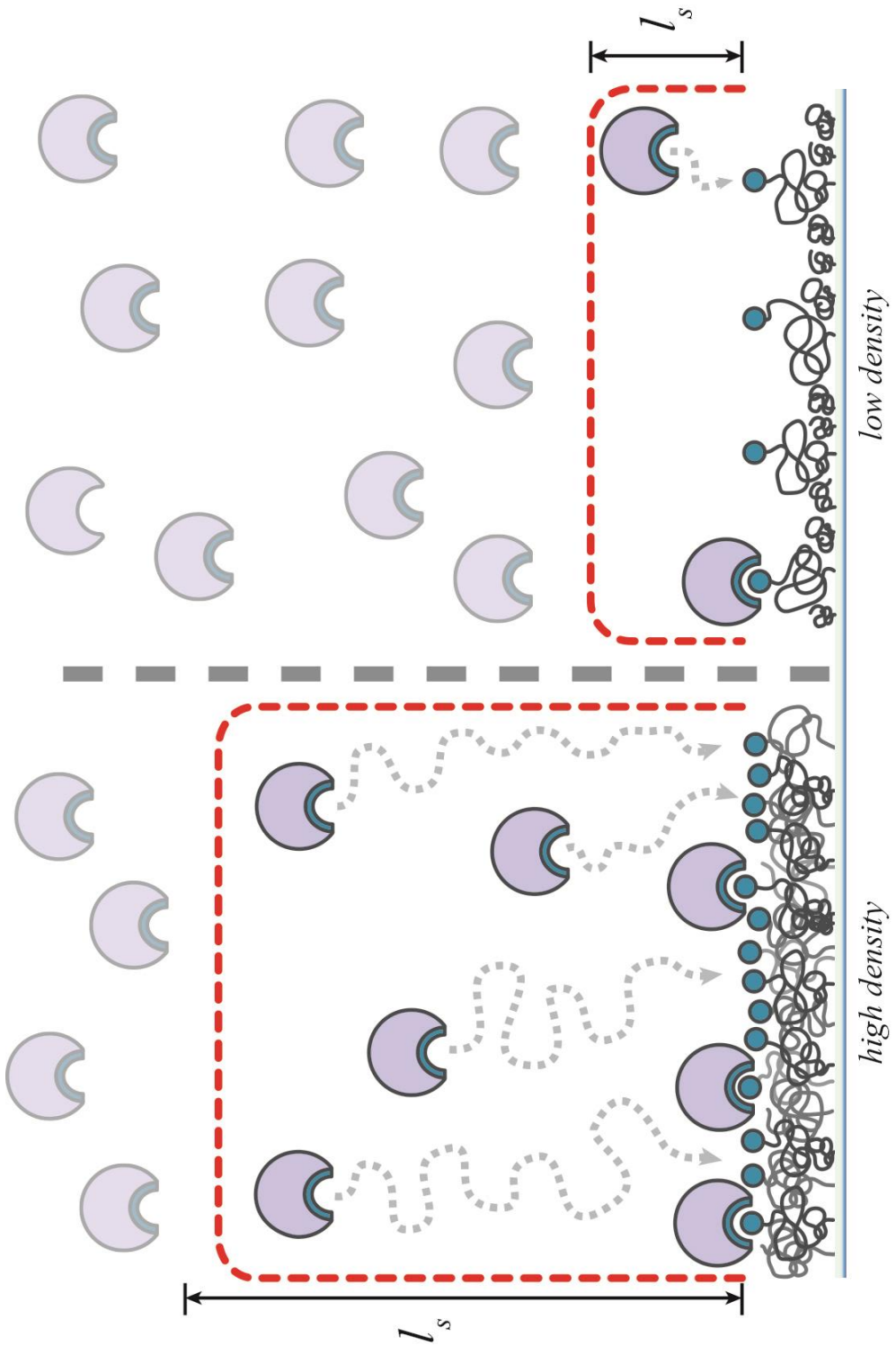
l_s
l_s
low density
high density

depletion layer, l_s, would be ~8 cm and would require ~4 years to satisfy the half-coverage coverage of R by diffusion. In contrast, using the density capture surfaces prepared in Chapter 3, having a receptor surface concentration of R ~1× 10^8 cm^{-2}, the depletion layer, l_s, would extend only ~0.8 μm from the surface and require just ~10 ms to relax the concentration gradient, τ, by diffusion

Flowing the solution over the surface is commonly used to overcome transport limitations associated with high-density capture surfaces. In the case where flow is used, molecules must still diffuse to the surface through an unstirred boundary of thickness, Δx, where the flux of ligand, L, to the surface is given by Fick's first law:

$$J = D\frac{dC}{dx} = \frac{[L]N_a}{\Delta x} \tag{1.3}$$

The time required in the presence of flow to relax the concentration gradient for half-coverage of the bound receptors, R, τ_{flow}, is given by:

$$\tau_{flow} = \frac{R}{2J} \tag{1.4}$$

Using the same diffusion coefficient as above, D ~3 × 10^{-7} cm^2s^{-1}, and an unstirred boundary layer thickness typical of very fast flow, Δx, 10 μm,[66] then the time required to relax the concentration gradient for a high density, R ~1 × 10^{13} cm^{-2}, capture surface would be ~8 hours. In the case of the low density capture surface, R ~1 × 10^8 cm^{-2} flow is not needed to speed up the mass transport rate since l_s << Δx ~ 10 μm; therefore, τ_{flow} = τ_s ≈ 10 ms. Although τ is greatly reduced in the case of the high density capture surface,

flow does not eliminate transport limitations. This demonstrates the important influence that the surface density of capture sites has on the observed kinetics associated with interfacial ligand-receptor interactions.

1.5 Surface Modification and Passivation

Proteins are composed of a variety of functionalities that cause them to readily adsorb onto glass substrates through Van der Waals, Lewis acid-base, electrostatic, and hydrophobic forces.[67] Often times upon adsorption to an interface, changes within the secondary and tertiary structures of the protein can lead to protein denaturation and decreased bioactivity.[68-70] To improve the efficacy of SPIs and observe protein-protein interactions that approach their *in vivo* activities, the solid-liquid interface must not only provide resistance to the nonspecific adsorption of biomolecules, but must also allow surface immobilized capture proteins to maintain native-like conformations and activities.

One of the most common and versatile methods to functionalizing glass surfaces, for use in biocompatible processes, has been through the use of silane chemistry.[71,72] Trifunctional alkoxy- or chloro-silanes monolayers are generally deposited onto glass surfaces using solution phase methods; however, such silanes are highly susceptible to oligomerization in the presence of water, and thus require the use of extremely dry solvents to prevent aggregation and formation of defects within the deposited monolayer during the reaction process.[73-76] Even trace levels of water in the reaction solvents can result in the deposition of nonuniform multilayers, codeposition of aggregated silanes, and the hydrolytic stripping of predeposited silanes.[76-79] Although less common than solution-phase deposition methods, the chemical-vapor-deposition (CVD) of small alkyl-

silanes onto glass-type substrates has been used as an efficient means to produce thin, uniform, and defect free functional monolayers.[76,77,80] The differences between solution-phase- and chemical-vapor- deposition techniques are illustrated in Figure 1.4.

Thin films produced from CVD techniques have been characterized using x-ray-photoelectron-spectroscopy (XPS), contact-angle-goniometry, spectroscopic-ellipsometry, atomic force microscopy (AFM), scanning-electron-microscopy (SEM), and time-of-flight-secondary-ion-mass-spectroscopy (ToF-SIMS).[75,77,81] Two commonly employed silane reagents, (3-Glycidyloxypropyl)trimethoxysilane (GOPTS) and (3-aminopropyl)triethoxysilane (APTES) have been deposited onto glass-type surfaces to prepare epoxide and amine functionalized coatings. These simple functionalities provide an extremely versatile means to further derivatized glass surfaces for a variety of applications, some of which are demonstrated in Figure 1.5.

Poly(ethylene glycol) (PEG) molecules are often grafted onto a variety of substrates at high densities as a means to prevent the nonspecific adsorption of proteins.[82-86] Owing to the large exclusion volumes and high degree of conformational mobility associated with PEG molecules, grafted PEG chains are highly resistant to biofouling;[87,88] however, depending on the density and molecular weight of the grafted PEG monolayer, their adsorption-resistant properties vary greatly.[89,90] In addition to the reduced protein adsorption, PEG monolayers have been shown to help surface-tethered proteins maintain more native-like conformations.[85] By depositing a mixture of biotin-functionalized PEG (biotin-PEG) and mPEG molecules, receptor proteins can easily be immobilized to the resulting monolayers through streptavidin intermediates.[91,92] In addition, it is important to have control over the surface concentration of biotin

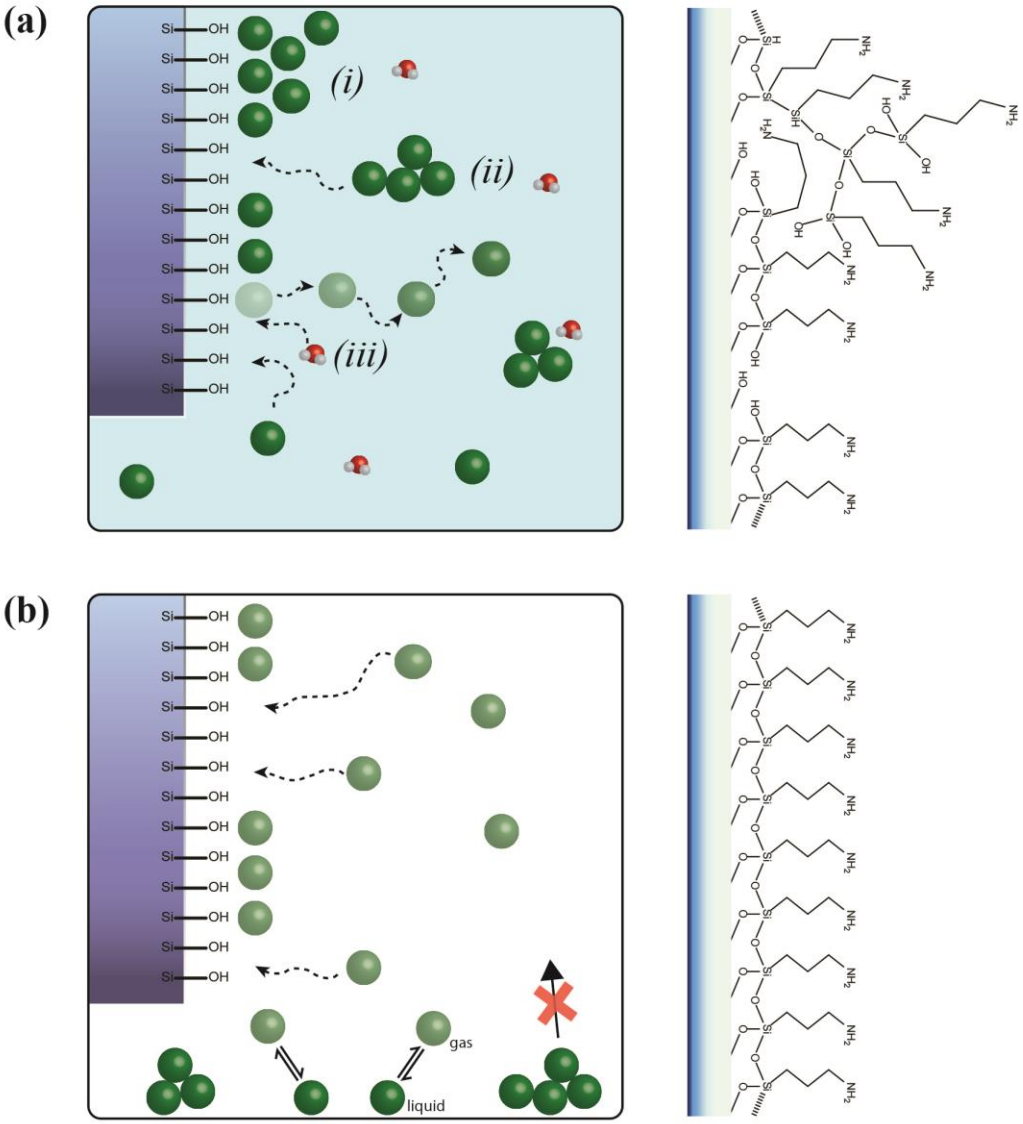

Figure 1.4: Comparison of silane deposition methods. (a) Solution-phase deposition of APTES. Trace levels of water in the reaction solution result in (i) the deposition of nonuniform monolayers, (ii) codeposition of aggregated silanes, and (iii) the hydrolytic stripping of predeposited silanes. (b) Chemical-vapor deposition (CVD) of APTES produces relatively uniform and defect-free monolayers. Only monomeric silanes are deposited, as large aggregated silanes are not volatile.

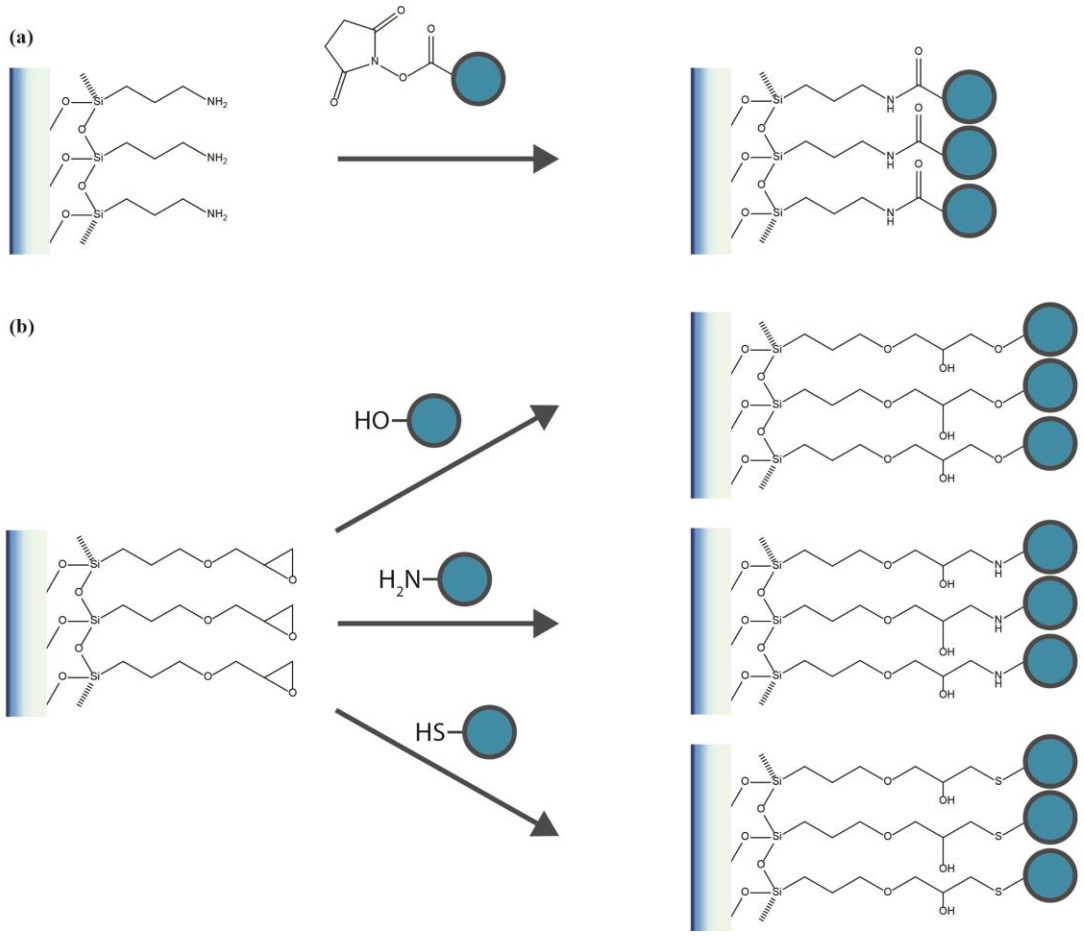

Figure 1.5: Silane chemistry: (a) The reaction of a N-hydroxysuccinimidyl (NHS) ester to an APTES modified surface forming a covalent amide bond. The blue circle represents any molecule capable of being modified with NHS functionality. (b) The reaction of GOPTS by nucleophilic substitution of any molecule (blue circle) containing hydroxyl-, amine-, or thiol-functionality to form a covalent ether, secondary amine or thioether bond.

conjugation sites because the density of receptor sites on an interface directly affects the signal response, sensitivity, kinetics, and capture activity of the resulting measurements.[12,20,93,94] By adjusting the ratio of biotin-PEG to the diluent mPEG, the density of biotin receptor sites can easily be controlled,[91,92]

Although the activities of immunoassays have been extensively studied using ensemble techniques such as radiometry,[15-18] ellipsometry,[19] SPR,[20,21] colorimetry,[22-24] and QCM,[25-27] little has been reported at the single-molecule level. By controlling the densities of immobilized receptor sites down to very small fractions of a monolayer, TIRF imaging can be employed to study the activities and heterogeneity of ligand-receptor interactions occurring at a glass-water interface at a single-molecule level. By studying such interactions at low receptor surface concentrations, the capture activities of individual receptor molecules can be characterized in the absence of transport limitations that govern the kinetic response of high density capture surfaces and bivalent interactions resulting from closely packed capture sites. Understanding these fundamental interfacial ligand-receptor interactions will aid in preparing SPIs with higher sensitivity, lower limits of detection, and that exhibit kinetics that more accurately represent the biorecognition processes.

1.6 Protein Immobilization through Streptavidin Tethering

The strept(avidin)-biotin interaction has commonly been applied to SPIs as a means to mediate the immobilization of capture proteins to a measurement surface. Strept(avidin) is an extremely stable homotetramer molecule that binds the small molecule biotin with an extremely high affinity (K_d= $10^{-14\ to\ -15}$M).[95-97] Capable of

simultaneously binding multiple biotins at once, the protein avidin binding complex (PABC) has previously been used as a bridge to immobilized biotin-functionalized antibodies to biotinylated-surfaces, as illustrated in Figure 1.6.[98] In some cases, capture antibodies immobilized through the strept(avidin) bridge exhibited up to 400 times more activity compared to antibodies passively adsorbed to a solid surface.[99] The strept(avidin)-biotin interaction not only helps maintain the activity of surface-immobilized capture proteins, but it also provides a nearly universal means to irreversibly immobilize any biotin-conjugated capture protein onto the aforementioned biotinylated-PEG modified surfaces at a controlled density.[91,100,101] Although the PABC immobilization strategy has many advantages, surface-immobilized strept(avidin) molecules exhibit poor capture yields.[8] The poor capture activity exhibited by surface immobilized strept(avidin) has been reported as a qualitative observation;[8] however, little quantitative information has been documented on the activity, behavior, and heterogeneity of surface-immobilized streptavidin.

1.7 Total Internal Reflection Fluorescence Microscopy

There are numerous measurement challenges that must be overcome in order to monitor discrete molecular interactions at a glass/water interface using optical based techniques. The instrumentation must be sensitive to submonolayer coverages, while having a high spatial resolution capable of resolving individual molecules. Total Internal reflection fluorescence (TIRF) has the ability to simultaneously fulfill these requirements by selectively illuminating and exciting fluorophores contained within a small distance from the glass-solution interface. In TIRF microscopy, an excitation laser is brought off-

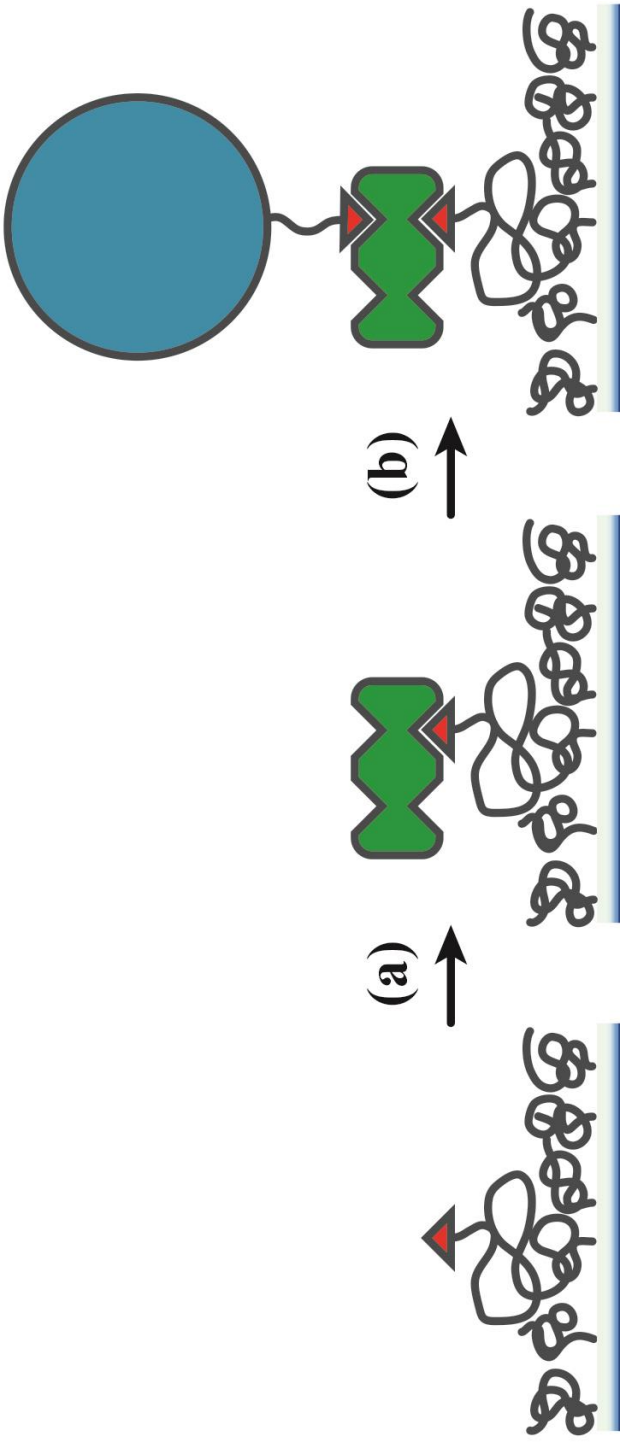

Figure 1.6: Protein immobilization through streptavidin intermediate: (a) Streptavidin (green rectangle) immobilized to surface bound biotin (red triangle) conjugation sites, (b) immobilization of a biotinylated-protein (blue circle) to the streptavidin modified surface.

center into the back of a high numerical aperture (NA) objective and projected onto a glass/water interface at an angle of incidence greater than the critical angle (θ_c). Total internal reflection (TIR) occurs when light hits an interfacial boundary traveling from a higher refractive index (n_1) medium to a lower refractive index (n_2) medium at an angle of incidence greater than the critical angle, θ_c, as defined by Snell's law:

$$\theta_c = sin^{-1}\frac{n_2}{n_1} \tag{1.5}$$

Upon TIR, an evanescent field (nonpropagating electromagnetic wave) is produced that decays exponentially in intensity (I(z)) with distance (z) normal from the interface, as defined by equation 1.6, where I_0 is the intensity at the interface (z=0) and d_p the penetration depth of the evanescent field into the lower refractive index medium.

$$I(z) = I_0 e^{-z/d_p} \tag{1.6}$$

The d_p, as defined by equation 1.7, is a function of the incident wavelength (λ_i), angle of incidence (θ_i), and two refractive indices (n_1 and n_2) of the glass and solution, respectively.[102]

$$d_p = \lambda_i/2\pi n_1\sqrt{\sin^2\theta_i-(n_2/n_1)^2} \tag{1.7}$$

As illustrated in Figure 1.7, our experimental setup utilized a 532 nm laser beam coupled into the back of a 1.45 NA oil-immersion objective causing the laser to strike the

Figure 1.7: A 532 nm laser is coupled into a single mode fiber and focused into the back of a 1.45 NA objective. TIR, achieved by translating the incoming light off center to the objective, produces an evanescent wave, exciting only fluorophores contained within the first 150 nm of the surface. Fluorescence from the excited molecules is then collected back through the same objective, passed through a 552 nm dichroic beamsplitter and 585/40 nm bandpass filter, and imaged using a CCD camera.

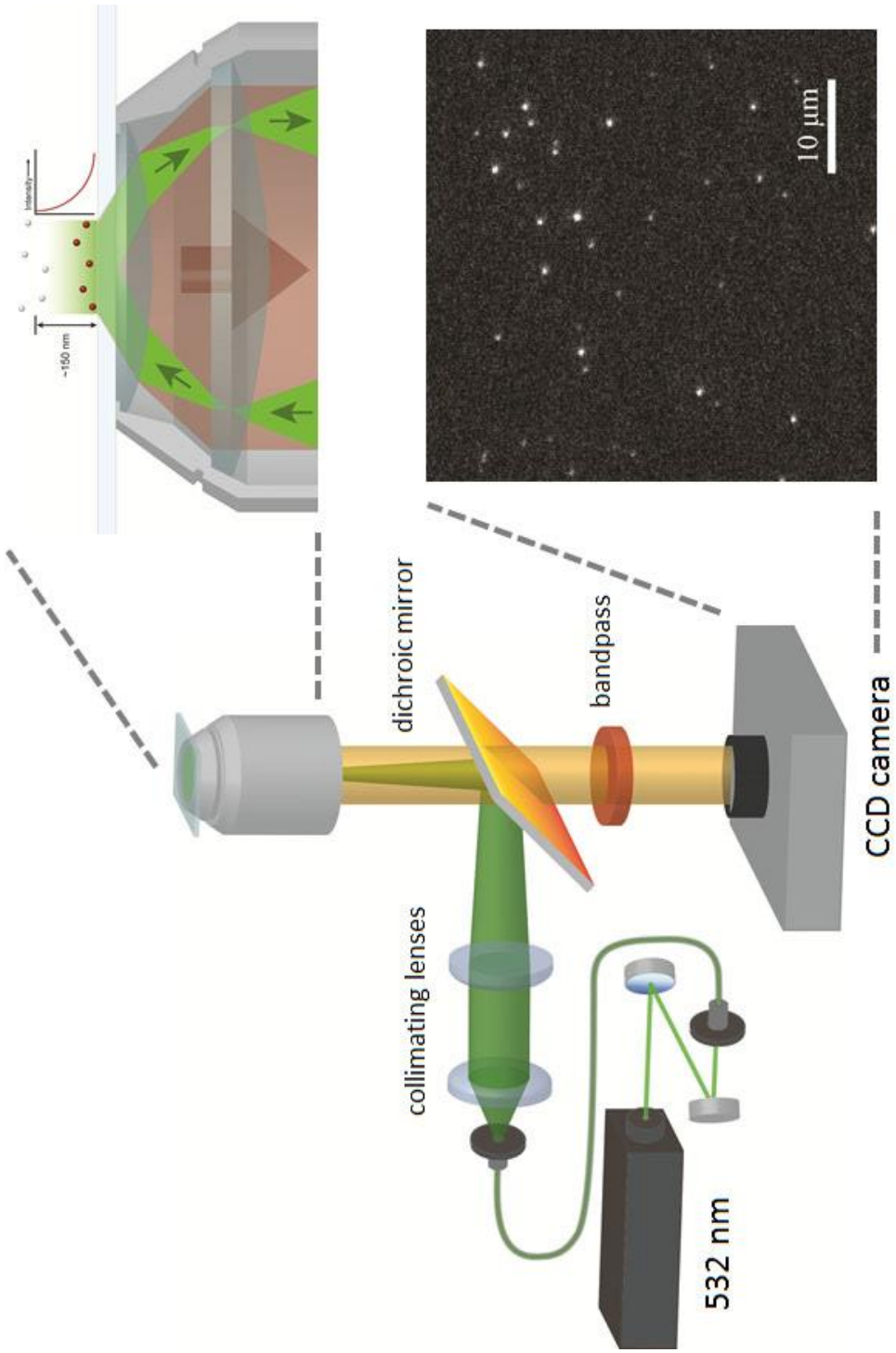
Intensity
~150 nm
10 µm
dichroic mirror
bandpass
CCD camera
collimating lenses
532 nm

sample interface at an angle $\theta_i \approx 65\text{-}75°$. The refractive indices, $n_1 = 1.47$ (borosilicate glass) and $n_2 = 1.33$ (water) generated TIR, which produces an evanescent wave penetration depth of ~150 nm. The emission from the excited fluorophores residing within the first ~150 nm from the glass surface is then collected back through the same objective and imaged onto a high efficiency charge coupled device (CCD) camera. Because only molecules within the first ~170 nm of the surface are excited, background signal from molecules in the bulk solution are minimized allowing TIRF imaging at high signal-to-noise and diffraction-limited spatial resolutions.

1.8 Single Molecule Imaging

Single molecule total internal reflection fluorescent (SM-TIRF) imaging has many advantages for interrogating the activity of proteins at interfaces. As previously discussed, it is well known that proteins immobilized to solid surfaces behave quite differently compared to that in free solution, and a large fraction of receptor proteins are inactivated when immobilized to a solid surface. Characterizing such processes using ensemble measurements such as radiometrically,[15-18] ellipsometry,[19] SPR,[20,21] colorimetry,[22] and QCM,[25-27] cannot report heterogeneity at individual receptor-ligand levels. Using single-molecule TIRF, it is possible to resolve individual receptor-ligand interactions and colocalize every subsequent capture event, or lack thereof, versus time. In addition, utilizing a low density of capture sites avoids transport limitations, bivalent interactions, and recapture processes.

Although SM-TIRF imaging has many advantages, this fluorescence-based technique requires ligand molecules to be conjugated to fluorescent dye molecules, which

are susceptible to photobleaching. By employing intermittent imaging, exposing the sample briefly to light and imaging at regular intervals in time, any protein-conjugated dye molecules are exposed to a minimal amount of excitation. When the intermittency factor is optimized, nearly all photobleaching can be eliminated. Using intermittent TIRF imaging, the ligand-receptor interactions can be monitored over many hours with negligible false negative observations arising from photobleaching of the fluorescent labels.

1.9 Overview of the Dissertation

The goal of this research is to develop single molecule TIRF techniques capable of characterizing biologically relevant ligand-receptor interactions at a solid-liquid interface. As previously discussed in this chapter, there are many challenges to overcome in order to observe and measure individual ligand-receptor interactions at glass-water interfaces. Because of the extreme sensitivity of single-molecule TIRF microscopy, the measurement surfaces must be resistant to the nonspecific adsorption of proteins, while maintaining the ability to control the site density of immobilized receptors.

In order to selectively monitor individual interfacial ligand-receptor interactions at the single-molecule level, the capture surface must first be highly resistant to nonspecific protein adsorption. As presented in Chapter 2, poly(ethylene glycol) (PEG) is grafted to glass slides in order to prepare a surface with resistance to the nonspecific adsorption of proteins. The goal of this research is not only to prepare a surface that has low biofouling properties, but also to investigate how the chemistry used to immobilize the PEG monolayer onto glass surfaces affects the protein adsorption properties of the

PEG-modified glass slide. Two small functional alkyl-silanes, (3-aminopropyl)triethoxysilane (APTES) and (3-Glycidyloxypropyl)trimethoxysilane (GOPTS), are deposited onto glass cover slides using CVD as a means to subsequently graft functional-PEG molecules. The amine-functionality of the APTES-derivatized slides is suitable for further modification using well-developed N-hydroxysuccinimide (NHS) ester chemistry. A monolayer of 2000 g/mol PEG-NHS is covalently grafted to APTES modified slides. In contrast, the epoxide-functionality of the GOPTS-derivatized slides readily undergoes substitutions with a variety of nucleophiles. Both 750 g/mol and 2000 g/mol PEG-amine are covalently grafted to the GOPTS-modified surfaces. The resistance to nonspecific adsorption of proteins is characterized using a monoclonal, mouse-derived cy3-labeled antibiotin (MsIgG) molecule. The higher resistance to protein adsorption exhibited by slides prepared by reaction of 2000 g/mol PEG-amine to an epoxide-modified surface suggests that the higher stability of epoxide functionality produced a more uniform surface with fewer defects. In addition, the results also indicate that, for similar grafting chemistries, the high conformational entropy associated with the larger PEG chain better resists the adsorption of antibodies.

Controlling the surface concentration of receptor molecules is not only critical in resolving single-molecule binding events, but it is also important in overcoming transport limitations and crowding effects that can influence interfacial ligand-receptor kinetics. In Chapter 3, the epoxide-based chemistry developed in Chapter 2 is adapted to control the surface concentration of biotin conjugation sites in an mPEG-diluent monolayer on glass slides. By diluting in a small concentration of 2300 g/mol biotin-PEG-amine into a higher concentration of 750 g/mol mPEG-amine reaction solution, the density of biotin

conjugation sites can be controlled. The extremely high affinity of biotin for strept(avidin) makes biotin an ideal choice for subsequent conjugation steps. Streptavidin, a tetravalent molecule, can simultaneously bind multiple biotin molecules, and has been extensively used as an intermediate tether to immobilize biotin conjugated biomolecules to surfaces.[21,91,92,103-105] The density of biotin conjugation-sites associated with the modified PEG surfaces are characterized using fluorescently-labeled streptavidin molecules. Increasing the concentration of biotin-PEG-amine in the reaction solution, containing a fixed concentration of mPEG-amine, results in a linear increase in the observed conjugation site density. The resulting surfaces produced conjugation site densities down to very low fractions (10^{-6}) of a streptavidin monolayer.

The modified surface prepared in Chapter 3 allows ligand-receptor interactions commonly utilized in solid-phase immunoassays (SPIs) to be investigated at a single-molecule level using TIRF imaging. In many cases the activity of surface immobilized capture antibodies differ greatly from free solution measurements. It is thought that the orientation of a protein receptor with respect to the surface affects the activity of the immobilized capture molecule. In Chapter 4, the activity of fluorescently-labeled rabbit derived antigoat IgG (anti-GtIgG) capture antibodies is tested using four different immobilization strategies: (i) passive adsorption to an mPEG surface, (ii) active, but random biotin-immobilization directly to streptavidin capture sites, (iii) an oriented two-step immobilization sequentially through streptavidin and *E. coli* protein A (EpA) intermediate, and (iv) an oriented one-step immobilization to streptavidin as a chimeric [EpA/anti-GtIgG] complex. The activity of each capture antibody immobilization strategy is characterized using a fluorescently labeled model goat antibody as an antigen

(GtIgG). The use of fluorescent labels in each step allows all subsequently bound proteins to be colocalized to previously known capture locations. As a result, the activities of individual capture proteins and protein-protein complexes are directly observed at a site-to-site basis. From these results, it becomes clear how the orientation of capture sites and the means of protein-receptor immobilization affects the activity of individual capture sites and how that correlates to the activity of the surface as a whole.

1.10 References

(1) Abul K. Abbas, A. H. L., Shiv Pillai. *Cellular and Molecular Immunology*; 7 ed.; Elsevier Suanders: Philadelphia, PA, 2012.

(2) Magi, B.; Liberatori, S. In *Immunochemical Protocols*; Burns, R., Ed.; Humana Press: 2005; Vol. 295, p 227.

(3) Wu, J.; Fu, Z.; Yan, F.; Ju, H. *Trends in Analytical Chemistry*. **2007**, *26*, 679.

(4) Shan, Guomin., *Immunoassays in Agricultural Biotechnology*; John Wiley & Sons, INC.: Hoboken, NJ, 2011.

(5) Facinelli, B. C. *Immunotherapy: Activation, Suppression, and Treatments*; Nova Science Publishers: Hauppauge, N.Y., 2010.

(6) Mason, D. W.; Williams, A. F. *Biochem. J.* **1980**, *187*, 1.

(7) Nygren, H.; Czerkinsky, C.; Stenberg, M. *J. Immunol. Methods*. **1985**, *85*, 87.

(8) Butler, J. E., *Immunochemistry of Solid-Phase Immunoassay*; CRC Press: Boca Raton, FL, 1991, p 221.

(9) Phillips, R.; Ursell, T.; Wiggins, P.; Sens, P. *Nature (London, U. K.)* **2009**, *459*, 379.

(10) Wild, D. *The Immunoassay Handbook*; Stockton Press: New York, NY, 1994.

(11) A. P. Johnstone, M. W. T. *Immunochemistry 2*. Oxford University Press: New York, NY, 2002.

(12) Stenberg, M.; Nygren, H. *J Immunol Methods*. **1988**, *113*, 3.

(13) Pesce, A. J.; Michael, J. G. *J. Immunol. Methods*. **1992**, *150*, 111.

(14) Butler, J. E. In *Immunoassays*; Eleftherios P. Diamandis, T. K. C., Ed.; Academic Press: New York, NY, 1996.

(15) Engvall, E.; Jonsson, K.; Perlmann, P. *Biochim. Biophys. Acta, Protein Struct.* **1971**, *251*, 427.

(16) Dierks, S. E.; Butler, J. E.; Richerson, H. B. *Mol. Immunol.* **1986**, *23*, 403.

(17) Catt, K. J.; Tregear, G. W. *Science (Washington, D. C.)* **1967**, *158*, 1570.

(18) Cantarero, L. A.; Butler, J. E.; Osborne, J. W. *Anal. Biochem.* **1980**, *105*, 375.

(19) Nygren, H.; Stenberg, M. *J. Colloid Interface Sci.* **1985**, *107*, 560.

(20) Vareiro, M. M. L. M.; Liu, J.; Knoll, W.; Zak, K.; Williams, D.; Jenkins, A. T. A. *Anal. Chem.* **2005**, *77*, 2426.

(21) Chung, J. W.; Park, J. M.; Bernhardt, R.; Pyun, J. C. *J. Biotechnol.* **2006**, *126*, 325.

(22) Ikawa-Yoshida, A.; Yoshii, K.; Kuwahara, K.; Obara, M.; Kariwa, H.; Takashima, I. *Microbiol. Immunol.* **2011**, *55*, 100.

(23) Procaccia, S.; Gasparini, A.; Colucci, A.; Lanzanova, D.; Bianchi, M.; Forcellini, P. *Boll Ist Sieroter Milan.* **1987**, *66*, 124.

(24) Broom, A. K.; Charlick, J.; Richards, S. J.; Mackenzie, J. S. *J Virol Methods* **1987**, *15*, 1.

(25) Guo, X.; Lin, C.-S.; Chen, S.-H.; Ye, R.; Wu, V. C. H. *Biosens. Bioelectron.* **2012**, *38*, 177.

(26) Kanno, S.; Yanagida, Y.; Haruyama, T.; Kobatake, E.; Aizawa, M. *J. Biotechnol.* **2000**, *76*, 207.

(27) Tang, D.-Q.; Zhang, D.-J.; Tang, D.-Y.; Ai, H. *J. Immunol. Methods*. **2006**, *316*, 144.

(28) Schuck, P.; Zhao, H. *Methods Mol. Biol.* **2010**, *627*, 15.

(29) Lipman, N. S.; Jackson, L. R.; Trudel, L. J.; Weis-Garcia, F. *ILAR Journal* **2005**, *46*, 258.

(30) Lansteiner, K. *The Specificity of Serological Reactions*; Harvard University Press: Cambridge, Massachusetts, 1947.

(31) Yalow, R. S.; Berson, S. A. *Nature*. **1959**, *184*, 1648.

(32) Catt, K. J.; Niall, H. D.; Tregear, G. W. *Nature*. **1967**, *213*, 825.

(33) Emami, M.; Shamsipur, M.; Saber, R.; Irajirad, R. *Analyst (Cambridge, U. K.)* **2014**, *139*, 2858.

(34) Tang, C. K.; Vaze, A.; Rusling, J. F. *Analytical Methods*. **2014**, *6*, 8878.

(35) Heineman, W. R.; Halsall, H. B. *Anal Chem*. **1985**, *57*, 1321A.

(36) Kurosawa, S.; Park, J.-W.; Aizawa, H.; Wakida, S.-I.; Tao, H.; Ishihara, K. *Biosens. Bioelectron.* **2006**, *22*, 473.

(37) Fratamico, P. M.; Strobaugh, T. P.; Medina, M. B.; Gehring, A. G. *Biotechnol. Tech.* **1998**, *12*, 571.

(38) Bokken, G. C. A. M.; Corbee, R. J.; van Knapen, F.; Bergwerff, A. A. *FEMS Microbiol. Lett.* **2003**, *222*, 75.

(39) Anderson, G. P.; Nerurkar, N. L. *J. Immunol. Methods*. **2002**, *271*, 17.

(40) Rijal, K.; Leung, A.; Shankar, P. M.; Mutharasan, R. *Biosens. Bioelectron.* **2005**, *21*, 871.

(41) Nanduri, V.; Kim, G.; Morgan, M. T.; Ess, D.; Hahm, B.-K.; Kothapalli, A.; Valadez, A.; Geng, T.; Bhunia, A. K. *Sensors*. **2006**, *6*, 808.

(42) Sapsford, K. E.; Shubin, Y. S.; Delehanty, J. B.; Golden, J. P.; Taitt, C. R.; Shriver-Lake, L. C.; Ligler, F. S. *J. Appl. Microbiol.* **2004**, *96*, 47.

(43) P. Singh, P. B. S., P. Tyle *Diagnostics in the year*. *2000*:*antibody, biosensor, and nucleic acid technologies*; Van Nostrand Reinhold: New York, NY, 1993.

(44) Diana, S. A.; Thurman, E. M. In *Immunochemical Technology for Environmental Applications*; American Chemical Society: 1997; Vol. 657, p 1.

(45) A. Paraf, G. P. *Immunoassays in Food and Agriculture*; Kluwer Academic Publisher: Boston, Massachusetts, 1991.

(46) Stenberg, M.; Stiblert, L.; Nygren, H. *J Theor Biol*. **1986**, *120*, 129.

(47) Kusnezow, W.; Syagailo, Y. V.; Rueffer, S.; Klenin, K.; Sebald, W.; Hoheisel, J. D.; Gauer, C.; Goychuk, I. *Proteomics.* **2006**, *6*, 794.

(48) Stenberg, M.; Nygren, H. *J. Theor. Biol.* **1985**, *113*, 589.

(49) DeLisi, C. *Q. Rev. Biophys.* **1980**, *13*, 201.

(50) Stenberg, M.; Nygren, H. *Anal. Biochem.* **1982**, *127*, 183.

(51) Azimzadeh, A.; Van Regenmortel, M. H. V. *J. Mol. Recognit.* **1990**, *3*, 108.

(52) Butler, J. E.; Ni, L.; Brown, W. R.; Joshi, K. S.; Chang, J.; Rosenberg, B.; Voss, E. W., Jr. *Mol. Immunol.* **1993**, *30*, 1165.

(53) Ferretti, S.; Paynter, S.; Russell, D. A.; Sapsford, K. E.; Richardson, D. J. *TrAC, Trends Anal. Chem.* **2000**, *19*, 530.

(54) Kennel, S. J. *J. Immunol. Methods*. **1982**, *55*, 1.

(55) Butler, J. E.; Ni, L.; Nessler, R.; Joshi, K. S.; Suter, M.; Rosenberg, B.; Chang, J.; Brown, W. R.; Cantarero, L. A. *J. Immunol. Methods.* **1992**, *150*, 77.

(56) Werner, S.; Machleidt, W. *Eur. J. Biochem.* **1978**, *90*, 99.

(57) Gersten, D. M.; Marchalonis, J. J. *J. Immunol. Methods.* **1978**, *24*, 305.

(58) Anderson, J. M.; Rodriguez, A.; Chang, D. T. *Semin. Immunol.* **2008**, *20*, 86.

(59) Bae, Y. M.; Oh, B.-K.; Lee, W.; Lee, W. H.; Choi, J.-W. *Biosens. Bioelectron.* **2005**, *21*, 103.

(60) Owaku, K.; Goto, M.; Ikariyama, Y.; Aizawa, M. *Anal. Chem.* **1995**, *67*, 1613.

(61) Spitznagel, T. M.; Jacobs, J. W.; Clark, D. S. *Enzyme Microb. Technol.* **1993**, *15*, 916.

(62) Lu, B.; Xie, J.; Lu, C.; Wu, C.; Wei, Y. *Anal. Chem.* **1995**, *67*, 83.

(63) Kausaite-Minkstimiene, A.; Ramanaviciene, A.; Kirlyte, J.; Ramanavicius, A. *Anal. Chem.* **2010**, *82*, 6401.

(64) Spinke, J.; Liley, M.; Schmitt, F. J.; Guder, H. J.; Angermaier, L.; Knoll, W. *J. Chem. Phys.* **1993**, *99*, 7012.

(65) Zhao, S.; Reichert, W. M. *Langmuir*. **1992**, *8*, 2785.

(66) Barry, P. H.; Diamond, J. M. *Physiol Rev.* **1984**, *64*, 763.

(67) Haynes, C. A.; Norde, W. *Colloids Surf., B.* **1994**, *2*, 517.

(68) Andrade, J. D.; Hlady, V. L.; Van Wagenen, R. A. *Pure Appl. Chem.* **1984**, *56*, 1345.

(69) Van Wagenen, R. A.; Rockhold, S.; Andrade, J. D. *Adv. Chem. Ser.* **1982**, *199*, 351.

(70) Kowalczyk, D.; Slomkowski, S.; Wang, F. W. *J. Bioact. Compat. Polym.* **1994**, *9*, 282.

(71) Plueddemann, E. P. *Silane Coupling Agents*; Plenum Press: New York, NY, 1982.

(72) Ulman, A. *An Introducation to Ultrathin Organic Films from Langmuir-Blodgett to Self Assembly*; Academic Press, Inc: Boston, Massachusetts, 1991.

(73) Bascom, W. D. *Macromolecules.* **1972**, *5*, 792.

(74) Vandenberg, E. T.; Bertilsson, L.; Liedberg, B.; Uvdal, K.; Erlandsson, R.; Elwing, H.; Lundstroem, I. *J. Colloid Interface Sci.* **1991**, *147*, 103.

(75) Popat, K. C.; Johnson, R. W.; Desai, T. A. *Surf. Coat. Technol.* **2002**, *154*, 253.

(76) Haller, I. *J. Am. Chem. Soc.* **1978**, *100*, 8050.

(77) Joensson, U.; Olofsson, G.; Malmqvist, M.; Roennberg, I. *Thin Solid Films.* **1985**, *124*, 117.

(78) Wong, A. K. Y.; Krull, U. J. *Anal. Bioanal. Chem.* **2005**, *383*, 187.

(79) Gray, D. E.; Case-Green, S. C.; Fell, T. S.; Dobson, P. J.; Southern, E. M. *Langmuir.* **1997**, *13*, 2833.

(80) Mittal, K. L.; O'Kane, D. F. *J. Adhes.* **1976**, *8*, 93.

(81) Zhang, F.; Sautter, K.; Larsen, A. M.; Findley, D. A.; Davis, R. C.; Samha, H.; Linford, M. R. *Langmuir.* **2010**, *26*, 14648.

(82) Goelander, C. G.; Kiss, E. *J. Colloid Interface Sci.* **1988**, *121*, 240.

(83) Beyer, M.; Felgenhauer, T.; Bischoff, F. R.; Breitling, F.; Stadler, V. *Biomaterials.* **2006**, *27*, 3505.

(84) Branch, D. W.; Wheeler, B. C.; Brewer, G. J.; Leckband, D. E. *Biomaterials.* **2001**, *22*, 1035.

(85) Harris, J. M.; Zalipsky, S. *Polyethylene Glycol: Chemistry and Biological Applications*; Plenum Press: New York, 1992.

(86) Piehler, J.; Brecht, A.; Valiokas, R.; Liedberg, B.; Gauglitz, G. *Biosens. Bioelectron.* **2000**, *15*, 473.

(87) Merrill, E. W.; Salzman, E. W. *ASAIO J.* **1983**, *6*, 60.

(88) Mori, Y.; Nagaoka, S.; Takiuchi, H.; Kikuchi, T.; Noguchi, N.; Tanzawa, H.; Noishiki, Y. *Trans Am Soc Artif Intern Organs.* **1982**, *28*, 459.

(89) Lee, J. H.; Kopeckova, P.; Zhang, J.; Kopecek, J.; Andrade, J. D. *Polym. Mater. Sci. Eng.* **1988**, *59*, 234.

(90) Kopeckova, P.; Kopecek, J.; Andrade, J. D. *New Polym. Mater.* **1990**, *1*, 289.

(91) Huang, N.-P.; Voeroes, J.; De Paul, S. M.; Textor, M.; Spencer, N. D. *Langmuir.* **2002**, *18*, 220.

(92) Ruiz-Taylor, L. A.; Martin, T. L.; Zaugg, F. G.; Witte, K.; Indermuhle, P.; Nock, S.; Wagner, P. *Proc. Natl. Acad. Sci. U.S.A.* **2001**, *98*, 852.

(93) Xu, H.; Lu, J. R.; Williams, D. E. *J. Phys. Chem. B.* **2006**, *110*, 1907.

(94) Herron, J. N.; Wang, H.-K.; Janatova, V.; Durtschi, J. D.; Christensen, D. A.; Caldwell, K.; Chang, I. N.; Huang, S.-C. *Surfactant Sci. Ser.* **2003**, *110*, 115.

(95) Swamy, M. J.; Heimburg, T.; Marsh, D. *Biophys. J.* **1996**, *71*, 840.

(96) Donovan, J. W.; Ross, K. D. *Biochemistry.* **1973**, *12*, 512.

(97) Green, N. M. *Methods Enzymol.* **1990**, *184*, 51.

(98) Suter, M.; Butler, J. E.; Peterman, J. H. *Mol. Immunol.* **1989**, *26*, 221.

(99) Suter, M.; Butler, J. E. *Immunol. Lett.* **1986**, *13*, 313.

(100) Rosano, C.; Arosio, P.; Bolognesi, M. *Biomol. Eng.* **1999**, *16*, 5.

(101) Hendrickson, W. A.; Paehler, A.; Smith, J. L.; Satow, Y.; Merritt, E. A.; Phizackerley, R. P. *Proc. Natl. Acad. Sci. U. S. A.* **1989**, *86*, 2190.

(102) Axelrod, D. *J Cell Biol.* **1981**, *89*, 141.

(103) Luo, S.; Walt, D. R. *Anal. Chem.* **1989**, *61*, 1069.

(104) Pollheimer, P.; Taskinen, B.; Scherfler, A.; Gusenkov, S.; Creus, M.; Wiesauer, P.; Zauner, D.; Schoefberger, W.; Schwarzinger, C.; Ebner, A.; Tampe, R.; Stutz, H.; Hytoenen, V. P.; Gruber, H. J. *Bioconjugate Chem.* **2013**, *24*, 1656.

(105) Vermette, P.; Gengenbach, T.; Divisekera, U.; Kambouris, P. A.; Griesser, H. J.; Meagher, L. *J. Colloid Interface Sci.* **2003**, *259*, 13.

CHAPTER 2

IMMOBILIZATION OF POLY(ETHYLENE GLYCOL) ON GLASS TO PREPARE PROTEIN-REPELLENT SURFACES

2.1 Introduction

Poly(ethylene glycol) (PEG) is a synthetic nontoxic water soluble polymer that exhibits excellent resistance to protein adsorption when immobilized at a solid/liquid interface.[1-4] The antifouling properties associated with PEG have made these coatings widely used for a variety of bioanalytical sensor surfaces.[5-7] Interfacial-based assays typically utilize heterogeneous platforms where one of the interacting biomolecules is immobilized to the sensor surface. The binding of a solution-phase biomolecule to a selective capture site results in a measured signal using a variety of optically based techniques, some of which include surface plasmon resonance (SPR), fiber-optic fluorescence, and total internal reflection fluorescence (TIRF).[8,9] The sensitivity and selectivity of such measurements highly depend on the ability of the sensor surface to resist the nonspecific adsorption of biomolecules.[10] As a result, many sensors have utilized PEG functionalization as the basis for low fouling interfacial supports. The ability PEG has to resist the adsorption of biomolecules has been attributed to steric interactions between densely packed PEG polymer chains,[11] high conformational

mobility that defines large exclusion volumes,[12-14] and a large free energy barrier to displacing tightly associated water molecules.[13,15-17] Both the molecular weight and the density of the grafted PEG layer directly influence the nonspecific adsorption properties exhibited by a functionalized surface.[18,19] In addition, the protein-resistant properties exhibited by these surfaces vary greatly depending on the chemistry used to graft monolayers of PEG. By better understanding how the immobilization chemistry used to deposit PEG molecules onto a surface affects the resulting protein resistance properties, sensor platforms with optimal protein-resistant properties can be reproducibly manufactured.

The excellent biocompatibility properties exhibited by poly(ethylene glycol) (PEG) in conjunction with the wide variety of commercially available functional conjugates has stimulated much research into developing methods for the immobilization of PEG chains to surfaces, as a means to reduce the nonspecific adsorption of biomolecules. For passivation of glass substrates, PEG has been deposited through three primary strategies: passive physisorption, electrostatic interactions, and covalent attachment. The simplest, yet least stable method for producing protein resistance coatings, has utilized nonspecific adsorption of PEG polymers onto glass surfaces.[20,21] In such cases, the physisorbed PEG polymers, weakly bound through Van der Walls interactions, readily desorb from the interface when exposed to aqueous solutions, resulting in surfaces that increasingly foul over time.[22,23] As a means to increase the attachment strength and stability of the PEG layer, poly-(L-lysine) modified with PEG (PLL-g-PEG) has been electrostatically deposited onto negatively charged oxide surfaces. Being cationic at neutral pH, the poly-(L-lysine) backbone readily adsorbs to anionic

glass or other oxide surfaces. These electrostatic interactions strongly anchor the PLL-g-PEG copolymers to the anionic oxide interfaces.[24] Although, this method has successfully shown to greatly reduce the nonspecific adsorption of proteins in comparison to untreated oxide surfaces, the electrostatic interactions holding the PLL-g-PEG layer to the surface can easily be disrupted by high ionic strength or high and low pH solutions. Exposure to such conditions can cause the PLL-g-PEG layer to desorb from the oxide surface, leaving the surface vulnerable to protein adsorption.[24-27]

In contrast to physisorption techniques, covalent immobilization of PEG has been shown to provide the most stable means of producing surfaces resistant to the adsorption of proteins. Organo-silanes, which are highly reactive with glass surfaces, have commonly been used to covalently immobilized functionalized-PEG molecules to glass-type surfaces through both direct and indirect methods. PEG monolayers have been directly immobilized to glass surfaces through the self-assembly of alkoxysilylated-PEG molecules.[28] The resulting PEG monolayers were capable of reducing the adsorption of fibrinogen by nearly 20 times compared to that of unmodified glass-type surfaces.[29] Although, these functionalized surfaces are highly stable and resistant to the adsorption of fibrinogen, the commercial sources of alkoxysilylated-PEG are very limited, and its synthesis is time consuming and difficult. With a wide variety of other functionalized-PEG molecules and alkyl-silanes commercially available, there have been many simple, yet indirect alternatives developted to covalently immobilize PEG monolayers onto glass surfaces using an intermediate layer of a functionalized-silane.[30-32]

The degree to which PEG functionalized surfaces are able to resist the nonspecific adsorption of proteins is greatly dependent on the density and homogeneity of the

deposited monolayer. When considering the indirect two-step deposition of monofunctional PEG molecules onto a glass surface, the density of the final grafted PEG monolayer can never be greater than that of the reactive alkyl-silane monolayer. It is vital that the reactive silane foundation exist as a uniform, defect-free monolayer in order to maximize the density and homogeneity of the subsequently deposited functionalized layers. Much work has been conducted to establish reproducible and simple methods to obtain uniform organo-functionalized silane monolayers on glass or other oxide surfaces.[33-35] Previously, glass supports have been modified with organo-functionalized silane monolayers using both solution-phase and gas-phase deposition methods;[34,36-40] however, the formation of uniform functionalized monolayers has proven to be quite challenging.[41,42] Trifunctional alkoxy- or chloro-silanes are advantangous for producing stable monolayers through cross-linking. These trifunctional silanes are susceptible oligomerization in the presence of water, so that solution-phase deposition methods require the use of extremely dry solvents in order to prevent the formation of silane aggregates in solution resulting in defects within the deposited monolayer.[34,43-45] These defects can be the result the accumulation of oligomers, or nonuniform multilayers, co-deposition of aggregated silanes, and hydrolytic stripping of predeposited silanes.[37,44,46,47] Such imperfections present within the functionalized foundation layers can often be propagated through succeeding reaction steps, which result in defect adsorption sites for biomolecules. In contrast, the chemical vapor deposition (CVD) of organo-functionalized silanes has been shown to overcome some of these limitations and reproducibly deposit uniform functional monolayers on silicon dioxide surfaces.[37] Wikstroem et al. reported the deposition of uniform and relatively defect free monolayers

of (3-Glycidyloxypropyl)trimethoxysilane (GOPTS) and (3-aminopropyl)triethoxysilane (APTES) onto porous silica surfaces using CVD methods.[33]

With the wide variety of functionalized PEG conjugates commercially available, both APTES and GOPTS have provided simple and cost effective means of covalently grafting PEG to glass surfaces. N-hydroxysuccinimide (NHS) active esters of PEG are reactive with primary amines at pH ranging from 7 to 9 and have previously been used to immobilize NHS conjugated molecules to APTES-modified surfaces through the formation of a stable amide bond. A major disadvantage to using NHS ester chemistry is that under high pHconditions, the reactive NHS esters readily hydrolyze to nonreactive carboxylic acids.[48] Yasuhiro et al. reported that for a 20 kDa NHS-PEG, the active-ester has a half-life of approximately 2 hours at pH 7.4, yet approximately 10 minutes at pH 9.[49] Given the pKa for an APTES monolayer on glass is approximately 9,[50] balancing the reaction pH to promote the formation of amide bonds with the neutral amine while limiting the hydrolysis of the active ester can be a challenge to overcome.

In contrast to NHS ester chemistry, the epoxide surface functionality resulting from the deposition of GOPTS onto glass can be reacted with a variety of nucleophiles to form covalent linkages.[32] Specifically at pH 10.1, the epoxide-group is highly reactive toward amine-conjugates.[51] Unlike the NHS ester functionality, the epoxide groups are stable at near neutral pH and above; therefore, reaction of amine with epoxide surface groups is not in competition with side reactions such as hydrolysis. As a result, this reaction requires less starting material and maintains activity over longer periods of time. Any reduction in reaction rates at lower amine conjugate concentrations can be compensated with longer incubation times.

In many cases, the covalent immobilization of PEG molecules at glass interfaces results in insufficient packing densities to optimally prevent the adsorption of proteins.[52,53] The low PEG densities in such cases have been attributed to the deactivation of terminal reactive groups through competing side reactions such as the hydrolysis of NHS ester functionality. Also, the steric constraints involved in densely packing large PEG polymers onto a surface can greatly slow reaction rates at high surface coverages.[30] It has been shown that the ability of PEG to resist the adsorption of proteins onto surfaces increases as a function of molecular weight up to 2000 g/mol;[54] however, the repulsive forces resulting from densely packing larger polymers onto a surface also increases proportionally with molecular weight. When higher molecular weight polymers are immobilized at a surface through small terminal reactive groups, there is a critical surface density where the rate of covalent bond formation decreases exponentially with surface coverage as a result of steric repulsive forces.[55] These decreased reaction rates in conjunction with competing side reactions can easily limit the final surface concentration of the grafted PEG layer. It becomes clear how the coupling chemistry used to covalently graft PEG and the size of the polymers being immobilized can greatly influence the resulting protein adsorption properties of the surface.

In this work, the protein adsorption properties of glass surfaces passivated by two common PEG immobilization strategies were characterized and compared using single molecule total internal reflection fluorescence (TIRF) imaging. As illustrated in Figure 2.1, glass surfaces were activated with either APTES or GOPTS monolayers using CVD in order to produce a uniform functionalized monolayer to which monofunctional PEG was further covalently grafted. As described in Figure 2.2, mPEG-NHS was reacted to

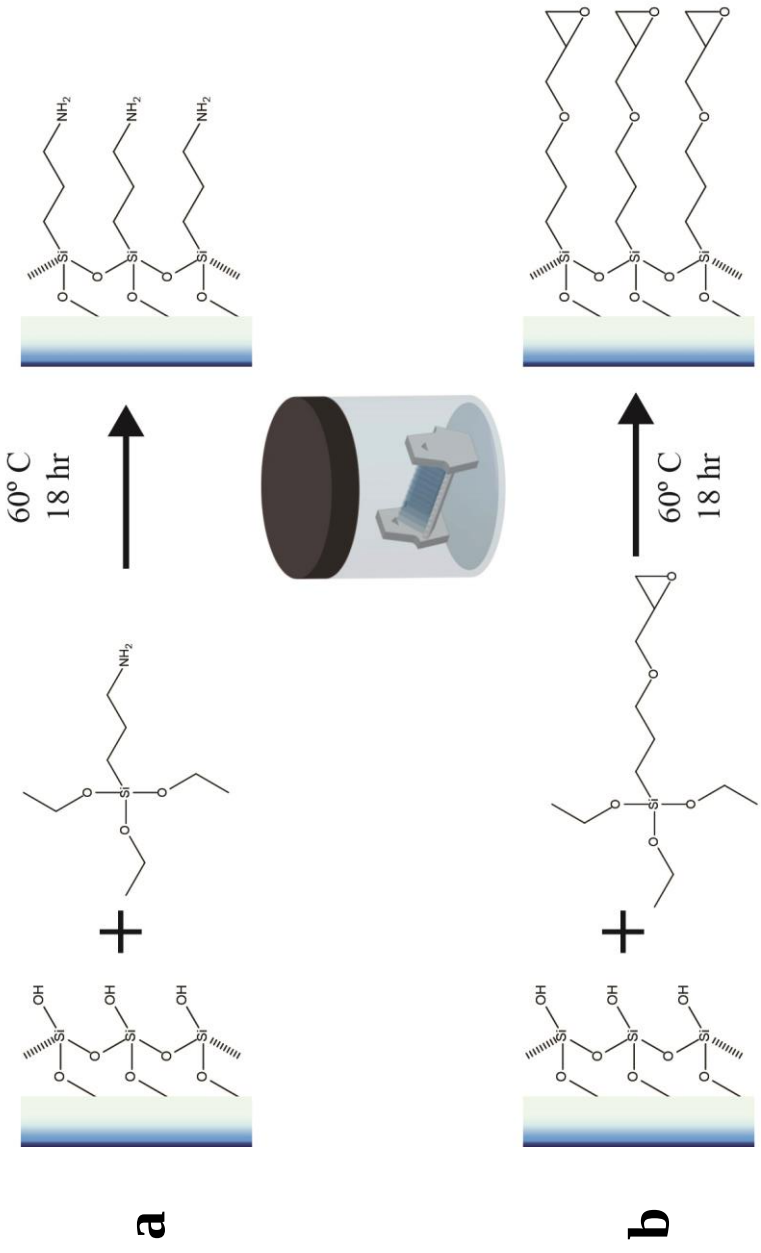

Figure 2.1: Chemical vapor deposition (CVD) of APTES (a) and GOPTS (b) to glass surfaces.

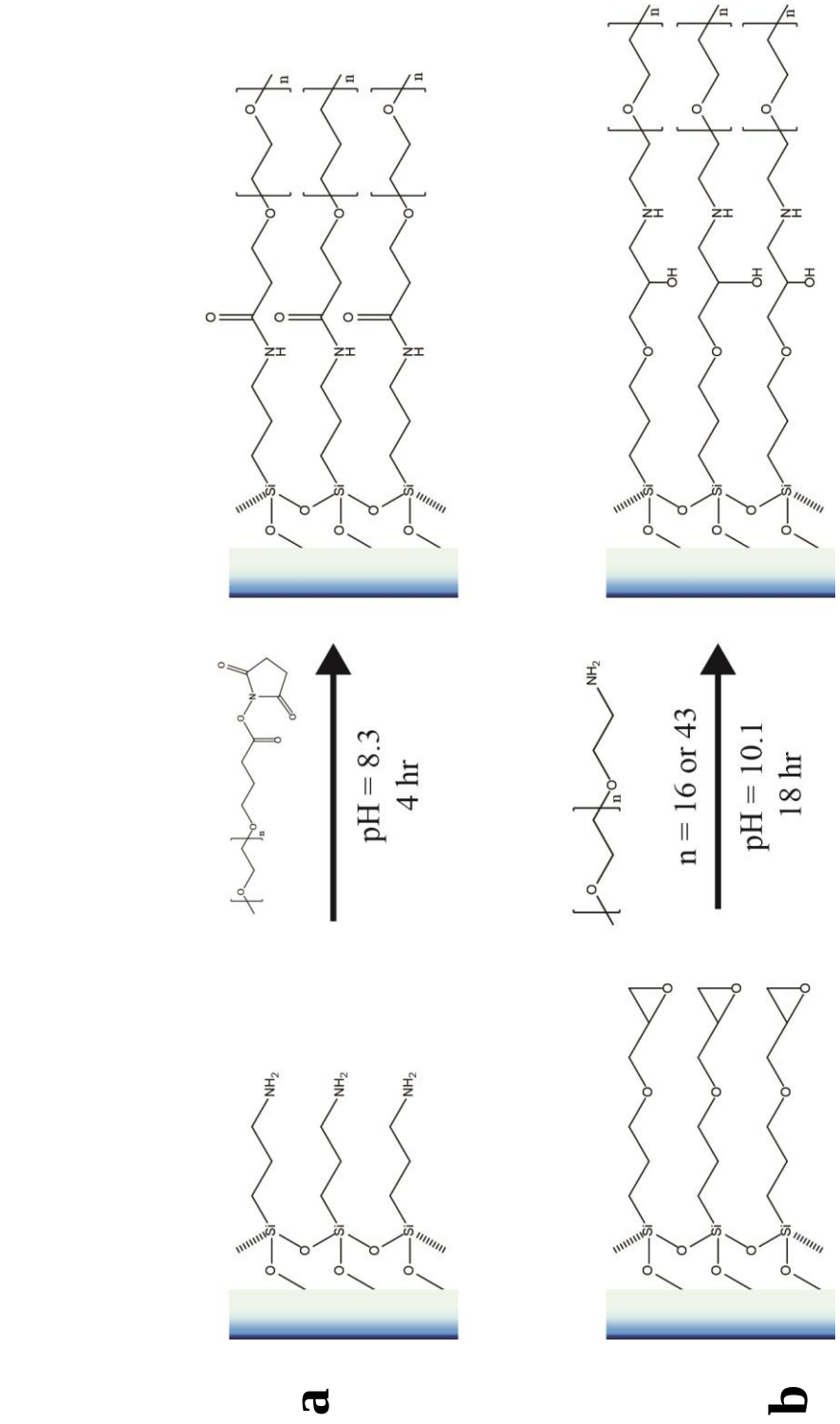

Figure 2.2: Surface reactions used to deposit PEG monolayers. (a) Reaction of NHS-PEG to APTES modified glass surface. (b) Reaction of amine-PEG to GOPTES modified glass surface.

the amine functionality resulting from glass slides modified with APTES, and for the glass slides modified with GOPTS, mPEG-amine was grafted to the surface epoxide functionality. In addition, two different molecular weight (750 g/mol and 2000 g/mol) mPEG-amine molecules were immobilized to GOPTS-modified surfaces and then compared. The adsorption of monoclonal cy3-labeled, mouse derived IgG (MsIgG) to each of the three surfaces was monitored using TIRF imaging. All three methods resulted in excellent resistance to the adsorption of cy3-MsIgG down to small (10^{-6}) fractions of a monolayer; however, significant differences in the adsorption of cy3-MsIgG were observed between each of the grafting methods at the single-molecule resolution limit. From these results, the influence in which the immobilization chemistry and molecular weight of immobilized PEG has on the protein adsorption properties of the surface was revealed.

2.2 Experimental

2.2.1 Reagents and Materials

(3-Glycidyloxypropyl)trimethoxysilane (GOPTS), (3-Aminopropyl)triethoxy-silane (APTES), methoxypoly(ethylene) glycol amine ($mPEG_{16}$-amine) with an average molecular weight (M_n) of 750 g/mol were purchased from Sigma Aldrich (St. Louis, MO). Methoxypoly(ethylene glycol) amine ($mPEG_{43}$-amine) with M_n=2000 g/mol and methoxypoly(ethylene glycol) succinimidyl carboxymethylester ($mPEG_{43}$-NHS) with M_n=2000 g/mol was obtained from JenKem Technology USA (Tianjin, China). Monoclonal mouse derived cy3-labeled antibiotin (MsIgG) was purchased from Jackson Immunoresearch Laboratories Inc (West Grove, PA). All chemicals were used as

received. The degree of cy3- labeling was characterized using a Thermo Scientific (Wilmington, DE) NanoDrop 2000 UV-vis spectrometer at wavelengths 280 and 550nm. Gold Seal microcover glasses (22 X 22mm No. 1.5) were purchased from VWR (West Chester, PA).

2.2.2 Surface Derivatization

The immobilization of PEG monolayers onto glass substrates began with the cleaning of 10 vertically racked glass cover slides by immersion in a freshly prepared mixture of H_2SO_4 and 30% H_2O_2 (2:1 vol). After a 20-minute incubation period, the slides were rinsed 6 times with 18MΩ-cm H_2O. This was immediately followed by treatment in a 75°C base bath composed of H_20, NH_4OH, and 30% H_2O_2 (5:1:1 vol) for 10 minutes. Slides were rinsed 3 times with 18MΩ-cm H_2O and dried under a stream of ultra-high purity nitrogen.

The deposition of APTES and GOPTS was achieved out of the vapor phase. In each case, the slide holder, containing 10 vertically racked clean glass cover slides, was placed in a glass vessel containing 500 μL of the respective alkyl-silane (APTES or GOPTS). The slide holder was an adequate height to suspend the cover slides above the bottom of the container in order to avoid direct contact with the reactive liquid alkyl-silane. The reaction vessel was then sealed and incubated, for 18 hours, in a convection oven previously heated to 60°C. After the reaction period, the rack of slides was removed from the container and further incubated in an empty oven for an additional 5 minutes at 60°C. The slides were removed from the oven and allowed to cool to room temperature before further derivatization.

The grafting of monofunctional PEG molecules, previously described in Figure 2.2, onto both APTES- and GOPTS-activated surfaces was started by separately placing each functionalized slide horizontally in the bottom of a 30 ml beaker. In the case of amine functionalized slides activated with APTES, a freshly prepared solution, containing 5 μM of 2000 g/mol mPEG-NHS in 100 mM pH 8.3 carbonate buffer, was then added in sufficient volume (~2 ml) to cover each individual slide. The beakers were then covered, placed on a titer plate shaker, and allowed to react under slow orbital shear for 4 hours at room temperature. After the reaction period was complete, the slides were then rinsed 3 times in 20-mM phosphate buffered saline (PBS) at pH 7.5, 100 mM ionic strength. The slides were stored in 20-mM PBS for no longer than 1 week prior to their characterization.

The 10 epoxide-functionalized slides activated with GOPTS were split into two groups where 5 slides were then reacted with mPEG-amine of either mean M_n of 750 g/mol or 2000 g/mol. The low molecular weight PEG was grafted to the GOPTS modified surface by freshly preparing a solution containing 1 mM 750 g/mol mPEG-amine in 100 mM pH 10.1 carbonate buffer. Approximately 4 ml of the 750 g/mol mPEG-amine solution was then added to each slide-containing beaker, from the first group of 5 slides, such that each slide was fully submerged in reaction solution. Similarly, the high molecular weight PEG was grafted from a solution containing 1 mM 2000 g/mol mPEG-amine in 100 mM pH 10.1 carbonate buffer. Sufficient volume (~4 ml) of the 2000 g/mol mPEG-amine solution was added to cover each slide. In both cases, the slide-containing beakers were then covered and placed on a titer plate shaker. The slides were allowed to react for 18 hours under slow orbital shear at room

temperature. After the reaction period was complete the mPEG functionalized slides were rinsed 3 times in 20-mM PBS, and then stored in PBS for no longer than 1 week prior to their characterization.

2.2.3 Characterization of Protein Adsorption

The degree of protein adsorption each surface exhibited was characterized by monitoring the accumulation of cy3-labeled monoclonal mouse-derived antibiotin (MsIgG) using single molecule total internal fluorescence (TIRF) imaging. Each respective slide was first assembled into a 4-μL flow cell, loaded onto the microscope, and rinsed under the continuous flow of 20 mM PBS with 0.1% Tween 20. The flow rate for all MsIgG incubation and rinse periods was 30 ml/h. While rinsing, the slides were photobleached for 15 minutes using a 532 nm laser operating at 12 mW of power in order to remove any inherent background fluorescence. Afterwards, 1 nM (150 ng / ml) cy3-MsIgG in of 20 mM PBS with 0.1% Tween 20 was continuously flowed through the sample cell. The accumulation cycle for each sample was allowed to reach saturation (50 to 100 minutes) where the protein surface density did not increase with time. After the accumulation cylce was complete, the sample was then rinsed with 20 mM PBS with 0.1% Tween 20 under continuous flow. Again, the protein surface density was allowed to reach steady state before stopping the rinse cycle (typically ~100 minutes).

2.2.4 Single Molecule Imaging

The single molecule imaging of the cy3-MsIgG was achieved using an Olympus inverted microscope. The frame was modified with an in-house built microscope stage

using a piezoelectric NanoFlex translation stage (ThorLabs), capable of maintaining focus over long observation times (> 5 hours). The cy3-antibody was illuminated using 1 mW, into the objective, of 532 nm laser (B&W TEK inc.) light. The laser beam was focused into a single mode fiber and refocused into the back of an Olympus plan apo 60X, 1.45 NA, oil immersion objective. The incoming laser light was translated off center until total internal reflection excitation was achieved. Emitted fluorescence was collected back through the same objective, passed through a 552 nm BrightLine dichroic beamsplitter (Semrock) and 585/40 nm BrightLine bandpass filter (Semrock), and imaged using an Andor iXon+ CCD camera. In order to ensure photobleaching did not occur over the course of the entire experiment, intermittent imaging was used. Images were obtained every 2 minutes at 150 mseconds integration exposures.

The resulting images were then imported into ImageJ to be analyzed.[56] The average pixel-to-pixel intensity and standard deviation were determined for three modified glass slides after photobleaching, yet prior to the injection of cy-MsIgG. For slides containing adsorbed cy-MsIgG, the identification of single-molecules was set such that a fluorescent spot must have an area >4 pixels^2 and an average intensity greater than a set threshold above background, as discussed below. All identified single molecules were located and counted for each of the prepared surfaces

2.3 Results

2.3.1 Surface Preparation

The ability of a PEG modified surface to resist the nonspecific adsorption of proteins depends critically on the density and uniformity of the grafted monolayer. When

immobilizing functionalized-PEG molecules to glass surfaces through reactive alkyl-silane intermediates, one of the most crucial steps to achieving optimal resistance to protein adsorption is the deposition of a uniform and defect-free functionalized silane foundation layer. In these experiments, silane monolayers were achieved by depositing APTES and GOPTS onto clean glass cover slides by CVD. Heating the reaction vessel to 60°C for 18 hours promotes an increase in alkyl-silane vapor pressure and crosslinking of the deposited silane monolayer to the glass surface. After the reaction period, the slides were further incubated in an empty oven at 60°C for 5 minutes in order to desorb any excess physisorbed silane from the surface, leaving a uniform amine or epoxide-functionalized monolayer. The unmodified glass slides were totally hydrophilic after the cleaning process, reflected by a nonmeasurable water contact angle. After the deposition of APTES and GOPTS, the hydrophobicity of each alkyl-silane modified surfaces increased. A water contact angle of $\Theta=15 \pm 3^{o}$ was observed for the APTES modified surfaces, compared to $\Theta=45 \pm 4^{o}$ for the surfaces modified with GOPTS.

The covalent immobilization of mPEG to glass slides was accomplished using two methods: (i) the reaction of N-hydroxysuccinimide (NHS) active esters of mPEG to the amine functionality of APTES modified glass slides, and (ii) the reaction of monofunctional mPEG-amine reacted to the epoxide functionality of GOPTS derivatized glass slides, both reactions are illustrated in Figure 2.2. The immobilization of mPEG-NHS to APTES derivatized glass slides was achieved by incubating the modified slides in an aqueous solution containing 100 mM mPEG-NHS at pH 8.3 for 4 hours. A major disadvantage of N-hydroxysuccinimide ester chemistry is that the active esters are highly susceptible to hydrolysis in the presence of even trace levels of water.[48] In competition

with the reaction of mPEG-NHS to surface amines, the hydrolysis of NHS decreases the concentration of reactive PEG in solution over time. Furthermore, the rate of hydrolysis for the mPEG-NHS is highly dependent on pH and increases rapidly with increasing pH. At pH 7, a 2000 g/mol mPEG-NHS has been reported to have a half-life of approximately 120 minutes, whereas at pH 9, the half-life is only 9 minutes.[49] By immobilizing the NHS-PEG to APTES modified slides from a solution of pH 8.3, the rate of hydrolysis of the NHS ester was slowed.[48] Because the pKa of the APTES modified surface (~9) was above the pH of reaction solution, the rate of aminolysis was also slowed. In an attempt to increase the formation of the amide bond to the amines on the surface, a large excess (100 mM) of NHS-PEG was used. After the 4-hour reaction was complete, the slides were rinsed 3 times with PBS in order to remove any physisorbed PEG molecules.

The second immobilization strategy utilized the reaction of mPEG-amine to the surface epoxide groups on the glass slides previously modified with GOPTS. Epoxide groups are very reactive with amine-functionalized molecules at pH 10.1, forming a covalent bond as shown in Figure 2.2. Unlike the NHS ester functionality, the epoxide groups are stable at high pH and are not in competition with side reactions such as hydrolysis. Thus, the reaction of mPEG-amine to the surface epoxide groups could be carried out over longer times and at a much lower (100-fold) concentration of the reactive-PEG compared to the N-hydroxysuccinimide ester method. The longer reaction times could help overcome the slowing of reaction rates at high coverages that arise from steric repulsion.[55] As the population of covalently immobilized PEG on the surface grows, it becomes increasingly more difficult for a large polymer to insert in a specific orientation in which the terminal amine can react with an epoxide group. By allowing the

GOPTS slides to incubate in the mPEG-amine solution for 18 hours, the slower reaction rates resulting from repulsive interactions between tightly packed polymer chains might be overcome. Both 750 g/mol and 2000 g/mol mPEG-amine were grafted to GOPTS modified glass slides in order to investigate how the molecular weight of the grafted PEG affects the protein resistant properties exhibited by each modified surface.

2.3.2 Single Molecule Imaging

The resistance to nonspecific adsorption of proteins was evaluated for each of the three methods used to prepare glass slides covalently modified with monofunctionalized PEG molecules by using single-molecule total internal reflection fluorescence (TIRF) imaging. By evaluating the ability of a surface to resist protein adsorption at the single-molecule level, information about the surface defects on the scale of individual molecules level could be revealed. Each PEGylated slide was assembled into a flow cell, loading onto an inverted TIRF microscope, and illuminated with a 532 nm laser. The modified-glass slides were photobleached, under continuous flow of 20-mM PBS, for 15 minutes in order to remove any background fluorescence from surface impurities. After photobleaching the glass surface, 1 nM (150 ng/ml) of cy3-labeled mouse derived monoclonal IgG antibiotin (cy3-MsIgG) was injected at a flow rate of 30 ml/hr. Considering the flow cell, illustrated in Figure 2.3, used in all experiments was 4 μl in volume, the sample cell volume was replenished in its entirety approximately once every 500 ms with fresh cy3-MsIgG solution. As a result, transport limitations of cy3-MsIgG to the surface and loss of cy3-MsIgG from solution due to the adsorption of protein to the sample cell walls and injection port should be negligible. Upon the injection of cy3-

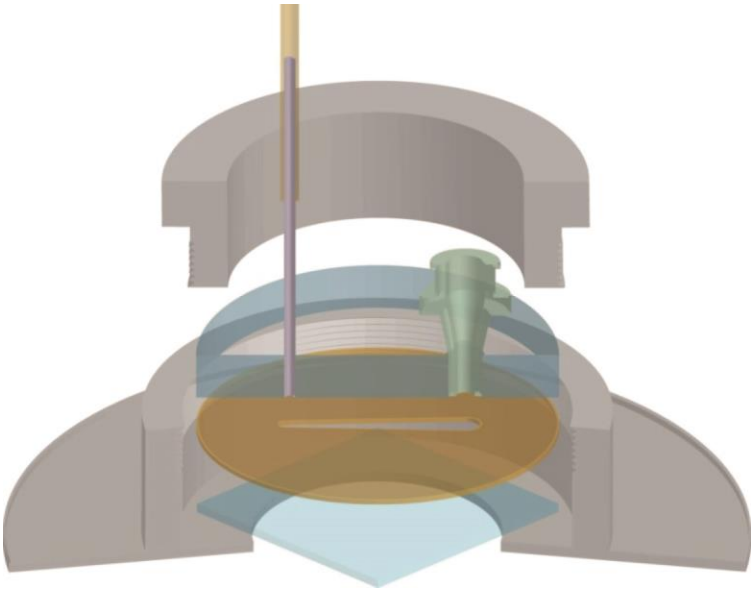

Figure 2.3: A ~4 µl flow cell. Dimensions: 1 cm × 0.26 cm × .015 cm.

MsIgG, accumulation of cy3-MsIgG was monitored until the population of surface associated antibodies remained constant, at which point the sample was washed with PBS with 0.1% Tween 20 until all weakly associated cy3-MsIgG was removed and the population of irreversibly adsorbed cy3-MsIgG remained constant. Images were collected intermittently, once every 2 minutes with a 150 ms exposure time, in order to prevent the photobleaching of strongly adsorbed molecules that persist over the duration of each experiment. If a cy3-MsIgG is adsorbed for the entire 180-minute experiment, the intermittent imaging would result in 13.5 seconds of exposure to 1 mW laser radiation. In a control experiment where immobilized cy3-MsIgG molecules were continuously exposed to 1 mW of laser radiation while images were collected in real-time at 150 ms integration periods, the rate of photobleaching of the cy3-mAb under continuous illumination had a time constant of $\tau_{PB} \approx 190$ seconds, as shown in Figure 2.4. Considering the molecules accumulate slowly over the 180-minute experiment, the typical molecule experiences much less than 13.5 seconds of illumination and the probability of a false-negative occurring from the result of photobleaching is small (<0.07).

The threshold for counting of single molecule cy3-MsIgG, plotted in Figure 2.5, was established by measuring the average background intensity of the photobleached slides prior to introduction to cy3-MsIgG. The average background fluorescence level of the photobleached slides was $\mu_B = 9.8$ photoelectrons, while a variation in pixel-to-pixel background counts had a standard deviation of $\sigma_B = 2.5$ photoelectrons. The threshold for counting single cy3-MsIgG molecules, L_c, was set such that a spot >4 pixels^2 in area have an average pixel intensity 10 times σ_B above $\mu_{B,}$ at 35 photoelectrons; thus, the

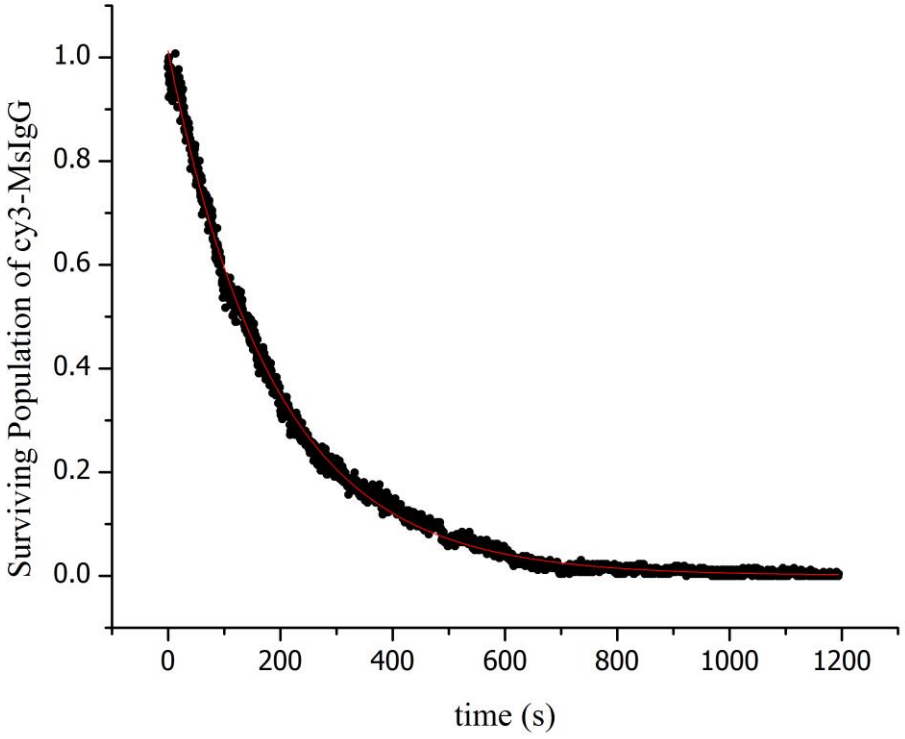

Figure 2.4: Histogram of survival times for the photobleaching of cy3-MsIgG with an average of 4.5 ± 1.2 dyes/protein at 1 mW of 532 nm laser light fit to a single exponential decay: $N = N_o \exp(t/\tau_{PB})$, where τ_{PB} ~190 s.

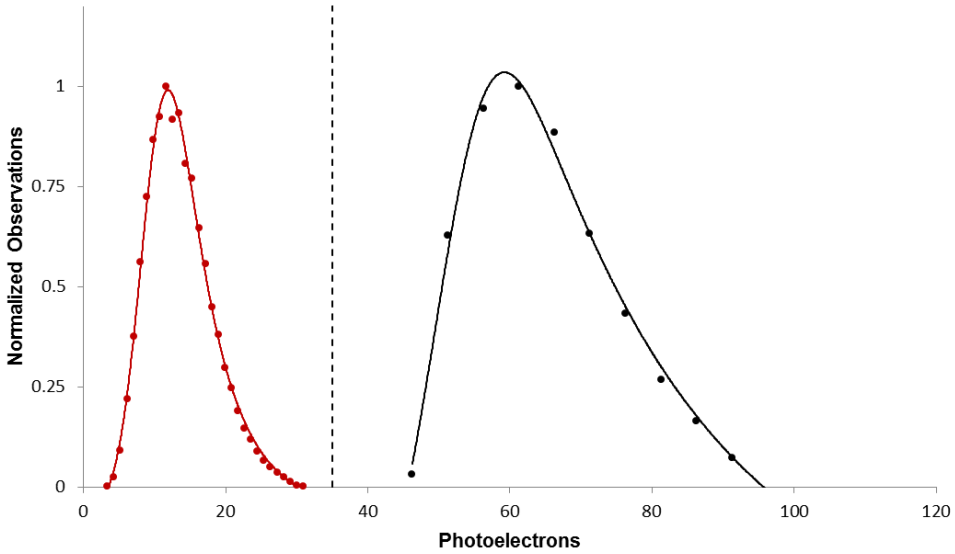

Figure 2.5: Histogram of background intensity fit to an exponentially modified Gaussian distribution (red) and the intensity of individual cy3-MsIgG adsorbed to a PEG modified surface fit to an exponentially modified Gaussian distribution (black). The dashed line sets the threshold for counting single-molecules.

probability of false positives arising from fluctuations in the background was negligible ($>10^{-10}$). The average fluorescence intensity, μ_{Ab}, collected from individual adsorbed cy3-MsIgG was 62 photoelectrons, with a standard deviation in spot-to-spot peak intensities of $\sigma_{MsIgG} = 11$ photoelectrons. The large variation in cy3-mAb intensity likely arises from variations in the number of labels covalently carried by each MsIgG molecule. Based on the relative absorbance at 280 nm and 550 nm,[57] MsIgG was labeled with 4.5 ± 1.2 cy3 molecules.

2.3.3 Protein Adsorption

Cy3-labeled mouse derived monoclonal IgG antibiotin (cy3-MsIgG) was used to assess the amount of protein adsorption exhibited by each of the three methods for PEGylating glass slides. Shown by the time-dependent accumulation experiments in Figure 2.6, the quantity of nonspecific adsorption, resulting from a 1 nM (150 ng/ml) solution of cy3-MsIgG, exhibited by each of the three PEG derivatized glass slides was very low. The amount of fouling ranged from approximately 10^{-5} to 10^{-6} fraction of a 150 kDa IgG monolayer, an estimate which ranges from ~ 0.2 to 0.5 $\mu g/cm^2$ (1.3 to 3.3pmol/cm^2) depending on IgG orientation.[58,59] Because of the sensitive nature of the single molecule fluorescence imaging used in this experiment, the nonspecific adsorption of cy3-MsIgG to untreated glass surfaces was much greater than the upper limit for resolving discrete molecules, which was approximately 32 pg/cm^2 (200 amol/ cm^2) or ~10^{-4} fraction of an IgG monolayer. The degree of fouling is illustrated in Figure 2.7, with images of adsorbed antibody to each of the three PEG modified surfaces and an unmodified bare glass slide.

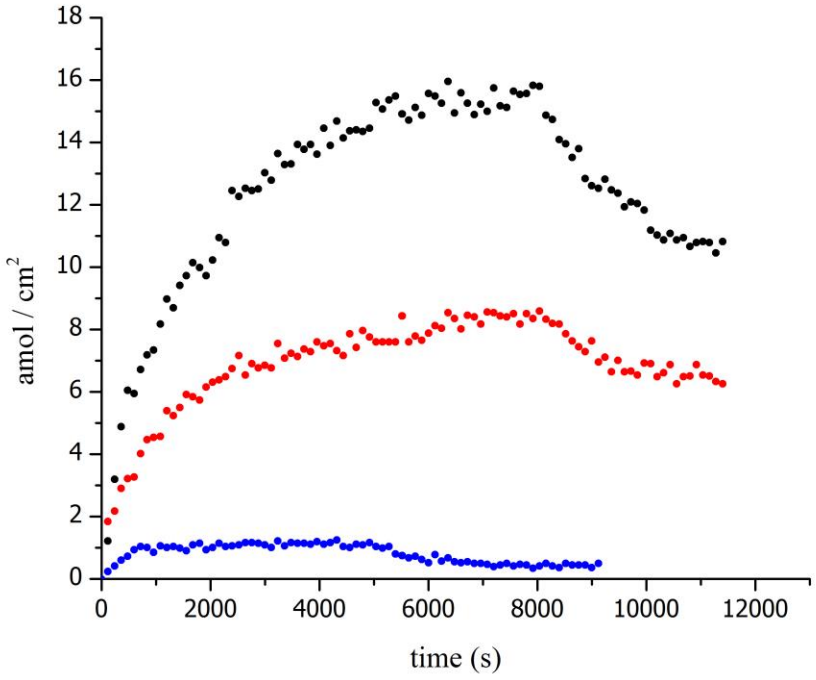

Figure 2.6: Accumulation and desorption of 1 nM cy3-MsIgG to each PEG modified surface: (black) 2000 g/mol NHS-PEG reacted to APTES derivatized glass surface, (red) 750 g/mol amine-PEG reacted to GOPTS modified glass surface, and (blue) 2000 g/mol amine-PEG reacted to GOPTS modified glass surface.

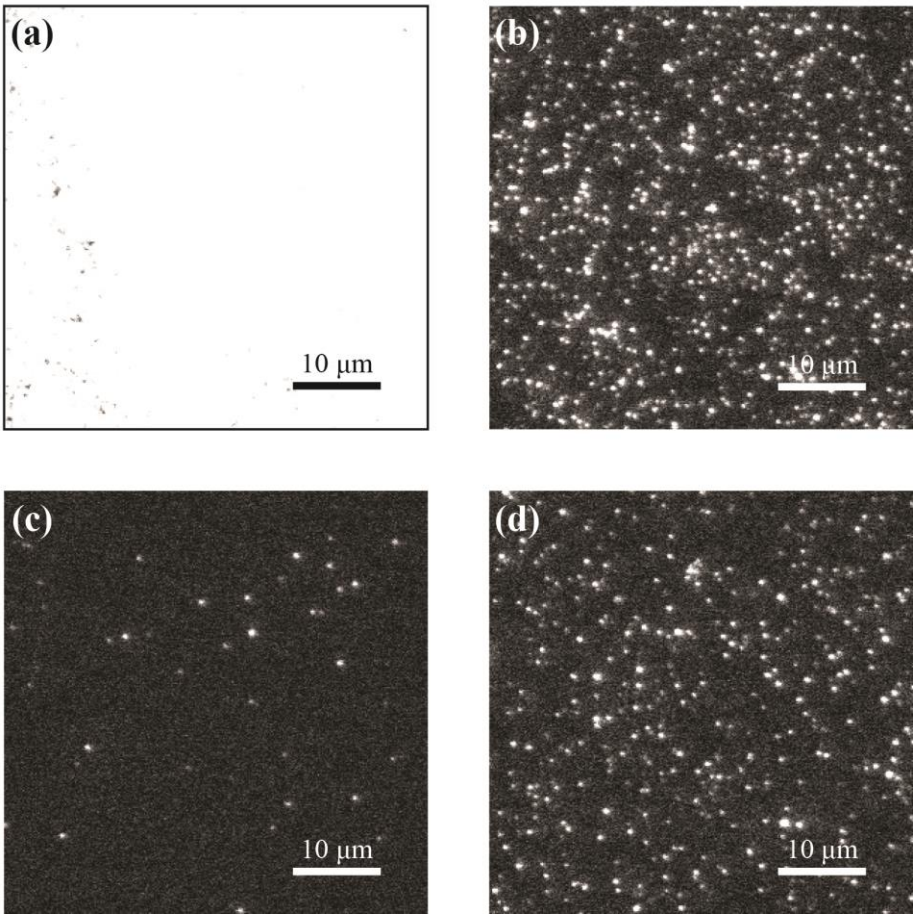

Figure 2.7: Images of individual cy3-MsIgG molecules remaining strongly adsorbed after the accumulation and wash cycle: (a) Bare glass, (b) 2000 g/mol amine-PEG reacted to APTES modified glass, (c) 2000 g/mol amine-PEG reacted to GOPTS modified glass, and (d) 750 g/mol NHS-PEG reacted to GOPTS modified glass.

All of the surfaces prepared in this experiment exhibited excellent resistance to the nonspecific adsorption of cy3-MsIgG in comparison to that of unmodified glass; however, when compared to each other, the various preparation methods resulted in significant differences in the amount of adsorbed cy3-MsIgG at the single molecule level, as tabulated in Table 2.1. These results give insight into surface properties at the molecular level with respect to preparation methods and immobilized polymer size.

The highest level of protein adsorption was exhibited by the surface where 2000 g/mol mPEG-NHS was reacted to the amine-functionality of glass slides modified with APTES. After the incubation with 1 nM cy3-MsIgG and rinse with PBS with 0.1% Tween 20 period, 4.1 ± 0.1 pg/cm^2 (27 ± 1 amol/cm^2) of cy3-MsIgG remained irreversibly adsorbed after rinsing. In direct comparison, the 2000 g/mol mPEG-amine reacted to the epoxide functionality of GOPTS-modified glass slides produced the greatest resistance to the nonspecific adsorption of cy3-MsIgG. The 2000 g/mol mPEG-amine slides resulted in 0.2 ± 0.02 pg / cm^2 (1.2 ± 0.2 amol / cm^2) adsorbed cy3-MsIgG remaining bound after the incubation and rinsing period. Although the APTES modified glass slides were reacted from a solution of mPEG-NHS at a concentration that was 100 times greater than that of the amine-PEG reaction, the epoxy-based PEG-immobilization chemistry produced a 25-fold smaller population of adsorbed cy3-mAb. Considering both surfaces were modified with the same molecular weight PEG, the difference in the nonspecifically adsorbed cy3-mAb population exhibited by the two preparation methods was likely due to differences in PEG surface densities.

The poorer resistance to mAb adsorption displayed by the N- hydroxysuccinimide ester immobilization strategy is consistent with the competitive hydrolysis of the active

Table 2.1: Surface concentration of strongly adsorbed antibody remaining after accumulation of 1 nM cy3-MsIgG and wash.

surface modification	*amol / cm^2*
Bare Glass	>> 200
2000 MW NHS-PEG	27 ± 1
750 MW NH_2-PEG	18 ± 1
2000 MW NH_2-PEG	1.2 ± 0.1

ester groups, leading to a lower density of covalently grafted PEG. As the reaction progressed over time, the concentration of active NHS-PEG in solution decreased due to hydrolysis. Eventually this grafting reaction prematurely stopped once the N-hydroxysuccinimide ester completely hydrolyzed. Simultaneously, as the density of covalently immobilized PEG increased on the surface, the rate of aminolysis at the surface slowed with time due to steric crowding.[60] Together these processes limit the surface density of the grafted PEG monolayer. The single molecule images collected from the NHS-PEG surfaces shows that the cy3-MsIgG typically nonspecifically adsorbed to the surfaces as discrete single-molecule events (see Figure 2.8). A smaller fraction of sites (~10%) appear to be clusters of adsorbed proteins, whose area exceeds the upper confidence bound of the point-spread function of the microscope (>36 pixels^2). The results suggest that the vast majority of the surface is PEG functionalized; however, there are isolated molecular scale defects and a smaller population of slightly larger defects, where PEG chains are missing and cy3-MsIgG adsorbs as single-molecules or clusters, respectively.

The surfaces prepared from the reaction of PEG-amine to epoxide-modified glass also resulted in discrete molecule adsorption sites; however, these surfaces exhibited 25 times smaller defect densities compared to the NHS chemistry. Unlike N-hydroxysuccinimide esters, the reactive epoxide groups of GOPTS modified slides do not undergo hydrolysis at alkaline pH. The higher stability of the reactive epoxide groups allows for longer reaction times, which helps overcome the slowed reaction rates caused by the steric crowding effect. By incubating the epoxide slides in a 1 mM amine-PEG solution for 18 hours, the hindered defect sites had more time to fill, and the increased

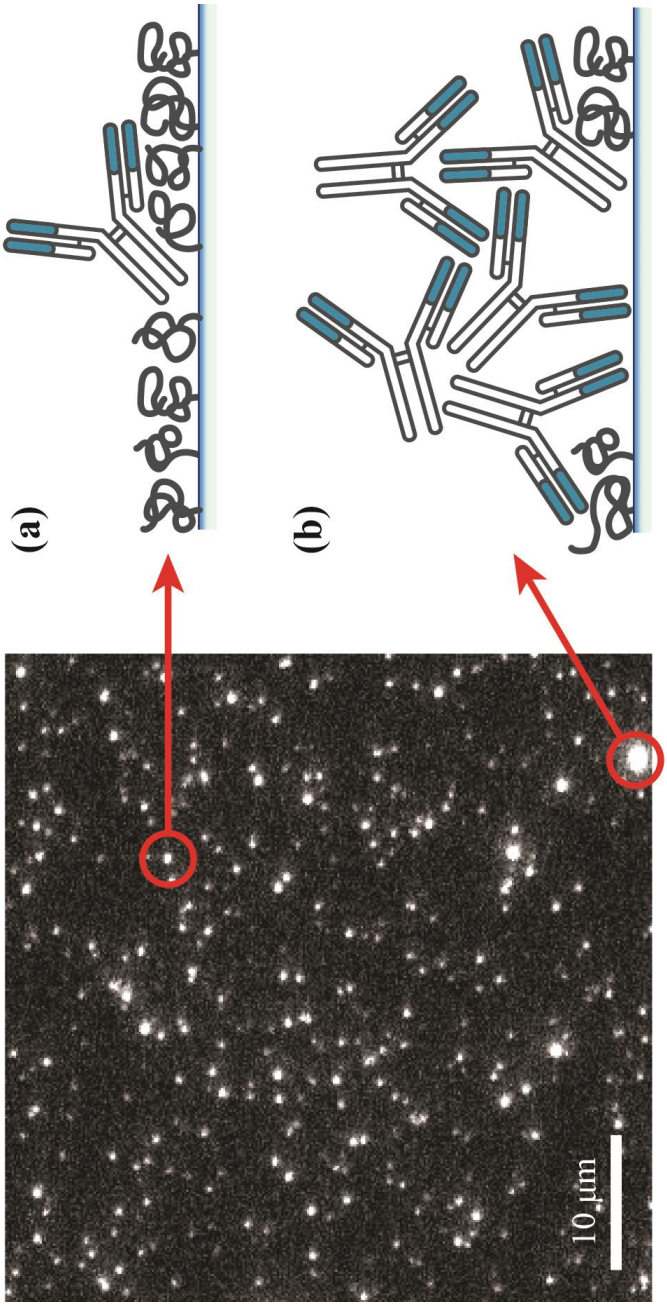

Figure 2.8: The ~15 amol/ cm^2 cy3-MsIgG remaining strongly adsorbed to 2000 g/moll NHS-PEG reacted to APTES modified glass. (a) Discrete defect sites, $\leq$ 36 pixels^2, account for > 90% of all adsorption events. (b) Large defect sites, >36 pixels^2, are composed of aggregated antibodies.

adsorption of cy3-MsIgG suggests that the epoxide-based chemistry was capable of producing a higher density of covalently grafted 2000 g/mol PEG onto the functionalized glass slides. This also suggests that given enough time and the proper chemistry, most of the defects sites within the grafted PEG monolayers could be functionalized with PEG molecules.

When considering the ability for epoxy-based chemistry to overcome the slow reaction rates of hindered sites, it is important to understand how the molecular weight of the grafted PEG affects protein adsorption properties of the PEG modified surface. In comparison to the 2000 g/mol mPEG-amine, the smaller, 750 g/mol, mPEG-amine resulted in 3.0 ± 0.1 pg/cm^2 (18 ± 1 amol/cm^2) of irreversibly adsorbed cy3-MsIgG, compared with the larger (2000 g/mol) amine-PEG, which exhibited 15-times fewer defects for adsorption of cy3-MsIgG. Although it is likely that the surface concentration of covalently immobilized PEG is higher in the case of the smaller (750 g/mol) mPEG-amine, the larger molecular weight PEG was superior at resisting the adsorption of cy3-MsIgG. In contrast, the 750 g/mol mPEG-amine resulted in approximately 1.6 times less adsorbed cy3-MsIgG compared to the 2000 g/mol mPEG-NHS surfaces, which is likely the result of a higher surface concentration and fewer defects in the case of the 750 g/mol mPEG-amine. These findings suggest that there are two issues that control optimal resistance to protein adsorption. First, a stable PEG reagent and intermediate functionalized layer are needed to provide ample time for surface defects in the immobilized PEG layer to fill in. This is illustrated by the 750 g/mol PEG-amine being able to achieve a grafted PEG layer with fewer defects than the 2000 g/mol PEG-NHS. Secondly, the larger exclusion volumes and conformational entropy of longer polymer

chains greatly improves the resistance to protein adsorption, as shown by the 2000 g/mol PEG-amine being much more resistant to the adsorption of cy-MsIgG compared to the 750 g/mol PEG amine. As a result, a PEG modified surface with optimal resistance to nonspecific protein adsorption should be composed of a uniform and dense monolayer of higher molecular weight grafted PEG chains. In order to produce such a surface, the proper grafting chemistry must be chosen in order to allow adequate time from the covalently deposited monolayer to achieve a maximum defect-free density.

2.4 Discussion

The goal of this research was to better understand how the chemistry used to immobilize monofunctional PEG molecules to glass surfaces affects the ability of a modified surface to resist the nonspecific adsorption of proteins. Comparing the reaction of N-hydroxysuccinimide active esters of PEG to APTES-modified glass slides and amine conjugated PEG to GOPTS-functionalized glass slides, we demonstrated that the resistance of the resulting surface to the nonspecific adsorption of proteins is influenced by chemistry used to prepare the PEG monolayer. Both methods produced surfaces with excellent resistance to the adsorption of cy3-MsIgG in comparison to unmodified glass surfaces, where the amount of fouling ranged from 10^{-5} to 10^{-6} of a full monolayer of IgG. At the single molecule level, it was revealed that there were significant differences in the degree of nonspecific protein adsorption exhibited by each prepared surface. The epoxide-based chemistry produced surfaces that were up to 25-times more resistant to the nonspecific adsorption of cy3-mAb in comparison to N-hydroxysuccinimide ester chemistry, thus demonstrating the importance that the immobilization chemistry plays in

the surfaces final properties. Considering the increased resistance observed with the epoxide-based chemistry, two different molecular weight (750 g/mol and 2000 g/mol) PEG-amine molecules were grafted to the GOPTS modified surfaces and compared. Although the 2000 g/mol PEG-amine was ~15-times more resistant to the adsorption of cy-MsIgG, the 750 g/mol PEG-amine was 1.6-times more resistant to adsorption compared to the 2000 g/mol PEG-NHS modified surface. From these results it is apparent that both the immobilization chemistry and molecular weight of the grafted polymer influence the nonspecific adsorption properties exhibited by the modified surface. Because of the stability of epoxide functional groups, the reaction PEG-amine to GOPTS modified glass slides achieved a relatively defect-free surface composed of high molecular weight PEG. With the large variety of heterofunctional amine-PEG molecules commercially available, epoxide-based chemistry provides a simple and cost effective means of producing sensor capture surfaces that are resistant to the nonspecific adsorption of proteins.

2.5 References

(1) Gombotz, W. R.; Wang, G.; Horbett, T. A.; Hoffman, A. S. *J. Biomed. Mater. Res.* **1991**, *25*, 1547.

(2) Leckband, D.; Sheth, S.; Halperin, A. *J. Biomater. Sci., Polym. Ed.* **1999**, *10*, 1125.

(3) Sofia, S. J.; Premnath, V.; Merrill, E. W. *Macromolecules.* **1998**, *31*, 5059.

(4) Emoto, K.; Van Alstine, J. M.; Harris, J. M. *Langmuir.* **1998**, *14*, 2722.

(5) Huang, N.-P.; Voeroes, J.; De Paul, S. M.; Textor, M.; Spencer, N. D. *Langmuir.* **2002**, *18*, 220.

(6) Ruiz-Taylor, L. A.; Martin, T. L.; Zaugg, F. G.; Witte, K.; Indermuhle, P.; Nock, S.; Wagner, P. *Proc. Natl. Acad. Sci. U. S. A.* **2001**, *98*, 852.

(7) Houseman, B. T.; Mrksich, M. *Chem. Biol.* **2002**, *9*, 443.

(8) Bally, M.; Halter, M.; Voros, J.; Grandin, H. M. *Surf. Interface Anal.* **2006**, *38*, 1442.

(9) Rabbany, S. Y.; Donner, B. L.; Ligler, F. S. *Crit Rev Biomed Eng.* **1994**, *22*, 307.

(10) Butler, J. E. *Methods.* **2000**, *22*, 4.

(11) Jeon, S. I.; Lee, J. H.; Andrade, J. D.; De Gennes, P. G. *J. Colloid Interface Sci.* **1991**, *142*, 149.

(12) Mori, Y.; Nagaoka, S.; Takiuchi, H.; Kikuchi, T.; Noguchi, N.; Tanzawa, H.; Noishiki, Y. *Trans Am Soc Artif Intern Organs.* **1982**, *28*, 459.

(13) Merrill, E. W.; Salzman, E. W. *ASAIO J.* **1983**, *6*, 60.

(14) Harris, J. M; Zalipsky, S. *Polyethylene Glycol: Chemistry and Biological Applications*; Plenum Press: New York, 1992.

(15) Chen, S.; Yu, F.; Yu, Q.; He, Y.; Jiang, S. *Langmuir.* **2006**, *22*, 8186.

(16) Holmberg, K.; Bergstroem, K.; Stark, M. B. *Immobilzation of Proteins via PEG Chains*; Plenum Press: New York, New York, 1992, p 303.

(17) Harris, J. M.; Yoshinaga, K. *J. Bioact. Compat. Polym.* **1989**, *4*, 281.

(18) Kopeckova, P.; Kopecek, J.; Andrade, J. D. *New Polym. Mater.* **1990**, *1*, 289.

(19) Lee, J. H.; Kopeckova, P.; Zhang, J.; Kopecek, J.; Andrade, J. D. *Polym. Mater. Sci. Eng.* **1988**, *59*, 234.

(20) Wasiewski, W.; Fasco, M. J.; Martin, B. M.; Detwiler, T. C.; Fenton, J. W., II *Thromb. Res.* **1976**, *8*, 881.

(21) Cheng, Y. L.; Darst, S. A.; Robertson, C. R. *J. Colloid Interface Sci.* **1987**, *118*, 212.

(22) Malmsten, M.; Van Alstine, J. M. *J. Colloid Interface Sci.* **1996**, *177*, 502.

(23) G.J. Fleer, M. A. C. S., J.M.H.M. Scheutjens, B. Vincent. *Polymers at Interfaces*; Chapman & Hall: New York, NY, 1993.

(24) Kenausis, G. L.; Voeroes, J.; Elbert, D. L.; Huang, N.; Hofer, R.; Ruiz-Taylor, L.; Textor, M.; Hubbell, J. A.; Spencer, N. D. *J. Phys. Chem. B* **2000**, *104*, 3298.

(25) Saxer, S.; Portmann, C.; Tosatti, S.; Gademann, K.; Zurcher, S.; Textor, M. *Macromolecules.* **2010**, *43*, 1050.

(26) Frey, B. L.; Corn, R. M. *Anal. Chem.* **1996**, *68*, 3187.

(27) Jordon, C. E.; Frey, B. L.; Kornguth, S.; Corn, R. M. *Langmuir.* **1994**, *10*, 3642.

(28) Lee, S.-W.; Laibinis, P. E. *Biomaterials.* **1998**, *19*, 1669.

(29) Jo, S.; Park, K. *Biomaterials.* **2000**, *21*, 605.

(30) Goelander, C. G.; Kiss, E. *J. Colloid Interface Sci.* **1988**, *121*, 240.

(31) Harris, J. M.; Struck, E. C.; Case, M. G.; Paley, M. S.; Yalpani, M.; Van Alstine, J. M.; Brooks, D. E. *J. Polym. Sci., Polym. Chem. Ed.* **1984**, *22*, 341.

(32) Piehler, J.; Brecht, A.; Valiokas, R.; Liedberg, B.; Gauglitz, G. *Biosens. Bioelectron.* **2000**, *15*, 473.

(33) Wikstroem, P.; Mandenius, C. F.; Larsson, P.-O. *J. Chromatogr.* **1988**, *455*, 105.

(34) Vandenberg, E. T.; Bertilsson, L.; Liedberg, B.; Uvdal, K.; Erlandsson, R.; Elwing, H.; Lundstroem, I. *J. Colloid Interface Sci.* **1991**, *147*, 103.

(35) Vallant, T.; Brunner, H.; Mayer, U.; Hoffmann, H.; Leitner, T.; Resch, R.; Friedbacher, G. *J. Phys. Chem. B.* **1998**, *102*, 7190.

(36) Mittal, K. L.; O'Kane, D. F. *J. Adhes.* **1976**, *8*, 93.

(37) Joensson, U.; Olofsson, G.; Malmqvist, M.; Roennberg, I. *Thin Solid Films.* **1985**, *124*, 117.

(38) Weetall, H. H. *Appl. Biochem. Biotechnol.* **1993**, *41*, 157.

(39) Plueddemann, E. P. *Silane Coupling Agents*; Plenum Press: New York, NY, 1982.

(40) Ulman, A. *An Introducation to Ultrathin Organic Films From Langmuir-Blodgett to Self Assembly*; Academic Press, Inc: Boston, Massachusetts, 1991.

(41) Parikh, A. N.; Allara, D. L.; Azouz, I. B.; Rondelez, F. *J. Phys. Chem.* **1994**, *98*, 7577.

(42) Brzoska, J. B.; Azouz, I. B.; Rondelez, F. *Langmuir.* **1994**, *10*, 4367.

(43) Bascom, W. D. *Macromolecules.* **1972**, *5*, 792.

(44) Haller, I. *J. Am. Chem. Soc.* **1978**, *100*, 8050.

(45) Popat, K. C.; Johnson, R. W.; Desai, T. A. *Surf. Coat. Technol.* **2002**, *154*, 253.

(46) Wong, A. K. Y.; Krull, U. J. *Anal. Bioanal. Chem.* **2005**, *383*, 187.

(47) Gray, D. E.; Case-Green, S. C.; Fell, T. S.; Dobson, P. J.; Southern, E. M. *Langmuir.* **1997**, *13*, 2833.

(48) Lim, C. Y.; Owens, N. A.; Wampler, R. D.; Ying, Y.; Granger, J. H.; Porter, M. D.; Takahashi, M.; Shimazu, K. *Langmuir.* **2014**, *30*, 12868.

(49) Nojima, Y.; Iguchi, K.; Suzuki, Y.; Sato, A. *Biol. Pharm. Bull.* **2009**, *32*, 523.

(50) Van der Maaden, K.; Sliedregt, K.; Kros, A.; Jiskoot, W.; Bouwstra, J. *Langmuir.* **2012**, *28*, 3403.

(51) Hermanson, G. T. *Bioconjugation Techniques*; 2 ed.; Academic Press: Amsterdam, 2008.

(52) Piehler, J.; Brecht, A.; Geckeler, K. E.; Gauglitz, G. *Biosens. Bioelectron.* **1996**, *11*, 579.

(53) Goelander, C. G.; Herron, J. N.; Lim, K.; Claesson, P.; Stenius, P.; Andrade, J. D. *Properties of Immobilized PEG Films and the Interaction with Proteins: Experiments and Modeling*; Plenum Press: New York, New York, 1992, p 221.

(54) Benhabbour, S. R.; Sheardown, H.; Adronov, A. *Macromolecules.* **2008**, *41*, 4817.

(55) O'Shaughnessy, B.; Sawhney, U. *Phys. Rev. Lett.* **1996**, *76*, 3444.

(56) Schneider, C. A.; Rasband, W. S.; Eliceiri, K. W. *Nat. Methods.* **2012**, *9*, 671.

(57) Hahn, C. D.; Riener, C. K.; Gruber, H. J. *Single Molecules.* **2001**, *2*, 149.

(58) Buijs, J.; Lichtenbelt, J. W. T.; Norde, W.; Lyklema, J. *Colloids Surf., B.* **1995**, *5*, 11.

(59) Caruso, F.; Furlong, D. N.; Ariga, K.; Ichinose, I.; Kunitake, T. *Langmuir.* **1998**, *14*, 4559.

(60) Trmcic, M.; Hodgson, D. R. W. *Beilstein J Org Chem.* **2010**, *6*, 732.

CHAPTER 3

CONTROLLING PROTEIN BINDING SITE DENSITIES ON PEG-MODIFIED GLASS SURFACE

3.1 Introduction

Controlling the density of covalently immobilized biomolecules at interfaces, while simultaneously preventing the nonspecific adsorption of proteins, has increasingly become an important task to overcome in the field of biosensors. Interfacial bioassays, including clinical diagnostics,[1] analytical measurements,[2] and assays of protein therapeutics,[3] utilize heterogeneous capture assays, where one of the interacting molecules is immobilized at a sensor surface. The selective binding of solution-phase analytes to surface-immobilized capture sites directly results in a measured signal from optical based microarray techniques such as surface plasmon resonance (SPR), fiber-optic fluorescence, and total internal reflection fluorescence (TIRF).[4,5] The ability of a sensor to optimally function requires the measurement interface to be resistant to nonspecific adsorption of biomolecules; yet simultaneously, the immobilized capture proteins must maintain native structure and preserve biological recognition. Furthermore, the capture-site density on a sensor surface directly affects the measured signal response, sensitivity, kinetics, and capture activity of the sensor.[6-9] Thus, the ability for bio-affinity

sensors to operate quantitatively and efficiently necessitates the reproducible manipulation and optimization of surface properties, including the minimization of nonspecific interactions and control over binding-site density.

Because proteins are composed of a variety of functional domains, they are highly surface active and readily adsorb to interfaces through hydrophobic, electrostatic, and hydrogen-bonding interactions.[10] In many cases, the interactions between immobilized (covalently bound or passively adsorbed) proteins and their solid supports result in conformational changes within their secondary and tertiary structures. In turn, this leads to the denaturation and deactivation of the immobilized receptor protein.[11] A surface must not only be resistant to the nonspecific adsorption of target proteins from solution, it must also provide an inert layer that preserves the native bioactivity and structure of the immobilized biomolecules. The surface density of immobilized capture proteins can also affect the bioactivity of a sensor. At high capture-site densities, closely packed biomolecules can cause the active domains of the receptor molecule to be inaccessible to solution phase analytes. This effectively deactivates a significant population of immobilized capture proteins and decreases the sensitivity and efficacy of the sensor.[7] It becomes clear that the functionalization chemistry used to prepare a capture surface is a complicated issue to address. The surface functionality for an optimal sensor platform requires a rigorous set criteria to be fulfilled: (i) the surface must be resistant to the nonspecific adsorption of proteins, (ii) the modified surface must not inhibit the activity of subsequently immobilized capture proteins, (iii) the chemistry used to functionalize the surface must allow for the control of the surface concentration of conjugation sites over a wide range, (iv) and the conjugation site linking chemistry must provide a highly

selective and easy means to immobilize capture biomolecules.

Attempts to control the density of covalently immobilized biomolecules to glass and other oxide surfaces for sensor applications have been undertaken through variety of strategies. Most commonly, the covalent immobilization of biomolecules on glass-type surfaces has been accomplished through deposited organic-silane monolayers. Composed of a high density of reactive functionalities, such as aldehydes,[12] epoxides,[13,14] and carbonyls,[15] these active monolayers target and react with accessible ε-amines of lysine within a protein to form covalent linkages with the surface. A major disadvantage to such methods is that both the immobilization orientation and density of biomolecules is uncontrollable and random. In addition, the reactive functionalities of organo-silane coatings commonly have poor resistance to nonspecific adsorption of proteins and require the addition of blocking agents such as bovine serum albumin (BSA), gelatin, or casein, all of which may further affect accessibility and conformation of the immobilized capture proteins.[16,17]

An alternate approach has employed grafted polyethylene glycol (PEG) monolayers on glass-type surfaces as a means to better fulfill the requirements for optimal sensor surfaces. PEG coatings have previously been shown to resist the nonspecific adsorption of proteins,[18-20] while simultaneously providing an inert foundation to tether biomolecules.[21-23] The protein repellent properties exhibited by PEG monolayers have been attributed to steric interactions between tightly packed PEG chains,[24] high conformational entropies of PEG molecules that define large exclusion volumes,[18,20] and high energy penalties associated with expelling tightly associated water molecules in order to allow protein adsorption.[22,25] The repulsive forces preventing

adsorption from occurring also help stabilize the secondary and tertiary structures of proteins near the PEG interface. As a result, proteins immobilized to PEG surfaces have shown to maintain a higher degree of bioactivity compared to that of other surface functionalities.[18] The indifferent nature of the PEG layer allows the covalently tethered capture biomolecule to exist in a more solution-like state above the surface. As a result, this provides the immobilized protein with an environment that may help preserve native properties.

The tethering of protein capture-sites to PEG monolayers has been accomplished through both covalent and affinity-based immobilization strategies. Hetero- and homo-bifunctionalized PEG polymers have been used to covalently link biomolecules onto glass surfaces activated with organo-silanes.[26] Diamino- (DAPEG) and dicarboxy- (DCPEG) functionalized PEG polymers have been grafted to (Glycidyloxypropyl)trimethoxysilane (GOPTS) functionalized glass slides as a means to form functionalized PEG layers that are resistant to the adsorption of proteins. Activated terminal amines or carbonyls of the PEG layer are then reacted to random nucleophilic groups in the protein to be immobilized.[27] In many cases, these activation steps result in poor reaction yields and little to no control over the orientation of the immobilized biomolecules. As a result, these methods fail to provide a selective means to immobilize capture proteins at a controlled site density and orientation.

Attempts to gain control over the density of immobilized capture sites within PEG layers have utilized mixed-functionality PEG coatings. Poly(L-lysine)-grafted-poly(ethylene glycol) (PLL-g-PEG) is known to spontaneously adsorb to glass and other negatively charged oxide surfaces at neutral pH, producing PEG coatings that are

resistant to the nonspecific adsorption of biomolecules.[28,29] By adjusting the ratio of a biotin-terminated PEG to mPEG molecules grafted onto the poly(L-lysine) (PLL) backbone, it was shown that the density of subsequent captured streptavidin molecules was controllable.[30,31] Although this method simultaneously fulfills the criteria required for optimal sensor functionality, a major limitation of the PLL-g-PEG method is that the electrostatic interactions binding PLL-g-PEG to glass surfaces can be disrupted with high ionic strength and high or low pH solutions, which can lead to desorption of the PLL-g-PEG layer.[29,32-34]

Despite this disadvantage, the mixed biotin-PEG/mPEG layer was successful at controlling conjugation site densities. Since it was first introduced by Suter et. al,[35] the biotin-(strept)avidin interaction has been extensively used as highly selective means to indirectly immobilize biomolecules onto interfaces through a streptavidin intermediate,[36] while varying the surface density of (strept)avidin molecules.[30] With the large variety of commercially available biotinylated and biotin conjugation products, the biotin-(stept)avidin complex provides a flexible means to selectively immobilize biomolecules to an interface. The biotin-(strept)avidin complex is one of the strongest noncovalent interactions in nature ($K_d = 10^{-14}$M) and is stable over a wide variety of pH values and temperatures.[37-39] (Strept)avidin is a homotetramer with four biotin-binding sites that allow for multiple biotin containing molecules to simultaneously bind to a single (strept)avidin tetramer.[40] As a result, (strept)avidin is an advantageous intermediate building block to immobilizing biotin conjugated biomolecules to interfaces.

In this work, a simple means to covalently immobilize heterogeneously functionalized PEG monolayers was investigated in order to prepare a surface resistant to

the nonspecific adsorption of proteins, inert to interfacially immobilized biomolecule, and with control over bioconjugation site density. As illustrated in Figure 3.1, glass surfaces were modified with a uniform GOPTS monolayer using chemical vapor deposition (CVD) methods. Utilizing the high reactivity of nucleophiles towards epoxide-functionalized surfaces,[27] amine functionalized poly(ethyleneglycol) (PEG-amine) molecules were grafted onto GOPTS modified glass surfaces at high pH. Discrete conjugation sites were created by diluting 2,300 g/mol biotin-PEG-amine at varied concentrations into 750 g/mol mPEG-amine to react with the GOPTS-activated surfaces. The density of surface biotins was characterized by monitoring the fluorescence of a cy3-conjugated streptavidin (cy3-streptavidn) binding to the surface-immobilized capture-sites using total internal reflection fluorescence (TIRF) imaging. The composition of this capture surface resists the nonspecific adsorption of proteins and provides control over capture-site densities down to very low fractions (10^{-6}) of a (strept)avidin monolayer.

3.2 Experimental

3.2.1 Reagents and Materials

(3-Glycidyloxypropyl)trimethoxysilane (GOPTS), methoxypoly(ethylene glycol) amine ($mPEG_{16}$-amine) with an average molecular weight (M_n) of 750 g/mol, and biotin poly(ethylene glycol) amine (biotin-PEG_{48}-amine) with M_n of 2300 g/mol were purchased from Sigma Aldrich (St. Louis, MO). Cy3-conjugated streptavidin was obtained from Jackson Immunoresearch Laboratories Inc. (West Grove, PA). The degree of cy3 labeling was characterized using a Thermo Scientific (Wilmington, DE) NanoDrop 2000 UV-vis spectrometer at wavelengths 280 and 550nm. All chemicals

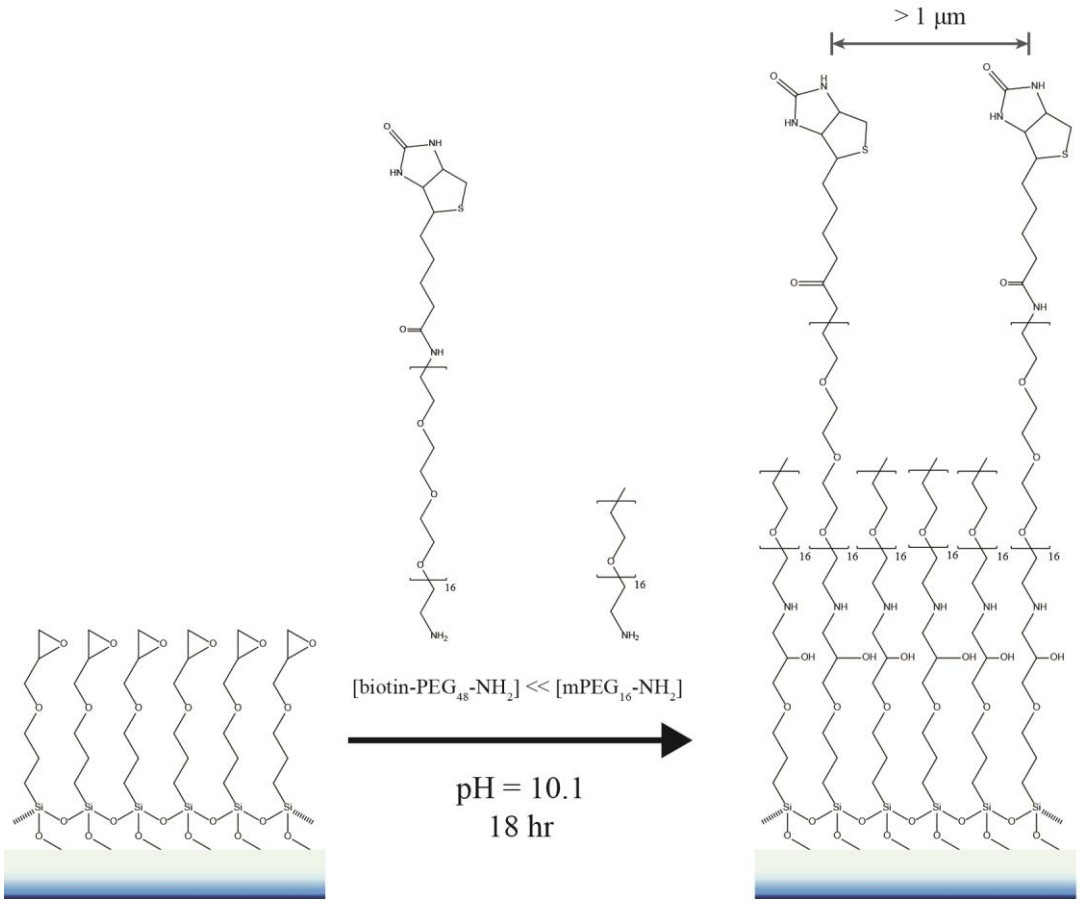

Figure 3.1: Reaction of a mixture of biotin-PEG-amine and mPEG-amine to GOPTS modified glass surface as a means to control the density of biotin conjugation sites.

were used as received. Gold Seal microcover glasses (22 X 22mm No. 1.5) were purchased from VWR (West Chester, PA).

3.2.2 Surface Derivatization

The grafting of PEG to glass substrates began with the cleaning of glass cover slides by immersion in a freshly prepared solution containing H_2SO_4 and 30% H_2O_2 (2:1 vol) for 20 minutes. This cleaning step was followed by 6 rinses in 18MΩ-cm H_2O. Residual surface siloxanes were then converted to silanols by treating the clean glass cover slides in a 75°C base bath composed of H_2O, NH_4OH, and 30% H_2O_2 (5:1:1 vol) for 10 minutes. After treatment with base, slides were rinsed 3 times with 18MΩ-cm H_2O and dried under a stream of ultra-high purity nitrogen.

The formation of an epoxide monolayer on glass cover slides was achieved through the deposition of GOPTS from the vapor phase.[41] A slide holder, containing 10 vertically racked clean glass cover slides, was placed in a glass vessel containing 500 μL of GOPTS. The slide holder was tall enough to completely suspend the cover slides above the bottom of the container in order to avoid direct contact with the reactive liquid GOPTS. The reaction vessel was then sealed and then placed in a convection oven, previously heated to 60°C, for 18 hours. After the silanization reaction was complete, the rack of slides was removed from the container and then further incubated for an additional 5 minutes at 60°C in an empty oven to evaporate physisorbed GOPTS. The slides were then removed from the oven and allowed to cool to room temperature before further derivatization.

In order to regulate the surface site density of biotin, a mixture of biotin-PEG_{48}-

amine and $mPEG_{16}$-amine was simultaneously reacted with the epoxide-functionalized slides. Five solutions consisting of (0.0, 0.42, 0.83, 1.3 and 1.7 μM) biotin-PEG_{48}-amine and 1 mM $mPEG_{16}$-amine in pH 10.1, 100-mM carbonate buffer were prepared. Individually, the epoxide functionalized slides were then placed horizontally in the bottom of separate 30 ml beakers and covered with 4 ml of the desired reagent solution. To ensure each slide was fully submerged, additional reactive solution was added to adequately cover each slide as required. The beakers were covered, placed on a titer plate shaker, and allowed to react for 18 hours under slow shear mixing. After the reaction period was complete, the slides were then rinsed 3 times in 18MΩ-cm H_2O and 3 times in 20 mM phosphate buffered saline (PBS) at pH 7.5, 100 mM ionic strength. Slides were stored in 20 mM PBS for no longer than 1 week prior to characterization.

3.2.3 Surface Site Density Characterization

Having a strong affinity for biotin ($K_d \sim 10^{-14}$ M),[40] fluorescently-labeled streptavidin was used to characterize the surface site density of biotin for the four dilutions of binding sites in the grafted PEG monolayers. Each slide at the respective dilution was assembled into a flow cell and loaded onto an inverted TIRF microscope. Each slide was first exposed to flowing (30 ml/hr) 20 mM PBS (pH 7.5, 100 mM ionic strength) with 0.1% Tween 20 and illuminated with 12 mW of 532-nm laser radiation, measured at the back of the objective, for ~15 minutes in order to photobleach any background fluorescence. All subsequent accumulation and rinse cycles were carried out at a flow rate of 30 ml/hr. A solution of 200-pM (30-ng/ml) cy3-streptavidin was then injected onto the sample and incubated for 100 minutes under continuous flow. After the

accumulation was complete, the slides were rinsed with 20 mM PBS with 0.1% Tween 20 under continuous flow for an additional 100 minutes. By monitoring the number of fluorescent molecules on the surface, it was determined that the accumulation time was adequate for the saturation of biotin with streptavidin, and the rinse time allowed desorption of weakly associated streptavidin to leave the surface.

3.2.4 Single Molecule Imaging

The single molecule imaging of cy3-streptavidin was achieved using an Olympus IX71 inverted microscope incorporating an in-house built microscope stage outfitted with piezoelectric NanoFlex translation stage (ThorLabs), capable of maintaining focus over long durations of time (> 5 hours). The samples were excited using a 532 nm laser (B&W TEK Inc.) operating at 1 mW of power into the objective. Using a single mode fiber launch, the laser light was focused into the back of an Olympus plan apo 60X, 1.45 NA, oil immersion objective. Total internal reflection was achieved by translating the incoming light off center into the objective. The emitted fluorescence was then collected back through the same objective, passed through a 552 nm BrightLine dichroic beamsplitter (Semrock) and a 585/40 nm BrightLine bandpass filter (Semrock), and then imaged using an Andor iXon+ CCD camera. TIRF images were acquired using Andor IQ software at 200 ms integration times. Image processing to count individual cy3-labeled streptavidin was achieved using the same procedures outlined in the previous chapter.

3.3 Results

3.3.1 Formation of PEG Surfaces

By diluting biotin-PEG-amine into a 750 g/mol mPEG-amine monolayer, a surface that is resistant to the nonspecific adsorption of protein is generated, while providing control over the bioconjugation site density. The grafting of PEG monolayers was accomplished through the nucleophilic substitution of PEG-amine to the epoxide functionality of a GOPTS-modified glass slide. Due to the relatively high stability of epoxides in aqueous solutions at neutral pH or above and their high reactivity with primary amines at high pH conditions,[27,42] epoxy-based chemistry provides a simple means to control conjugation site density during the formation of mixed PEG monolayers. The production of highly uniform epoxy functionalized monolayers was accomplished through the deposition of GOPTS out of the vapor phase.[41,42] Heating this reaction to 60°C for 18 hours promoted a high GOPTS vapor pressure allowing the deposition of alkyl silane to occur.

The immobilization scheme depicted in Figure 3.2 illustrates the chemistry used to form a mixed functional PEG ($mPEG_{16}$ and biotin-PEG_{48}) monolayer through the reaction between amine terminated PEG polymers and epoxide-functionalized glass surfaces. The zero binding site $mPEG_{16}$-amine grafted glass surfaces had sufficient resistance to the nonspecific adsorption of streptavidin, and resulted in a nonspecifically adsorbed population of streptavidin at 10^{-9} fraction of a monolayer (~6.7 pmol/cm^2)[30] from a 200 pM (30-ng/ml) solution, shown in Figure 3.2.

By using a longer chain tether length (biotin-PEG_{48}-amine), the biotin conjugation sites were more likely to be accessible to target molecules in solution and not sterically

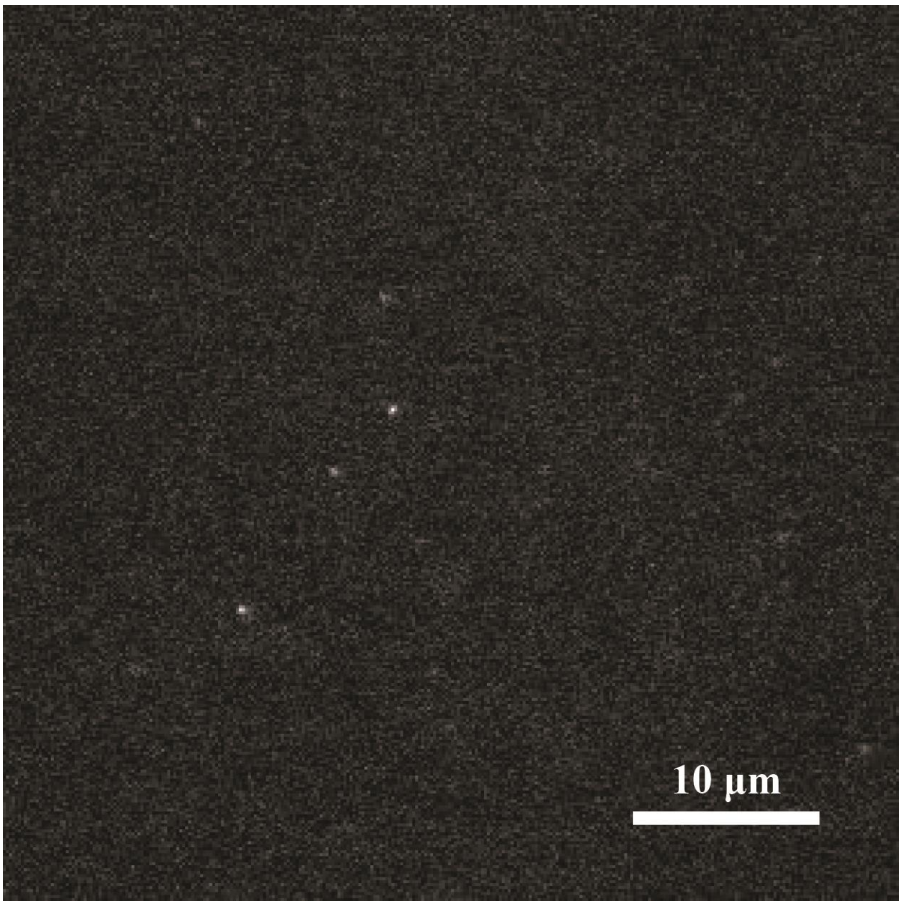

Figure 3.2: Nonspecific polulation of streptavidin remaining strongly adsorbed to 750 g/mol PEG surface containing no biotin-conjugation sites after exposure to 200 pM cy3-streptavidin and wash.

hindered or engulfed by the surrounding polymer chains. By grafting a mixed monolayer from a solution containing a dilute concentration of biotin-PEG_{48}-amine (0.42-1.7 μM) and a much higher $mPEG_{16}$-amine concentration (1 mM), a surface resistant to the nonspecific adsorption of biomolecules, yet containing a low density of biotin sites, was produced. Achieving a conjugation site density near 10^{-6} of a fraction of a streptavidin monolayer allows the conjugation sites to be separated by micron distances, and the bound (strept)avidin intermediates can easily be resolved within the diffraction limits of optical microscopy. By adjusting the ratio of biotin-PEG_{48}-amine and $mPEG_{16}$-amine contained within the reaction solution, the surface concentration of biotin conjugation sites was controlled, allowing for the optimization of a sensor response to suit the requirements of a given technique.

3.3.2 (Strept)avidin Labeling of Biotin Conjugation Sites

The tethering of biotin-labeled biomolecules to surfaces through (strept)avidin intermediates has commonly been employed as a means to immobilized antibodies, enzymes, and cells to interfaces.[35,43,44] In order to measure the interactions between individual biomolecules at a single-molecule level, it is important to control biotin surface sites down to very small fractions (10^{-6}) of a (strept)avidin monolayer. In this study, the biotin site density within the grafted diluent PEG monolayer was characterized using single-molecule imaging of cy3-streptavidin. Its relatively low nonspecific adsorption properties, likely due to its near-neutral isoelectric point, and high affinity for biotin-conjugates makes streptavidin an ideal intermediate to immobilize capture proteins to sensor platforms.[40] To assay the streptavidin capture, the biotinylated cover slides

were loaded into a flow cell, illuminated with 532 nm laser radiation, and allowed to photobleach for 15 minutes. The slides were then exposed to 2×10^{-10} M cy3-labeled streptavidin. A concentration of streptavidin >20,000-times greater than the K_d was used in order to ensure the complete saturation of available biotin binding sites.

Assessing the time required for cy3-streptavidin to completely saturate the biotin surface sites was achieved by collecting an image once every 10 minutes by exposing the sample to 200 ms of laser light. By intermittently imaging over the duration of the entire experiment, the photobleaching of the fluorescent cy3 dye conjugated to streptavidin was minimized, where the total exposure time over the entire course of the experiment was 3.6 seconds, which is <2% of the photobleaching time observed under continuous illuminations (see previous chapter). Monitoring of the accumulation and rinsing of cy3-streptavidin, as shown in Figure 3.3, revealed that 1 hour was sufficient time to reach equilibrium; however, flow of cy3-streptavidin was maintained for an additional 1 hour to allow all biotin-streptavidin complexes to assemble. The desorption of weakly associated streptavidin molecules from the surface by rinsing for 2 hours produced a constant surface site density of strongly bound streptavidin. Even after 60 hours under continuous flow of rinse buffer in the absence of laser excitation, the capture slide showed < 20% decrease in the immobilized streptavidin surface population. At micron distances between surface biotin sites, the strongly-bound complex formed by the streptavidin-biotin interaction is not the result of bivalent interactions or rebinding to nearby biotin sites.[45] As a result, the interfacial complex formed by a single streptavidin and a single biotin appears to be irreversible on the time scale of ≥24 hours,[46] which exemplifies it usefulness as an intermediate immobilization strategy for detection of

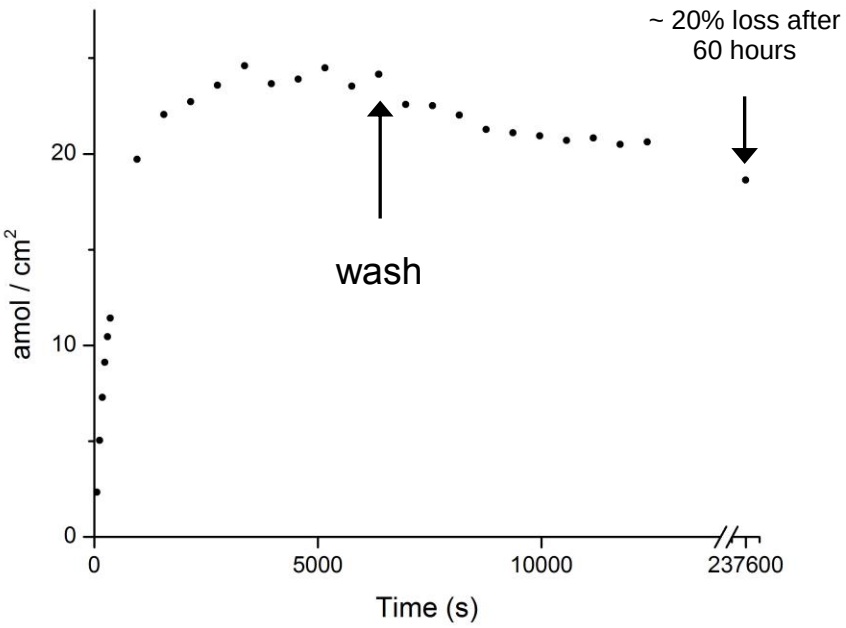

Figure 3.3: Accumulation of 200 pM cy3-streptavidin and wash from 750 g/mol PEG surface containing a low density of 2000 g/mol biotin-PEG conjugation sites.

subsequently investigated protein-protein interactions on sensor platforms.

After establishing the required accumulation/rinse times, the biotin surface site density was characterized, on separate slides, by 2 hours of exposure to 2×10^{-10} M cy3-labeled streptavidin, followed by 2 hours of rinsing with buffer. Each accumulation/rinse cycle was conducted in the absence of light as a means to avoid any photobleaching of the cy3- labels covalently attached to each streptavidin molecule. At the end of the cycle, the slides were immediately imaged using TIRF microscopy. The fluorescence from interfacially bound cy3-streptavidin had an average intensity $\mu_S = 52$ photoeletron counts, with a spot-to-spot variation in peak intensities having a standard deviation $\sigma_S = 11$ photoelectons. The large variation in streptavidin-to-streptavdin intensity most likely arises from differences in the number of cy3-labels carried by each individual streptavidin molecule, where the average streptavidin was labeled with 3.7 ± 1.9 cy3 molecules. The threshold for counting single-molecule surface sites was determined from the background intensity and noise level of the biotinlylated slides after photobleaching, but prior to exposure with cy3-labeled streptavidin. The average background level was measured to be $\mu_B = 10$ photoelectrons counts, with a variation in pixel-to-pixel background counts having a standard deviation of $\sigma_B = 2$ photoelectrons. The threshold for counting cy3-labeled molecules, shown in Figure 3.4, was set such that a spot >4 pixels^2 in area have an average pixel intensity 10 times σ_B above μ_B at 30 photoelectrons, meaning the probability of false positives arising from fluctuations in the background was negligible.

Quantifying the biotin site density was accomplished by counting the number of fluorescent spots, above the threshold previously set, contained within a 2×10^{-8} m^2

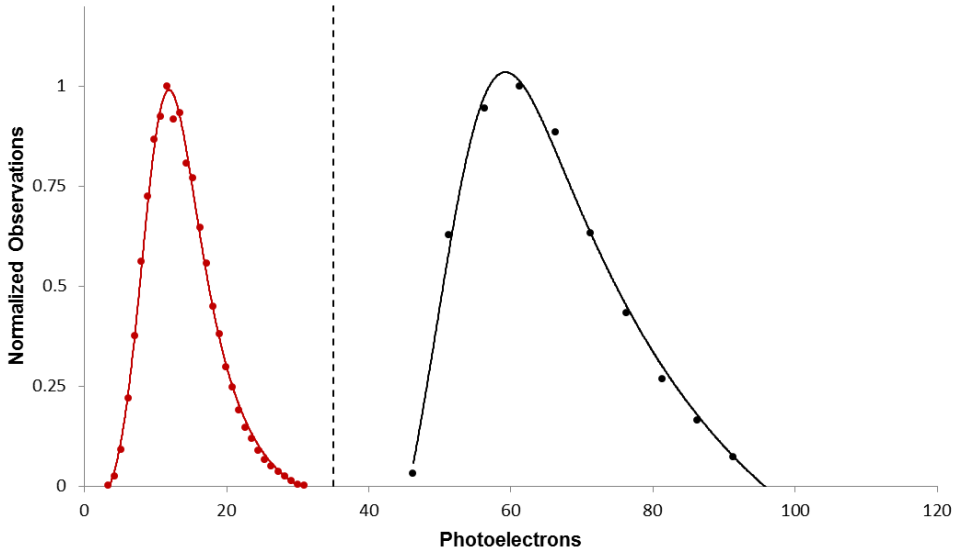

Figure 3.4: Histogram of background pixel intensities fit to an exponentially modified Gaussian distribution (red) and the intensity of individual cy3-MsIgG spots, adsorbed to a PEG modified surface, fit to an exponentially modified Gaussian (black) distribution. The dashed line sets the threshold for counting single molecules.

field of view, as illustrated by Figure 3.5. Images from each of the four biotin-PEG-amine dilutions including a "blank" surface containing no biotin-PEG revealed a monotonic increase in streptavidin surface concentration, as demonstrated by the images in Figure 3.6 and the tabulated data in Table 3.1. The relationship between the biotin-PEG dilution ratio and the streptavidin binding site density was linear and was evaluated using a linear least-squares fit. As plotted in Figure 3.7, the slope was determined to be 0.79 ± 0.04 nmols/m^2, for a single lot of slides, with a 0.29 ± 0.02 amols/m^2 intercept that corresponds to the zero-binding site, blank slide. While the site density varies linearly with the biotin-PEG concentration within a given lot, there is up to a ~30% variation in slope between separately prepared lots of slides.

In order to test whether the incorporation of biotin-PEG into the monolayer is stoichiometric, the surface density of the 750 g/mol PEG diluent can be estimated from its radius of gyration, which has been measured to be ~0.9 nm.[47] If the surface immobilized 750 g/mol PEG adopts a spherical conformation equivalent to its radius of gyration in solution, then the grafted surface concentration for a monolayer of PEG would be ~4.7 nmols/ cm^2. The density of the biotin-PEG, extrapolated from the results in Figure 3.7 to 100% biotin-PEG in the reaction solution, is 0.79 ± 0.04 amol/cm^2. This is ~600-times lower than the expected surface concentration predicted by the stoichiometric ratio of the biotin-PEG in a monolayer of the 750 g/mol mPEG diluent.

The lower than expected value observed for density of biotin conjugation sites in the PEG monolayer may arise from several possible origins. One likely cause would be the difference in reaction rates of the two PEG molecules. The surface grafting of linear polymers through a single, terminal reactive group is an intrinsically slow process.[48]

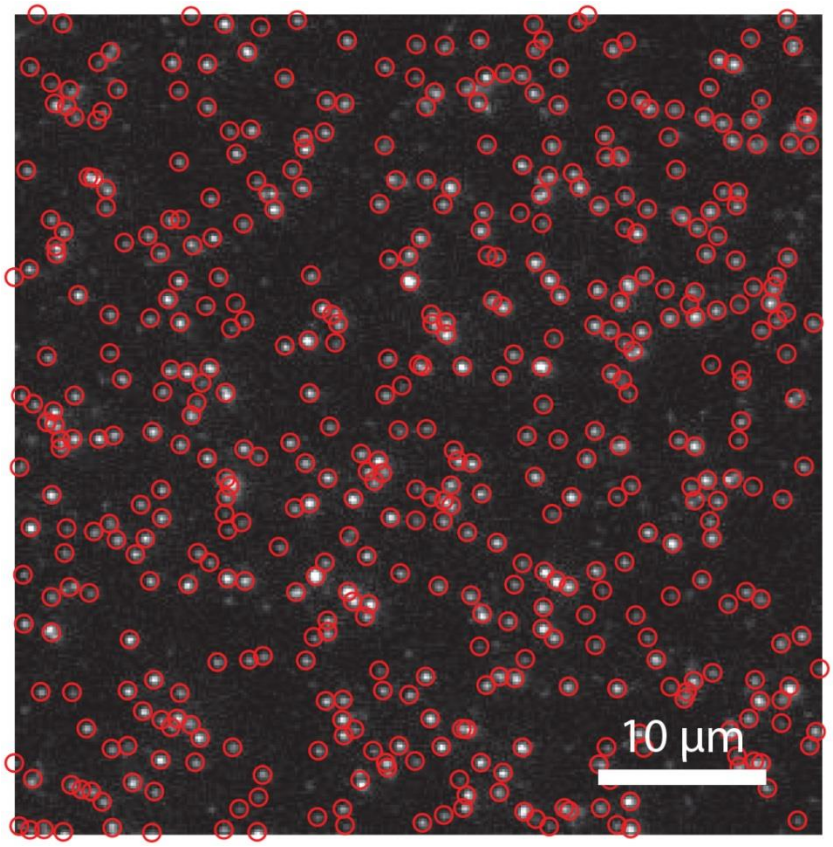

Figure 3.5: Located single cy3-streptavidin molecules captured by biotin conjugation sites.

Table 3.1: Surface concentration of cy3-streptavidin captured by biotin conjugation sites for each dilution.
See corresponding images in Figure 3.6.

	biotin-PEG_{48}:$mPEG_{16}$	*amol/cm^2*
a	"blank"	0.29 ± 0.02
b	0.4×10^{-3}	35 ± 3
c	0.8×10^{-3}	62 ± 2
d	1.3×10^{-3}	95 ± 2
e	1.7×10^{-3}	140 ± 10

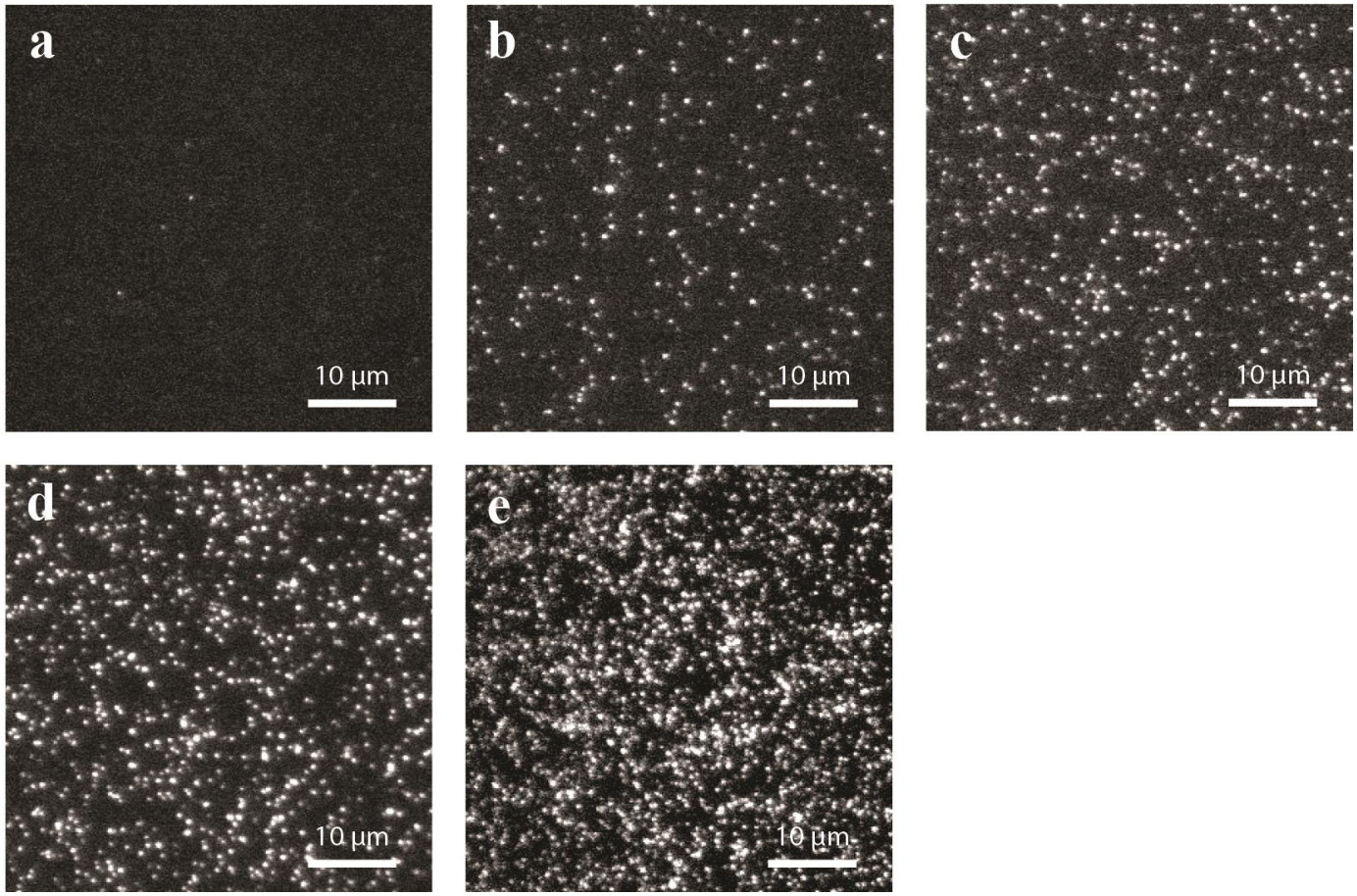

Figure 3.6: Images of individual cy3-streptavidin molecules in the blank (a) and captured by biotin conjugation sites (b-e). The dilution ratio and concentration of bound streptavidin for each image is listed in Table 3.1.

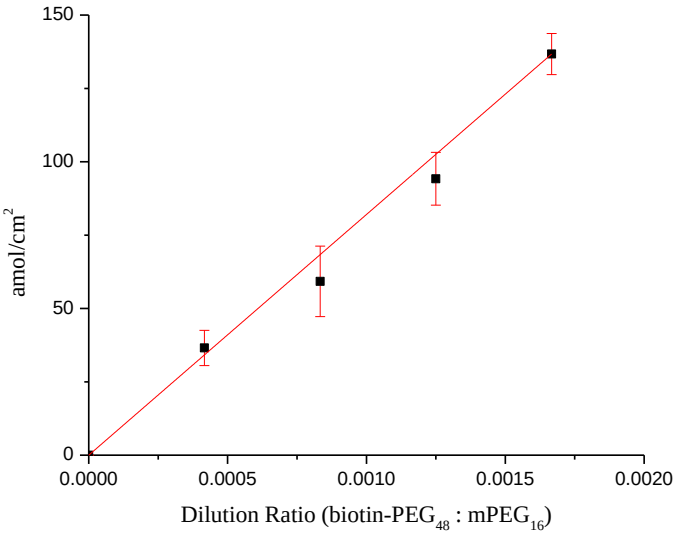

Figure 3.7: Biotin-PEG conjugation site density as a function of the dilution ratio of biotin-PEG_{48}-amine and $mPEG_{16}$-amine. The slope of the fitted line: 0.79 ± 0.04 amol/cm^2.

Access to the surface by a terminal reactive group is inhibited by collisions with the surrounding polymer structure on the surface. This steric reaction rate inhibition is more significant with higher molecular weight polymers, where the probability of a reactive collision decreases with increasing interference by the surrounding polymer.[49] This trend would predict that the reactive amine groups of the 2300 g/mol biotin-PEG-amine would experience a much smaller fraction of collisions, leading to reactions with surface epoxide groups, than the 750 g/mol diluent PEG-amine. Furthermore, the larger molecular weight polymer would exhibit slower diffusion in solution and collide with the surface less frequently. Finally, surface binding of the larger, biotin-carrying PEG would be further inhibited as the coverage of the 750 g/mol diluent PEG increases and fills in the surface,[50] where the remaining small residual areas might only be accessible to the small M_n PEG.

In addition to the effect of the slower reaction rate of the biotinylated PEG, some surface-immobilized biotin may be inaccessible. Well solvated PEG chains covalently immobilized to interfaces have been shown not to adopt an extended brush-like conformation, but collapsed mushrooms.[51] It is possible that some biotin capture sites are within these collapsed structures and therefore inaccessible to solution phase streptavidin molecules. The relatively slow accumulation rates observed for streptavidin binding to surface immobilized biotin conjugation sites during the accumulation experiments would suggest that the accessibility of an individual biotin site might dynamically evolve over time. The small biotin molecules on long PEG tethers are likely distributed between residing polymers chains, in an inaccessible state, or being accessible to solution. Therefore, some loss of binding site density might arise from the existence of an

inaccessible population of biotin conjugation sites that are irreversibly buried within the polymer layer. Unlike a large protein, biotin is a small hydrophobic molecule that is capable of accessing and interacting with the underlying functionalized glass surface. The biotin population that is accessible to streptavidin binding produces a bioconjugate interaction that is irreversible on the timescale of a day.[46,52,53]

The capture surfaces produced in this experiment simultaneously fulfill the criteria earlier discussed for an optimal sensor platform. The PEG surface functionality exhibits sufficient resistance to the nonspecific adsorption of proteins while providing a means to control conjugation site densities down to 10^{-6} fractions of a streptavidin monolayer. By adjusting the concentration of 2300 g/mol biotin-PEG-amine in a 1 mM solution of 750 g/mol mPEG-amine, the density of biotin conjugation sites was readily controlled. The relationship between the ratio concentration of 2300 g/mol biotin-PEG-amine in the reaction solution and the counted cy3-streptavidin molecules per unit area was linear. Furthermore, the surface density of the immobilized streptavidin molecules was well resolvable with optically based fluorescence imaging, potentially allowing these surfaces to be used for single molecule investigation of individual protein-protein interactions. The streptavidin-biotin interaction is a highly specific, yet generic means to surface immobilize any biotin conjugated protein for a day or more. By first immobilizing fluorescently labeled streptavidin molecules, individual conjugation-site positions could first be localized and then photo-bleached. Upon further conjugation with any biotinylated-protein, the locations of the streptavidin-biotin-protein pair could be colocalized defining active binding sites, in which subsequently investigated interactions could be referenced. Because PEG does not completely eliminate the

nonspecific adsorption of proteins to interfaces, the use of colocalization diminishes the need to fully prevent nonspecific interactions. By referencing measured spots to known binding sites, specific and nonspecific interactions can be discriminated from each another.

3.4 Discussion

The goal of this research was to produce a sensor capture surface that resisted the adsorption of nonspecific biomolecules, while maintaining the ability to control the density of bio-conjugation sites on glass slides. Furthermore, the surface functionalization process provided a simple means to selectively immobilize capture proteins. The 750 g/mol PEG-amine surface was highly resistant to the nonspecific adsorption of streptavidin, amongst other proteins, from aqueous solutions. The conjugation site density was uniformly controlled down to very low fractions (10^{-6}) of a streptavidin monolayer by diluting in biotin-PEG-amine into an mPEG-amine monolayer. At such low densities, the discrete conjugation sites are spaced out over micron distances between adjacent molecules, which were easily resolvable using single-molecule fluorescent imaging. Using cy3-streptavidin molecules, the linear relationship between biotin-PEG-amine reaction solution concentration and the surface site density of immobilized biotin was established. It was possible to control the density of biotin conjugations sites on glass surfaces by adjusting the concentration of biotin-PEG-amine in a 1 mM mPEG-amine reaction solution. Using the biotin functionality for conjugation sites, these surfaces are able to further employ the well-developed biotin-(strept)avidin

interaction as an intermediate tether to selectively immobilize subsequent biotin-conjugated capture proteins.

3.5 References

(1) McNeil, C. J.; Athey, D.; Renneberg, R. *EXS.* **1997**, *81*, 17.

(2) Stefan-van Staden, R.-I.; Bokretsion, R. G.; van Staden, J. F.; Aboul-Enein, H. Y. *Crit. Rev. Anal. Chem.* **2015**, *45*, 2.

(3) Kambhampati, D. *Protein Microarray Technology*; Wiley; Hoboken, New Jersey, 2004.

(4) Bally, M.; Halter, M.; Voros, J.; Grandin, H. M. *Surf. Interface Anal.* **2006**, *38*, 1442.

(5) Rabbany, S. Y.; Donner, B. L.; Ligler, F. S. *Crit Rev Biomed Eng.* **1994**, *22*, 307.

(6) Stenberg, M.; Nygren, H. *J Immunol Methods.* **1988**, *113*, 3.

(7) Xu, H.; Lu, J. R.; Williams, D. E. *J. Phys. Chem. B.* **2006**, *110*, 1907.

(8) Herron, J. N.; Wang, H.-K.; Janatova, V.; Durtschi, J. D.; Christensen, D. A.; Caldwell, K.; Chang, I. N.; Huang, S.-C. *Surfactant Sci. Ser.* **2003**, *110*, 115.

(9) Vareiro, M. M. L. M.; Liu, J.; Knoll, W.; Zak, K.; Williams, D.; Jenkins, A. T. A. *Anal. Chem.* **2005**, *77*, 2426.

(10) Hlady, V.; Buijs, J. *Curr. Opin. Biotechnol.* **1996**, *7*, 72.

(11) Guo, A.; Zhu, X. Y. *Drug Discovery Ser.* **2007**, *8*, 53.

(12) Madoz-Gurpide, J.; Wang, H.; Misek, D. E.; Brichory, F.; Hanash, S. M. *Proteomics.* **2001**, *1*, 1279.

(13) Zhu, H.; Klemic, J. F.; Chang, S.; Bertone, P.; Casamayor, A.; Klemic, K. G.; Smith, D.; Gerstein, M.; Reed, M. A.; Snyder, M. *Nat. Genet.* **2000**, *26*, 283.

(14) Mateo, C.; Fernandez-Lorente, G.; Abian, O.; Fernandez-Lafuente, R.; Guisan, J. M. *Biomacromolecules.* **2000**, *1*, 739.

(15) Latterich, M.; Corbeil, J. *Proteome Sci.* **2008**, *6*, 31.

(16) Haynes, C. A.; Norde, W. *Colloids Surf., B.* **1994**, *2*, 517.

(17) Norde, W. *Adv. Colloid Interface Sci.* **1986**, *25*, 267.

(18) Harris, J. M; Zalipsky, S. *Polyethylene Glycol: Chemistry and Biological Applications*; Plenum Press: New York, New York, 1992.

(19) Zhang, M.; Desai, T.; Ferrari, M. *Biomaterials.* **1998**, *19*, 953.

(20) Mori, Y.; Nagaoka, S.; Takiuchi, H.; Kikuchi, T.; Noguchi, N.; Tanzawa, H.; Noishiki, Y. *Trans Am Soc Artif Intern Organs.* **1982**, *28*, 459.

(21) Harris, J. M.; Yoshinaga, K. *J. Bioact. Compat. Polym.* **1989**, *4*, 281.

(22) Merrill, E. W.; Salzman, E. W. *ASAIO J.* **1983**, *6*, 60.

(23) Holmberg, K.; Bergstroem, K.; Stark, M. B. *Immobilzation of Proteins via PEG Chains*; Plenum Press: New York, New York, 1992, p 303.

(24) Jeon, S. I.; Lee, J. H.; Andrade, J. D.; De Gennes, P. G. *J. Colloid Interface Sci.* **1991**, *142*, 149.

(25) Chen, S.; Yu, F.; Yu, Q.; He, Y.; Jiang, S. *Langmuir.* **2006**, *22*, 8186.

(26) Rusmini, F.; Zhong, Z.; Feijen, J. *Biomacromolecules.* **2007**, *8*, 1775.

(27) Piehler, J.; Brecht, A.; Valiokas, R.; Liedberg, B.; Gauglitz, G. *Biosens. Bioelectron.* **2000**, *15*, 473.

(28) Huang, N.-P.; Michel, R.; Voros, J.; Textor, M.; Hofer, R.; Rossi, A.; Elbert, D. L.; Hubbell, J. A.; Spencer, N. D. *Langmuir.* **2001**, *17*, 489.

(29) Kenausis, G. L.; Voeroes, J.; Elbert, D. L.; Huang, N.; Hofer, R.; Ruiz-Taylor, L.; Textor, M.; Hubbell, J. A.; Spencer, N. D. *J. Phys. Chem. B.* **2000**, *104*, 3298.

(30) Huang, N.-P.; Voeroes, J.; De Paul, S. M.; Textor, M.; Spencer, N. D. *Langmuir.* **2002**, *18*, 220.

(31) Ruiz-Taylor, L. A.; Martin, T. L.; Zaugg, F. G.; Witte, K.; Indermuhle, P.; Nock, S.; Wagner, P. *Proc. Natl. Acad. Sci. U. S. A.* **2001**, *98*, 852.

(32) Saxer, S.; Portmann, C.; Tosatti, S.; Gademann, K.; Zurcher, S.; Textor, M. *Macromolecules.* **2010**, *43*, 1050.

(33) Frey, B. L.; Corn, R. M. *Anal. Chem.* **1996**, *68*, 3187.

(34) Jordon, C. E.; Frey, B. L.; Kornguth, S.; Corn, R. M. *Langmuir.* **1994**, *10*, 3642.

(35) Suter, M.; Butler, J. E. *Immunol. Lett.* **1986**, *13*, 313.

(36) Luo, S.; Walt, D. R. *Anal. Chem.* **1989**, *61*, 1069.

(37) Donovan, J. W.; Ross, K. D. *Biochemistry.* **1973**, *12*, 512.

(38) Swamy, M. J.; Heimburg, T.; Marsh, D. *Biophys. J.* **1996**, *71*, 840.

(39) Green, N. M. *Methods Enzymol.* **1990**, *184*, 51.

(40) Green, N. M. *Adv. Protein Chem.* **1975**, *29*, 85.

(41) Wikstroem, P.; Mandenius, C. F.; Larsson, P.-O. *J. Chromatogr.* **1988**, *455*, 105.

(42) Hermanson, G. T. *Bioconjugation Techniques*; 2 ed.; Academic Press: Amsterdam, 2008.

(43) Dontha, N.; Nowall, W. B.; Kuhr, W. G. *Anal. Chem.* **1997**, *69*, 2619.

(44) Jasiewicz, M. L.; Schoenberg, D. R.; Mueller, G. C. *Exp. Cell Res.* **1976**, *100*, 213.

(45) Hendrickson, W. A.; Paehler, A.; Smith, J. L.; Satow, Y.; Merritt, E. A.; Phizackerley, R. P. *Proc. Natl. Acad. Sci. U. S. A.* **1989**, *86*, 2190.

(46) Suter, M.; Butler, J. E.; Peterman, J. H. *Mol. Immunol.* **1989**, *26*, 221.

(47) Yanagisawa, M.; Yoshida, T.-a.; Furuta, M.; Nakata, S.; Tokita, M. *Soft Matter*. **2013**, *9*, 5891.

(48) Zdyrko, B.; Luzinov, I. *Macromolecular Rapid Communications.* **2011**, *32*, 859.

(49) Minko, S. In *Polymer Surfaces and Interfaces*; Stamm, M., Ed.; Springer Berlin Heidelberg: 2008, p 215.

(50) O'Shaughnessy, B.; Sawhney, U. *Phys. Rev. Lett.* **1996**, *76*, 3444.

(51) Nelson, K. E.; Gamble, L.; Jung, L. S.; Boeckl, M. S.; Naeemi, E.; Golledge, S. L.; Sasaki, T.; Castner, D. G.; Campbell, C. T.; Stayton, P. S. *Langmuir.* **2001**, *17*, 2807.

(52) Pollheimer, P.; Taskinen, B.; Scherfler, A.; Gusenkov, S.; Creus, M.; Wiesauer, P.; Zauner, D.; Schoefberger, W.; Schwarzinger, C.; Ebner, A.; Tampe, R.; Stutz, H.; Hytoenen, V. P.; Gruber, H. J. *Bioconjugate Chem.* **2013**, *24*, 1656.

(53) Li, Y.-J.; Bi, L.-J.; Zhang, X.-E.; Zhou, Y.-F.; Zhang, J.-B.; Chen, Y.-Y.; Li, W.; Zhang, Z.-P. *Anal. Bioanal. Chem.* **2006**, *386*, 1321.

CHAPTER 4

PROTEIN CAPTURE ACTIVITY AT SOLID-LIQUID INTERFACES

4.1 Introduction

Since the enzyme-linked immunosorbent assay (ELISA) was first introduced in 1971, solid phase immunoassays have become one of the most widely used tools for clinical diagnostics and immunosensing applications.[1-4] Surface-immobilized antibodies serve as the foundation for heterogeneous-type immunoassays owing to their high specificity toward a wide variety of biologically relevant molecules. The fundamental principle behind such measurements relies on the ability of immobilized capture antibodies (CAbs) to efficiently bind homologous antigens (Ags) from solution. The measured signal obtained from "sandwich-type" immunoassays is commonly the result of subsequently captured biomolecules, where the compounded activity from each capture step governs the amplitude and sensitivity of the observed immunosensor response.[5-7] In many cases, capture proteins immobilized at solid surfaces exhibit a significant decrease in observed activity compared to that in free solution, which decreases the efficacy of the sensor.[8] This reduction in bioactivity has been attributed to two primary phenomena. First, surface induced alterations of the secondary and tertiary structures of interfacially immobilized biomolecules can lead to protein denaturation and deactivation of the

binding domain.[9-11] Second, the orientation of an immobilized protein with respect to the plane of the capture surface can be such that the active domain(s) of the protein are inaccessible to solution phase antigen/hapten molecules.[12] With respect to both mechanisms of deactivation, the decreased activity associated with interfacially immobilized proteins is not fully understood at an individual molecule level. As a result, there is a need to better understand the fundamental processes that govern interfacial protein activity at the molecular level in order to produce immunosensor capture surfaces with higher sensitivity and lower limits of detection.

Several procedures have been used to immobilize capture-antibodies onto solid supports for immunosensing applications. Despite the overwhelming evidence indicating that protein-surface interactions promote structural and functional changes in surface-immobilized proteins,[13-16] passive adsorption techniques remain one of the most commonly used methods to deposit capture antibodies onto solid supports.[1,17,18] It has previously been shown that ~75% of polyclonal antibodies (PoAb) physically adsorbed to solid surfaces are rendered inactive and are incapable of capturing homologous antigens.[11] Antibodies have also been immobilized covalently to amino- and carboxyl-modified surfaces using chemical linkers, such as N-hydroxysuccinimidyl ester and glutaraldehyde through random accessible lysines contained within the protein.[19] For both passively and covalently surface immobilized antibodies, inefficient capture activities are observed, which have been attributed to surface induced structural changes within the active domains of the capture protein.[20,21]

In an attempt to circumvent direct contact with solid surfaces, CAbs have been immobilized at interfaces using noncovalent bioaffinity docking through intermediate

protein-tethers. Butler et al. used species-specific antiglobulins as a means to immobilized CAbs onto polystyrene surfaces.[22] In numerous cases, CAbs immobilized to surfaces through intermediate antiglobulins showed >100% surface activity, indicating the existence of a population of bivalently active capture antibodies; however, the efficiency of the surface-immobilized antiglobulins capturing homologous-IgG molecules was extremely poor in most cases. The compounded capture capacity (total apparent activity) of the two-step immobilization strategy was only comparable to the activity associated with the direct passive adsorption of the capture antibody.[11]

Strept(avidin), a homotetrameric protein that selectively binds biotin with an extremely strong affinity,[23] has also been used as an intermediate protein tether to bridge biotinylated-molecules to interfaces. Since first being proposed in 1986,[24] the protein-avidin-biotin-capture (PABC) method has been extensively used in a variety of immunosensor applications.[25-29] Similarly to antiglobulins, the PABC method showed a significant increase in antigen capture capacity for monoclonal antibodies (MoAbs) that were immobilized, but again, the efficiency of surface-immobilized strept(avidin) for capturing biotinylated-CAbs was quite low.[11,30] Under optimal conditions, substantially more CAbs could be immobilized using physical adsorption techniques.[18,24]

Despite these inefficiencies, the strept(avidin)-biotin bridge has proven to provide many other advantages, over passive adsorption techniques, as a means to immobilize proteins to solid interfaces. Passive adsorption techniques rely on hydrophobic, electrostatic, and hydrogen bonding surface/protein interactions to adsorb biomolecules at a surface; as a result, the properties associated with such techniques vary greatly from surface-to-surface and protein-to-protein.[31] In some cases, proteins will not

spontaneously adsorb to a given solid surface, which renders passive adsorption techniques as not a viable option. In addition, controlling the surface concentration of passively adsorbed proteins can be an extremely difficult task, yet the density of surface capture sites can greatly affect the activity, measured signal, and sensitivity of a sensor.[32,33] In contrast, the PABC method provides a reproducible means to immobilize any biotinylated-biomolecule to a solid interface.[34] Described in the previous chapter as well as by other researchers, the surface concentration of subsequently immobilized streptavidin molecules has been shown to be controllable by adjusting the ratio of biotinylated-PEG and mPEG molecules deposited onto glass substrates.[25,26]

Regardless whether the interfacially immobilized CAbs are in direct contact with the surface or spaced above the surface through an intermediate protein tether, the measured capture efficiency is always much less than theoretically achievable.[11] It has been suggested that surface-induced structural changes are not exclusively responsible for the decreased activity. It has also been hypothesized that the orientation of immobilized CAbs with respect to the solution interface could influence the activity of the sensor.[35] The molecular basis of most immunoassays is the macromolecule immunoglobulin G (IgG), which is composed of two identical "heavy" polypeptide chains that pair with two identical "light" polypeptide chains to form the well-known Y-shape structure. The IgG molecule contains two identical variable regions (Fab) that bind antigens with extremely high specificity and a constant region (Fc) that regulates effector functions.[36] Because of this asymmetric shape, surface immobilized IgG molecules can have varying degrees of antigenicity depending on their orientation with respect to the interface.[37] In all of the previously discussed CAb immobilization strategies (passive adsorption, direct covalent

binding, and indirect protein bridging), the deposition results in random uncontrollable distribution of antibody orientations with respect to the surface. In such cases, a significant fraction of CAbs can be oriented in such a manner that one or both of the Fab domains are hindered by the surface and inaccessible to solution phase antigens. This distribution of orientations could result in severe heterogeneity in activity between individual CAbs on the surface.

Since it was first applied to immunoassays in 1978,[38,39] protein A, derived from *Staphyloccus aureus*, has become one of the most commonly utilized methods to noncovalently immobilize IgG molecules onto solid surfaces in a more controlled orientation. [40-42] Protein A, as well as protein G and protein A/G specifically bind the Fc region of the IgG molecule for a variety of species of vertabrates.[43] Surface immobilized CAbs tethered through Fc binding protein intermediates are aligned with both $(Fab')_2$ extended away from the plane of the surface. In such an orientation, both Fab domains are accessible to solution and could simultaneously bind homologous Ags. Chung et al. utilized the PABC method to sequentially immobilize NeutrAvidin, biotinylated-Protein A, and donkey-derived antihuman IgG (anti-hIgG) onto gold surfaces. Immobilized through the Fc domain, the efficiency of surface-tethered anti-hIgG capturing hIgG was ~3-fold greater than a single layer of passively adsorbed anti-hIgG.[29] Although it is well documented that the use of protein A increases surface immobilized CAb activity, the capture efficiency of protein A has not been studied at the single-molecule level.

The activities of surface immobilized antibodies deposited using passive adsorption, covalent attachment, and intermediate bioaffinity tethering have been investigated using a variety of techniques, including radiometry,[1,8,17,44] surface plasmon

resonance (SPR),[29,45] ellipsometry,[46] colorimetry,[47-49] and quartz crystal microbalance (QCM).[10,50,51] These methods produce ensemble signals that report the activities of the entire surface population. Little information is revealed about the distribution of activities from site-to-site, and yet the response of multipart immunoassays resulting from the sequential immobilization of strept(avidin), biotinylated-protein A, CAb, Ag, and reporter-Ab' can be extremely complex. For each additional layer, an individual surface-immobilized capture-protein can be the result of either a specific ligand-receptor interaction or nonspecific surface adsorption; therefore, for a system with N layers, there are N possible configurations for a surface immobilized capture-antibody as illustrated in Figure 4.1. In addition, each possible complex potentially has differing activities,[22,29] causing the combined apparent activity to be composed of a highly complex subset of activities. Although well studied at a macroscopic level, little has been reported about the activities of solid-phase immunoassays at the single-molecule level.

In this work, we applied single-molecule imaging, based on total internal reflection fluorescence (TIRF) microscopy, to address molecular-scale issues associated with the observed activities for solid-phase immunosorbent assays at site-to-site resolution. A (polyethylene)glycol modified glass surface containing biotin binding sites was used to immobilized a very low density (10^{-13} mol/m^2) of cy3-labeled streptavidin molecules. Cy3-conjugated antigoat IgG (anti-GtIgG-cy3) was immobilized to the modified-surfaces using four techniques: (i) passive adsorption to an mPEG-modified surface, (ii) indirect bioaffinity tethering with streptavidin, (iii) sequentially with streptavidin and protein A, (iv) and a one-step deposition of a chimeric (protein A-anti-IgG) complex through a surface immobilized streptavidin. Each of the methods was then

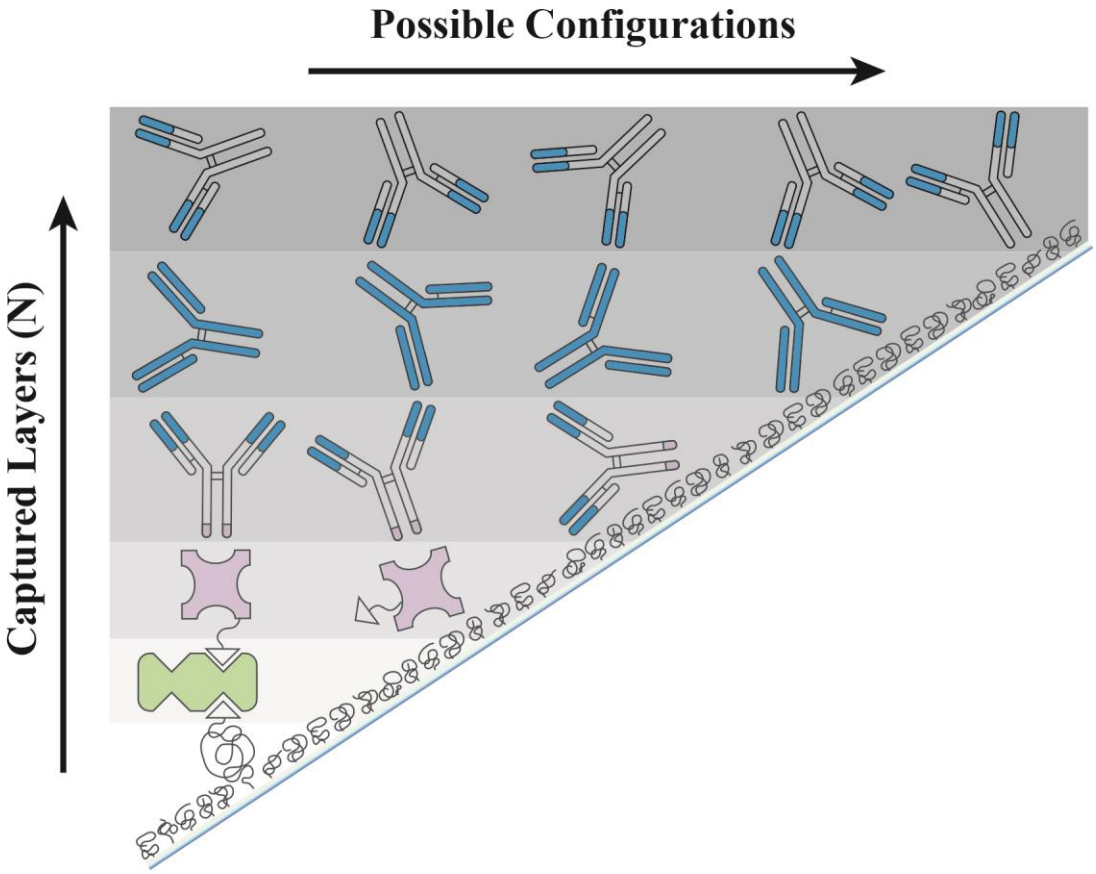

Figure 4.1: Sandwich capture assay with N capture steps had N possible conformations.

sequentially exposed to GtIgG, and the capture activity for each surface preparation was measured at the single-molecule level using sequential colocalization. The compounded capture activities were then compared for each of the four methods of immobilization. The results demonstrate the inefficiency of interfacially immobilized proteins in recognizing their homologous counterparts; however, depending on the method by which the CAbs were immobilized, significant differences in the capture activities were observed.

4.2 Experimental

4.2.1 Chemicals and Materials

(3-Glycidyloxypropyl)trimethoxysilane (GOPTS), methoxypoly(ethylene glycol) amine ($mPEG_{16}$-amine) with an average molecular weight (M_n) of 750 g/mol, and biotin poly(ethylene glycol) amine (biotin-PEG_{48}-amine) with a M_n of 2300 g/mol were purchased from Sigma Aldrich (St. Louis, MO) and used as received. Rabbit antigoat $IgG_{(H+L)}$ (anti-GtIgG), goat IgG (GtIgG), and cy3-conjugated streptavidin (cy3-streptavidin) were obtained from Jackson Immunoresearch Laboratories Inc. (West Grove, PA). Recombinant Protein A from *E. coli* (EpA) and EZ-link NHS-PEG_4-biotin were purchased from Thermo Scientific (Rockford, IL). Cy3 monoreactive N-hydroxysuccinimidyl ester was purchased from GE Health Care Life Sciences (UK). Gold Seal microcover glasses (22 X 22mm No. 1.5) and 10 kDa cutoff Pall Life Sciences Nanosep Centrifugal dialysis filters were purchased from VWR (West Chester, PA).

4.2.2 Protein Labeling

The monofunctional labeling of anti-GtIgG, GtIgG, and EpA with biotin and cy3 functional tags was accomplished using succinimidyl ester linking chemistry as outlined by Hans et al.[52] For hetero-bifunctional labeling of anti-GtIgG and EpA simultaneously with cy3 and biotin, the protocol was adapted as follows: Biotin-PEG_4-NHS (2 mg) was dissolved in 500 μL of pH 8.3 carbonate buffer (6.8 mM), Cy3-NHS (1 mg) was dissolved in 200 μL of DMF (6.5 mM), and 3.33 nmol of each respective protein was dissolved in 500 μl (6.7 μM) of pH 8.3, 100 mM carbonate buffer. 5.5 μl (75 μM) of the biotin-PEG_4-NHS and 5.7 μl (75 μM) of the cy3-NHS containing solutions were the added to the protein solution. The mixture was slowly vortexed at room temperature and in the absence of light for 30 minutes. After the reaction was complete, the free dye/biotin was separated from labeled protein solution using 10 kDa cutoff nanosep centrifugal dialysis filters. The labeled protein solution was centrifuge filtered at 10,000 rpm with 20 mM phosphate buffered saline (pH 7.5, 100 mM ionic strength) until negligible fluorescence at 550 nm was detected in the supernatant.

4.2.3 Measurement of Protein and Degree of Dye Labeling

The protein concentration and dye-to-protein ratio (D/P) for each protein was determined using UV-vis absorption measurements at 280 nm and 550 nm in conjunction with reported molar extinction coefficients (ε_{550} = 150000 $M^{-1}cm^{-1}$ for Cy3, ε_{280} = 170000 $M^{-1}cm^{-1}$ for IgG, and ε_{280} = 6406 $M^{-1}cm^{-1}$ for protein A).[52] Because biotin-PEG_4-NHS and cy3-NHS solutions were prepared and reacted simultaneously and biotin-PEG_4-NHS has an estimated ~25% faster diffusion coefficient compared to cy3-NHS based on

molecular weight, it is expected that the degree of biotin labeling was slightly greater than that of cy3, assuming the NHS reactivity of the two reagents are equivalent.

4.2.4 Surface Preparation

Glass cover slides were first cleaned by immersion into a freshly prepared mixture of H_2SO_4 and 30% H_2O_2 mixture (2:1 vol) for 20 minutes followed by extensive rinsing in 18MΩ-cm H_2O. The clean slides were then treated in an H_2O, NH_4OH, and 30% H_2O_2 mixture (5:1:1 vol) at 75°C for 10 minutes; after which, the slides where rinsed 3 times with 18MΩ-cm H_2O and dried under a stream of ultra-high purity nitrogen. The unmodified glass slides were totally hydrophilic after the cleaning process, such that water spreads and results in a nonmeasurable water contact angle.

In order to achieve a uniform reactive monolayer, GOPTS was deposited out of the vapor phase.[53] Ten clean glass cover slides were vertically racked into a ceramic slide holder and placed into a glass vessel containing 500 μl of GOPTS. The glass vessel was then sealed and incubated for 18 hours in a convection oven previously set to 60°C. After the silanization periods concluded, the slides were removed from the container and further incubated in an empty oven for an additional 5 minutes at 60°C in order to remove physisorbed GOPTS and to prevent residual gas phase GOPTS from condensing on the slide's surface. The slides were then allowed to cool to room temperature before further derivatization occurred.

The reaction of PEG-amine to GOPTS modified surfaces utilized the high reactivity of epoxide functional groups with primary amines at high pH. A solution containing 100 mM $mPEG_{16}$-amine and 1 μM biotin-PEG_{48}-amine in pH 10.1 carbonate

buffer was prepared. Each epoxide functionalized cover slide was separately placed horizontally in the bottom of a 30 ml beaker and covered with 4 ml of the mPEG/biotin-PEG solution. If any slide was not fully wetted and submerged, additional reaction solution was added. The beakers were then placed on a titer plate shaker, covered, and slowly mixed under orbital shear for 18 hours at room temperature. After completion, the slides were washed three times with 20mM phosphate buffered sailine (PBS) at pH 7.5, 100 mM ionic strength). The PEG-modified cover slides were stored up to 1 week in PBS prior to their characterization.

4.2.5 Streptavidin Surfaces

For each immunoassay experiment, the biotinylated capture surface was first assembled into a 4 μl flow cell and loaded onto an inverted microscope stage. The sample was then rinsed with 20 mM PBS (pH 7.5, 100 mM ionic strength) with 0.1% Tween 20 and illuminated with 12 mW of 532-nm laser radiation. In order to remove all inherent background fluorescence, the sample was photobleached for 15 minutes prior to any surface modification. A streptavidin-modified surface was prepared by treatment of a photobleached biotin-modified slide with 11 ng/ml (200 pM) cy3-streptavidin in PBS. Under continuous flow (30 ml/h), the sample was incubated for 120 minutes with the streptavidin containing solution and then rinsed with PBS (0.1% Tween 20) for an additional 60 minutes.

4.2.6 Anti-GtIgG Surface

Prior to the injection of each additional protein layer, the sample was photobleached for 15 minutes using 12 mW of 532-nm laser radiation. Biotin-anti-GtIgG-cy3 at a concentration of 75 ng/ml (500 pM) in PBS was injected onto a photobleached streptavidin-modified surface. The sample was treated for 120 minutes and then rinsed with PBS (0.1% Tween 20) for an additional 60 minutes under continuous flow (30 ml/h). After photobleaching the previously immobilized biotin-anti-GtIgG-cy3 layer, 75 ng/ml (500 pM) GtIgG-cy3 in PBS was accumulated under continuous flow for 120 minutes and rinsed for 60 minutes with PBS (0.1% Tween 20).

4.2.7 Protein A-anti-GtIgG Surface

A photobleached streptavidin-modified slide was sequentially exposed to 10 ng/ml (250 pM) biotin-EpA-cy3, 75 ng/ml (500 pM) anti-GtIgG-cy3, and 75 ng/ml (500 pM) GtIgG-cy3 in PBS. Prior to the injection of each subsequent protein layer, the sample was photobleached with 12 mW of 532-nm laser radiation for 15 minutes. Each protein was accumulated under continuous flow (30 ml/h) for 120 minutes followed by 60 minutes of rinsing with PBS (0.1% Tween 20).

4.2.8 Protein A-anti-GtIgG Chimeric Complex Surface

The single step immobilization of the protein [EpA/anti-GtIgG] chimeric complex was accomplished by first pre-equilibrating 6 μg/ml (125 nM) of biotin-EpA and 75 μg/ml (500 nM) anti-GtIgG-cy3 in 20 mM PBS *ex situ* for 1 hour. The chimera containing solution was diluted by 500 times and injected onto a photobleached

streptavidin-modified slide. The chimeric complex was accumulated under continuous flow (30 ml/h) for 120 minutes and then rinsed with PBS (0.1% Tween 20) for 60 minutes. After photobleaching the immobilized chimeric complex with 12 mW of 532-nm laser radiation for 15 minutes, 75 ng/ml (500 pM) GtIgG-cy3 in PBS was then injected, accumulated for 120 minutes, and rinsed with PBS (0.1% Tween 20) for an additional 60 minutes.

4.2.9 Single Molecule Imaging

The fluorescent imaging of cy3-labeled proteins used for monitoring each immunoassay step was achieved using an Olympus IX71 inverted microscope retrofitted with an in-house built stage utilizing a piezoelectric NanoFlex translation stage (ThorLabs), capable of maintaining focus over many hours of observation. The cy3-labeled proteins were excited with 1mW, measured at the back of the objective, of 532 nm laser (B&W TEK Inc.) light. The laser was coupled into a single mode fiber and launched off-center into the back of an Olympus plan apo 60X, 1.45 NA, oil immersion objective to achieve total internal reflection. Emitted fluorescence was then collected back through the same objective, passed through a 552 nm BrightLine dichroic beamsplitter (Semrock) and 585/40 nm BrightLine bandpass filter (Semrock), and imaged using an Andor iXon+ CCD camera.

The accumulation and rinse of each sequentially deposited protein layer was monitored using total internal reflection fluorescence (TIRF) by intermittently collecting images every 10 minutes at 150 mseconds integration times. Each accumulation was monitored for 12 image cycles (120 minutes) and then rinsed for an additional 6 image

cycles (60 minutes). This was sufficient time to reach saturation and desorption of weakly-bound proteins, while minimizing the photobleaching of any conjugated cy3 label. At the end of each accumulation/wash cycle, 5 images were acquired at 20-seconds intervals and 150 mseconds integration times. The 5 images were then imported into image J,[54] where they were co-added and analyzed. The fluorescent background measured for 5 coadded images obtained from a photobleached surface prior to the accumulation of protein had an average intensity of μ_B = 103 photoelectron counts, while having a variation in pixel-to-pixel intensity of σ_B = 13 photoelectrons. The threshold for counting single molecules, plotted in Figure 4.2, was set such that a spot >4 pixels^2 in area have an average pixel intensity 10 times σ_B above μ_B at 233 photoelectrons. Each spot above threshold was then fit to a point spread function and its center of mass was plotted. For sequential images from a single accumulation, the average frame-to-frame variation in plotted locations, over 180 minutes, had a radius σ_r = 0.5 pixel. For each capture experiment, the location of subsequently adsorbed protein pairs were plotted on top of each other, where the threshold radius for colocalization was set 6.4 times σ_R, R_c = 3 pixels. Under these conditions, the probability of missing a colocalized molecule was 0.001 based on 2-D Gaussian distribution. The positions of sequentially immobilized protein layers were plotted on top of each other using Microsoft Excel (Redmond, WA). Subsequent positions were colocalized within an 0.5 μm radius of overlap and then counted.

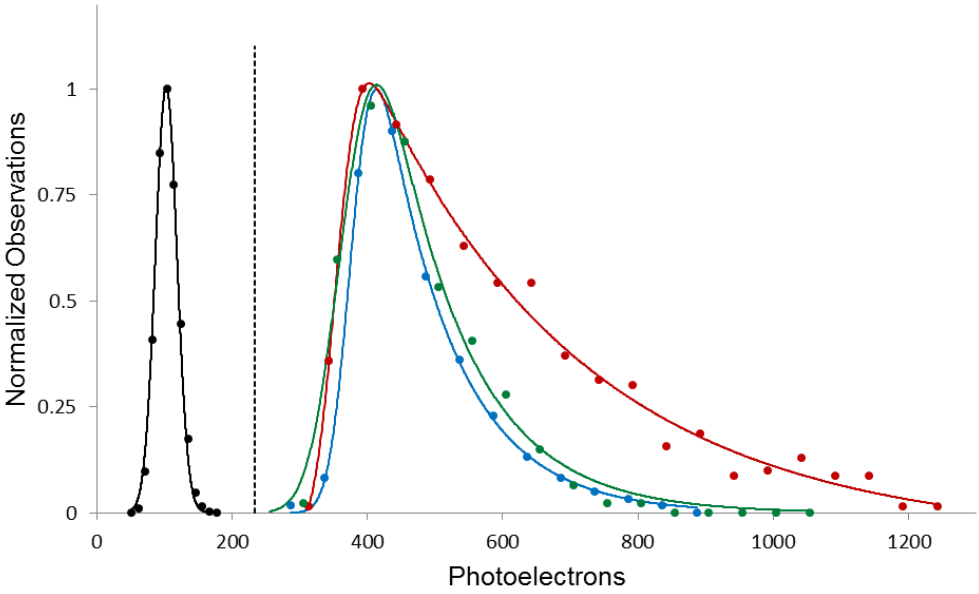

Figure 4.2: Histogram of background intensity (black) fit to a Gaussian distribution and histograms of individual (green) biotin-antiGtIgG-cy3, (blue) biotin-EpA-cy3, and (red) GtIgG-cy3 intensities each fit to an exponentially modified Gaussian function. The dashed line marks the threshold set for counting single-molecules.

4.3 Results

4.3.1 Protein Labeling and Counting

The average dye-to-protein ratio (D/P) was measured for each labeled protein. When labeling with cy3, polyclonal goat IgG (GtIgG-cy3) had an average D/P of 4.4 and rabbit antigoat (anti-GtIgG-cy3) had an average D/P of 3.7. With respect to the biotinylation of protein A (biotin-EpA), the biotin-to-protein ratio (B/P) was not measured as it was assumed that EpA without biotin would not be captured by surface immobilized streptavidin. In the case of the hetero-bifunctional labeling, the B/P could be inferred from the dye labeling result. Because the biotin-PEG_4-NHS has a diffusion coefficient ~25% faster than cy3-NHS and the NHS reactivities were assumed to be equivalent, the B/P should be greater than D/P for the simultaneous bifunctional labeling of proteins. For bifunctional labeled proteins, rabbit antigoat (biotin-anti-GtIgG-cy3) was measured to have a D/P of 4.2 and protein A (biotin-EpA-cy3) had a D/P of 3.4. The variation in molecule-to-molecule intensities using TIRF imaging was quite large in some cases (~30%). This large variation in spot-to-spot intensity suggests there was a distribution in the number of fluorescent labels carried by each protein. Because of the labeling variation and complicated photo-physics of multilabeled proteins,[52] single-molecule imaging is incapable of resolving multiple bound proteins to a single capture site based on individual spot intensities. Although streptavidin, IgG, and protein A are multivalent, the measured capture activities of these surface immobilized proteins are much less than 50%, so the likelihood of multiple bound ligands should be even smaller.

4.3.2 Surface Preparation and Streptavidin Immobilization

Immunoassays

The heterogeneous PEG functionalized surfaces were prepared by reacting a solution containing a mixture of dilute biotin-PEG_{48}-amine and a much higher concentration of diluent $mPEG_{16}$-amine with GOPTS-modified glass slides. A PEG functionalization of the surface was chosen for its ability to reduce the nonspecific adsorption of biomolecules, while providing an inert layer where interfacially tethered proteins would be able to maintain a native-like structure and activity.[55-57] In the previous chapter, it was shown that by diluting biotin-PEG-amine into an mPEG-amine monolayer, the density of biotin conjugation sites on glass surfaces is controllable. The use of the well-developed and stable biotin-streptavidin interaction provided a generic, yet highly specific means to further immobilize any biotin-conjugated biomolecule through interfacially tethered streptavidin intermediates.[34] The properties exhibited by the prepared PEG surfaces were previously characterized and discussed in the previous chapter. The mPEG-modified surfaces without PEG-biotin tethers exhibited low levels ($2.9 \pm 0.7 \times 10^{-15}$ mols/m^2) of nonspecifically adsorbed cy3-streptavidin, while increasing the ratio of surface immobilized biotin-PEG-amine-to-mPEG-amine resulted in a monotonic rise in the concentration of specifically immobilized cy3-streptavidin. By preparing PEG modified surface with low conjugation site densities ($\leq 2.9 \times 10^{-12}$ mols/m^2), individual immobilized proteins could be easily resolved within the diffraction limits of optical microscopy allowing individual protein-protein interactions to be observed and quantified.

In our previous work, it was observed that the interfacially associated biotin-

streptavidin complex was an extremely stable interaction. Demonstrated in Figure 4.3, there was little observable dissociation (<20%) of the bound biotin-streptavidin complex during a 60 hour wash period, so that surface-bound biotin-streptavidin molecules were found to be irreversible on the time scales $\leq$ 24 h.[27,34,58] The irreversible nature of the interaction was exploited in this experiment to investigate the activities of a variety of ligand-protein-receptor interactions intermediately tethered to a PEG-modified surface through streptavidin molecules. The strong affinity ($K_d \sim 10^{-14 \text{ to } -15}$ M)[23] streptavidin exhibits for biotin requires a minimal concentration of streptavidin to completely saturate a low-density of surface immobilized biotin conjugation sites. At such low concentrations (200 pM), cy3-streptavidin was found to exhibit minimal nonspecific adsorption ($2.9 \pm 0.7 \times 10^{-15}$ mols/m^2) to mPEG-modified glass slides, as discussed in the previous chapter. As a result, the specific interactions accounted for 0.99996 of the total observed binding events on modified slides containing a low ($\leq 7.2 \times 10^{-13}$ mols/m^2) density of biotin conjugation-sites. By locating the positions of discretely immobilized cy3-streptavidin molecules on a modified glass surface using TIRF microscopy, all successively observed protein-protein interactions could be colocalized to known streptavidin locations, allowing specific and nonspecific surface interactions to be discriminated from each other. The use of colocalization avoids the need to eliminate all nonspecific protein-surface interactions for the subsequent investigation of protein-protein interactions, as the history of each observed binding-site location is well known.

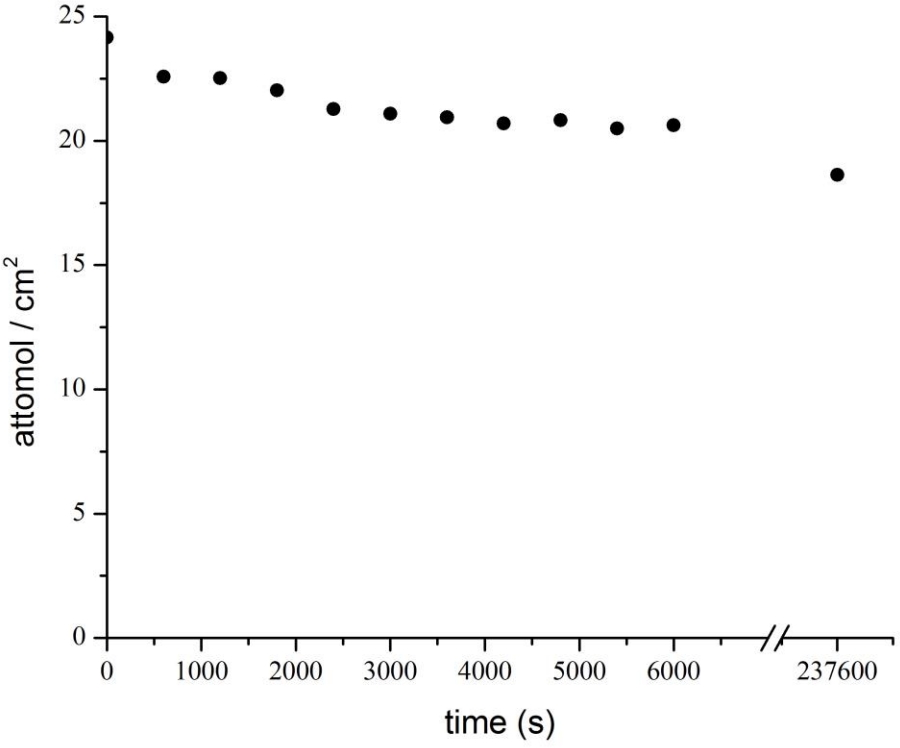

Figure 4.3: Washing of cy3-streptavidin from a 750 g/mol mPEG surface containing a low density of 2000 g/mol biotin-PEG conjugation sites. After ~60 hr >90% of the streptavidin population remained strongly immobilized.

4.3.3 Testing Capture Efficiency of Immobilized Antibodies

Figure 4.4 illustrates the sequential association of cy3-streptavidin, biotin-anti-GtIgG-cy3, and GtIgG–cy3 onto the biotin containing PEG surfaces. Prior to the injection of each protein, the cy3- labels associated with the previously-immobilized capture biomolecules were photobleached by exposing the conjugated slides with 12 mW laser light until no observable fluorescent spots remained (~15 minutes). The sequential deposition of each protein layer was then monitored by intermittently imaging the sample over the duration (180 minutes) of the accumulation experiment. By collecting an image every 10 minutes, at 150 msecond integration periods, and 1 mW laser power, the accumulation of protein was observed over several hours with negligible photobleaching of the cy3-conjugated fluorescent labels. At 1 mW of continuous 532 nm laser power, the time constant of complete photobleaching for a protein modified with an average of 4.4 ± 0.2 cy3- labels was measured in Chapter 2 to be $\tau_{PB} \approx 190$ seconds. For a labeled-biomolecule present for an entire 180 minutes accumulation/wash, the conjugated fluorescent dyes would have been exposed to 2.7 s of 532 nm laser radiation. As a result the probability of a false negative occurring as a result of photobleaching was small (< 0.015).

Following the injection of 75 ng/mL (500pM) biotin-anti-GtIgG-cy3 to a photobleached streptavidin-modified surface, antibody slowly accumulated, reaching a maximum in ~120 minutes. Any weakly associated biotin-anti-GtIgG-cy3 was then removed by rinsing with PBS (0.1% Tween 20) for an additional 60 minutes, as shown in Figure 4.5. Following the accumulation and rinse period, 5 images where then collected at 20 s intervals, 150 ms integration times, and 1 mW laser power. The 5 images were

Figure 4.4: Heterogeneous sandwich assay and colocalization: (a) capture of cy3-streptavidin by surface immobilized biotin sites, (b) image and photobleach cy3-streptavidin, (c) capture of biotin-anti-IgG-cy3 by photobleached streptavidin, (d) image and photobleach biotin-anti-GtIgG-cy3, and (e) capture of GtIgG-cy3 by photobleached anti-GtIgG.

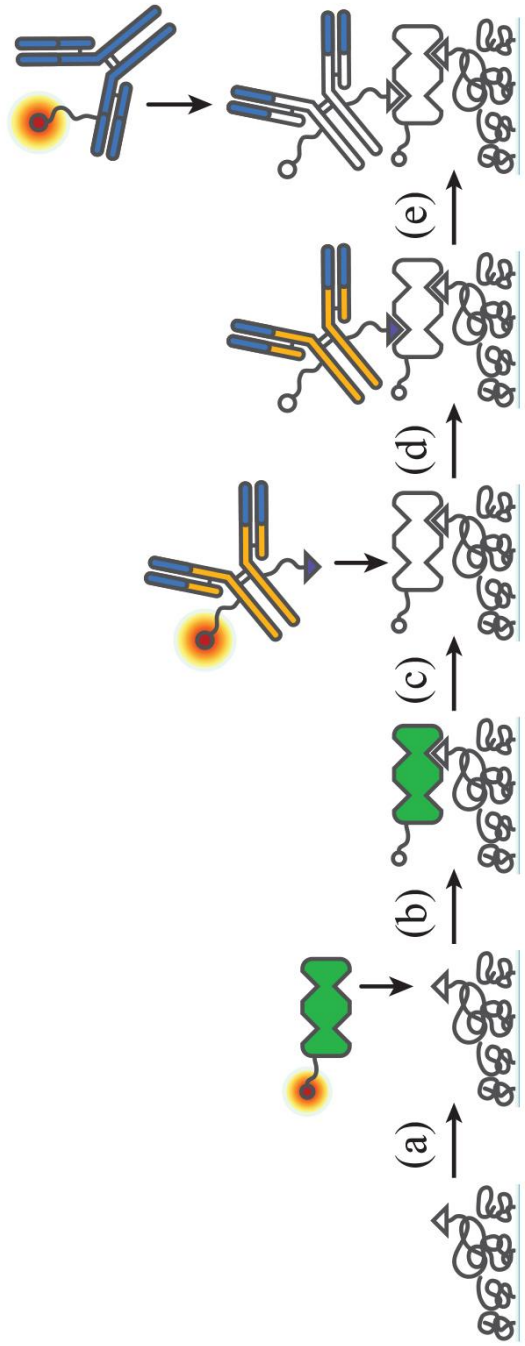
(a)
(b)
(c)
(d)
(e)

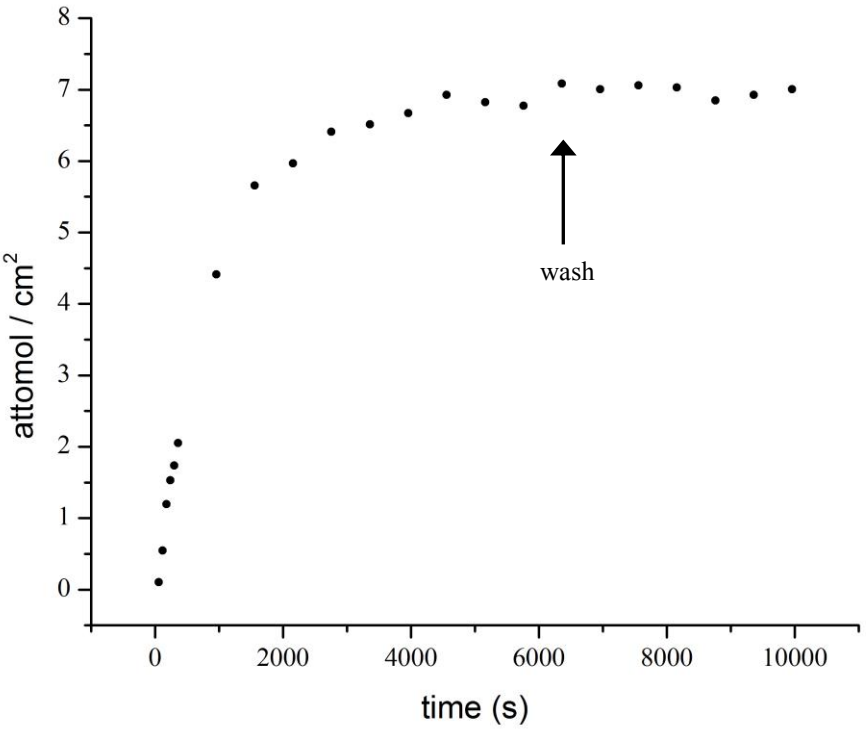

Figure 4.5: Accumulation and wash of 500 pM biotin-anti-GtIgG-cy3 to surface immobilized streptavidin.

then co-added in order to average out intensity fluctuations. The population of surface-associated biotin-anti-GtIgG-cy3 molecules had an average fluorescence intensity of $\mu_{\text{biotin-anti-GtIgG-cy3}} = 326$ photoelectron counts with a variation in spot-to-spot intensity counts, $\sigma_{\text{biotin-anti-GtIgG-cy3}} = 38$ photoelectrons. The variation in the intensity between individual biotin-anti-GtIgG-cy3 spots likely arises from a distribution of labels carried by each biomolecule (see Figure 4.2).

On average, the immobilized surface concentration of the streptavidin-capture sites was measured to be $3 (\pm 1) \times 10^{-13}$ mol/m^2, which was well within the resolution limits ($\leq 2 \times 10^{-12}$ mol/m^2) of imaging discrete single molecules using TIRF microscopy. The ~30% variation in immobilized streptavidin from slide-to-slide made comparing absolute protein surface concentrations from experiment-to-experiment irrelevant; as a result, all values reported in the following experiments are in terms of fractional activities of surface-bound proteins and not surface concentrations. The colocalization of cy3-streptavidn with biotin-anit-GtIgG-cy3 (Figure 4.6) revealed that only 8 ± 2 % of the total streptavidin population was able to capture biotin-anit-GtIgG-cy3 molecules; however, because of the small chance of random spot overlap, $\leq 2\%$, depending on streptavidin surface concentration, this value is an upper bound on the activity. Considering the degree of biotin labeling (B/P ~ 4) and the concentration of anti-GtIgG (500 pM) injected, the streptavidin capture surface was exposed to an effective biotin concentration $>2 \times 10^5$ times K_d, which should have been an adequate concentration to saturate all available streptavidin binding sites in the given time.

The low capture efficiency exhibited by streptavidin capture surfaces for biotinylated proteins has been previously been observed. For high-density biotin

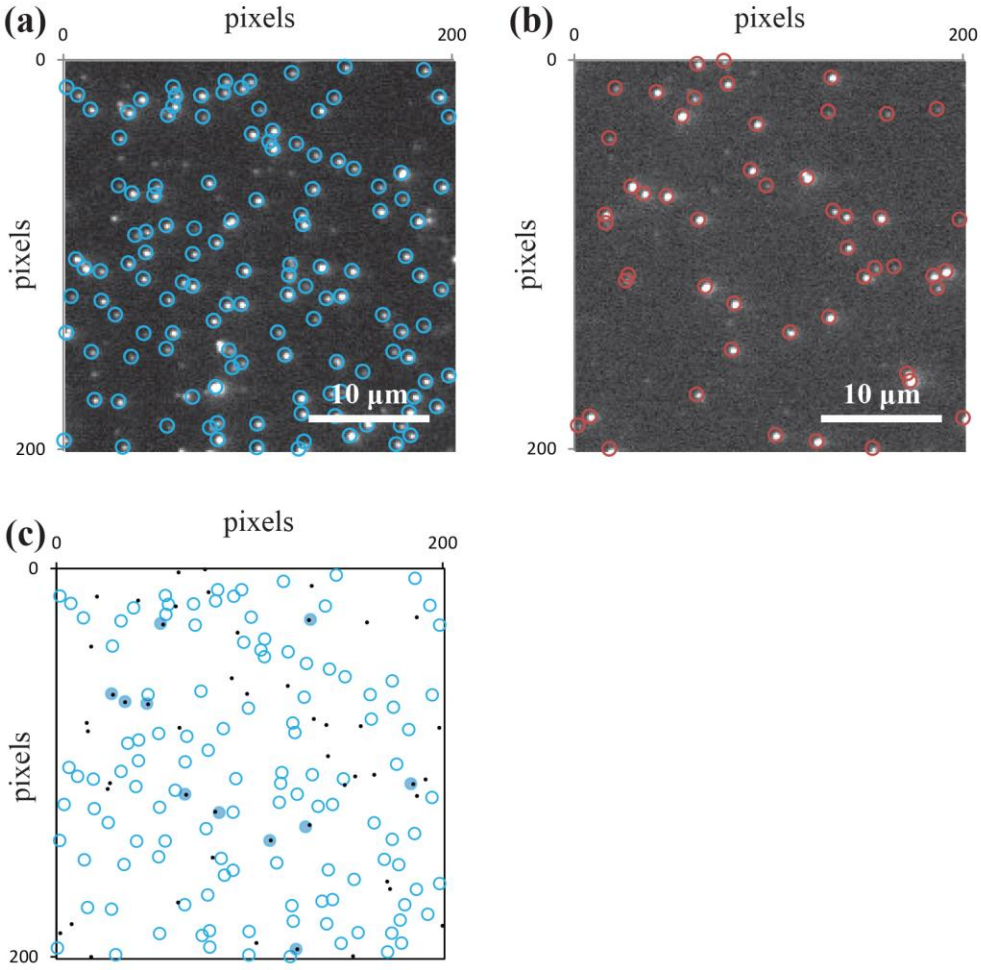

Figure 4.6: Steptavidin capture efficiency: (a) The locations of individual cy3-streptavidin molecule captured by surface immobilized biotin sites, (b) the location of individual biotin-anti-GtIgG-cy3 molecules strongly adsorbed to the streptavidin modified surface, and (c) colocalized streptavidin (blue circles) and anti-IgG (black dots).

modified surfaces, it has been hypothesized that a single tetrameric streptavidin molecule could be immobilized through multiple biotins within a close proximity.[26] This would render the remaining capture sites within a single streptavidin incapable of subsequently capturing and immobilizing additional biotinylated-proteins. Given the extremely low surface concentration of biotin on the surfaces in this experiment, it is highly improbable that any streptavidin molecule is immobilized to the surface through more than one biotin.[26,28] This fact suggests that the decrease in observed activity is not the result of the remaining binding sites of the immobilized streptavidin molecule being occupied by surface tethered biotin. Another possibility may have resulted from some of the active sites on streptavidin being hindered by the surrounding surface; however, the long PEG (2000 MW) tether, through which the streptavidin was immobilized, should have allowed mobility above the surface. If the PEG tether allows streptavidin to have dynamic motion above the surface, this should allow accessibility to the remaining biotin binding sites; however, as demonstrated by Figure 4.7, the capture of biotin-anti-GtIgG by surface immobilized streptavidin is not efficient, which implies the conformational mobility of the tethered streptavidin is limited.[59] It is likely that the tethered streptavidin is also adsorbed to the modified interface through protein-surface interactions. These interactions may have induced structural changes that disrupted the remaining active domains rendering them incapable of capturing additional biotin molecules.

After the colocalization of the observed biotin-anti-GtIgG-cy3 events with known streptavidin locations, two populations of immobilized CAbs were revealed. On average, 36 ± 2% of the biotin-anti-GtIgG-cy3 population is associated (colocalized) with a streptavidin molecule, whereas the remaining 64 ± 2% was strongly adsorbed to the PEG-

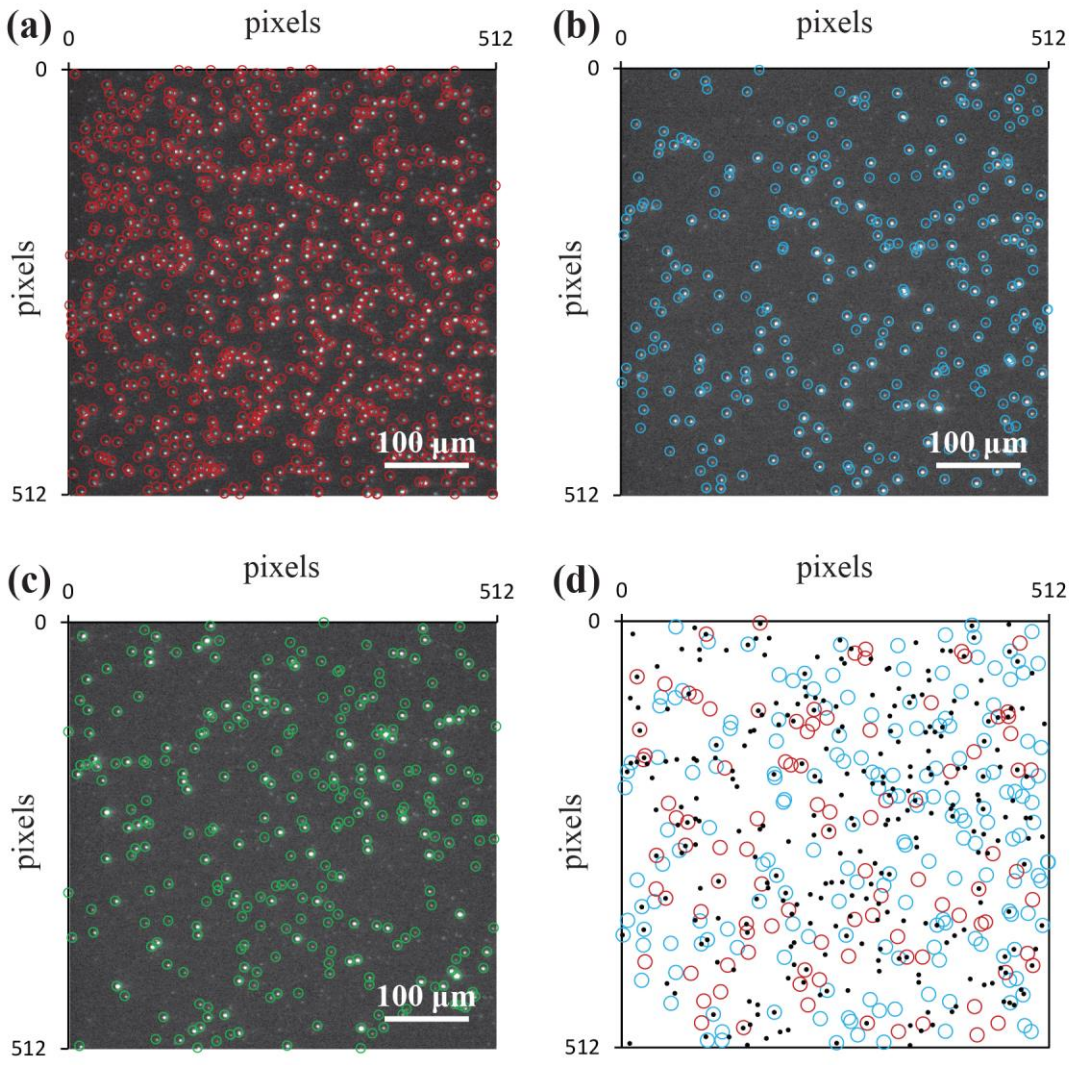

Figure 4.7: Sequential capture of streptavidin, anti-GtIgG, and GtIgG: (a) located individual cy3-steptavidin molecules, (b) located individual biotin-anti-GtIgG-cy3 molecules, (c) located individual GtIgG-cy3 molecules, and (d) colocalized events: (red circles) biotin-anti-GtIgG-cy3 molecules colocalized with cy3-streptavidin, (blue circles) anti-GtIgG passively adsorbed (not colocalized), and (black dots) GtIgG-cy3 molecules.

modified surface, but not tethered through streptavidin. The capture efficiency of CAbs immobilized to surfaces through both streptavidin intermediates (PABC) and passive adsorption techniques has previously been reported;[11] however, it becomes clear from the single molecule results that the heterogeneity of a capture surface increases as the complexity of the protein-scaffold layer increases, as illustrated in Figure 4.7. In such cases where intermediate tether proteins are employed, the apparent capture efficiency of a CAb modified surface will represent an average of the heterogeneity of each contributing protein-protein interaction. To better understand how the two populations of CAbs contribute to the total observed capture capacity of a surface, a model antigen (GtIgG-cy3) was injected over the anti-GtIgG-conjugated capture surfaces, accumulated, rinsed, and imaged.

Individual interfacially adsorbed GtIgG-cy3 molecules had an average fluorescent intensity of $\mu_{GtIgG\text{-}cy3}$ =353 photoelectron counts with a variation in spot-to-spot intensity of $\sigma_{GtIgG\text{-}cy3}$ = 25 photoelectrons counts (see Figure 4.2). When examining the colocalized events (Figure 4.7), 26 ± 1% of the streptavidin-biotin-anti-GtIgG complexes captured GtIgG-cy3 biomolecules, where in contrast, only 14 ± 4% of the passively adsorbed biotin-anti-GtIgG population captured GtIgG-cy3 molecules. The total apparent capture activity of the surface (an average of the two antibody populations) is 18 ± 8%. The activities of PoAbs immobilized to polystyrene surfaces using the PABC were previously measured to be 32 ± 27%, compared to 22 ± 3 % for passively adsorbed PoAbs, which agrees quite well with the single-molecule measurements.[11] Although PEG functionalization was previously reported to help interfacially immobilized proteins maintain activity,[60] the 750 g/mol PEG surface modification used to dilute the biotin

tethers in these experiments do not appear to significantly improve the activity of surface immobilized streptavidin or polyclonal CAbs in comparison to polystyrene surfaces.

From these experiments, it is clear that the total apparent capture activity measured for a surface prepared by the PABC method is actually dominated by a population of passively adsorbed CAbs, which may explain the large standard deviations in activities previously reported for PABC methods. In this research, it is evident that CAbs immobilized to surfaces through intermediate streptavidin molecules are nearly 2 times more active compared to passively adsorbed CAbs, which may be explained by a protein cushion effect. As a protein becomes further away from underlying surface functionality on an intermediate protein tether, interactions with the underlying glass/PEG surface are shielded, allowing the protein to maintain secondary and tertiary structures that may help preserve a more native-like activity. Although the antibodies immobilized through streptavidin intermediates exhibited ~1.8 times greater capture activity compared to passively adsorbed antibodies, the total apparent activity derived from the streptavidin-biotin-anti-GtIgG (PABC) capture antibodies was ~5 fold lower than that from the passively adsorbed CAbs. The extremely low efficiency (7.8 ± 0.2%) of surface immobilized streptavidin for immobilizing biotinylated-CAbs dominated the small total observed antigen capture activity of the initial streptavidin sites (2.1 ± 0.4%).

4.3.4 Oriented Antibody Immobilization through Protein A

The low capture yields associated with CAb immobilized using the passive adsorption or PABC techniques were likely influenced by the orientation of the biomolecules with respect to the interface.[20] Given the asymmetric structure of an

antibody, the orientation of a surface immobilized CAb might result in one or both Fab domain(s) being inaccessible to target antigens in solution. In the case of biotinylated-antibodies, the biotin tags were conjugated using N-hydroxysuccinimidyl (NHS) ester chemistry through randomly accessible ε-amines distributed throughout the entire antibody molecule. The capture of the biotinylated-CAb by a surface immobilized streptavidin likely resulted in a distribution of random orientations of the antibody with respect to the interface, as illustrated in Figure 4.8. Considering ~74% of the streptavidin-biotin-anti-GtIgG complexes were rendered inactive once immobilized to an interface, the orientation of the capture antibody must be factor.

Protein A is a cell wall component of the *Staphylococcus aureus* and is well known to bind the Fc region of IgG antibodies.[61] *E. coli* protein A (EpA), which functions similarly to native protein A, has four binding domains and was chosen to be used in this experiment because of its high affinity for rabbit derived IgG molecules (our capture antibody) and poorer affinity for goat derived IgG, our model antigen.[62] Illustrated in Figure 4.9, biotin-EpA-cy3 and anti-GtIgG-cy3 were sequentially injected onto a streptavidin-modified surface using a two-step immobilization procedure. Solutions containing 10 ng/ml (250 pM) of biotin-EpA-cy3 in PBS, 75 ng/ml (500 pM) of anti-GtIgG-cy3 in PBS, and 75 ng/mL (500 pM) of GtIgG-cy3 in PBS were sequentially captured and localized using the previously described methods (see above). Because of the extremely low efficiencies associated with the two-step method (see below), a much higher density (~4×10^{-12} mol/m^2) streptavidin capture surface was needed to accumulate sufficient protein to acquire statistically relevant data on the second capture step. At this higher density, the streptavidin surface concentration was above the

Figure 4.8: The immobilization strategies used. (a) Random immobilization of biotin-anti-IgG with an average of four biotin labels per protein to a streptavidin conjugated surface. (b) Capture of solution IgG molecules by randomly immobilized biotin-anti-IgG molecules.

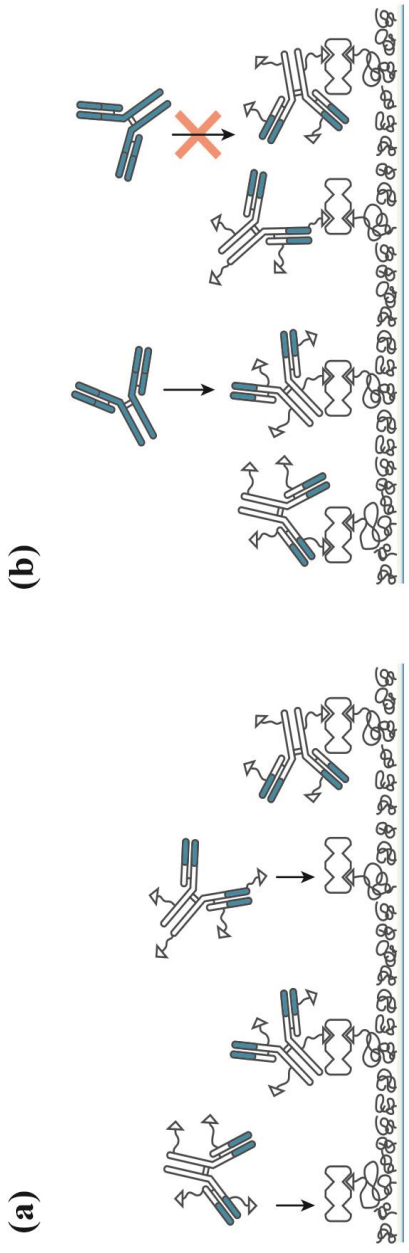
(b)
(a)

Figure 4.9: Two-Step capture-antibody immobilization using protein A: (a) Random immobilization of biotin-EpA with an average of three biotin labels per protein to a streptavidin conjugated surface. (b) Protein A capturing the Fc domain of anti-GtIgG-cy3. (c) The binding of solution GtIgG molecules to oriented anti-GtIgG capture molecules.

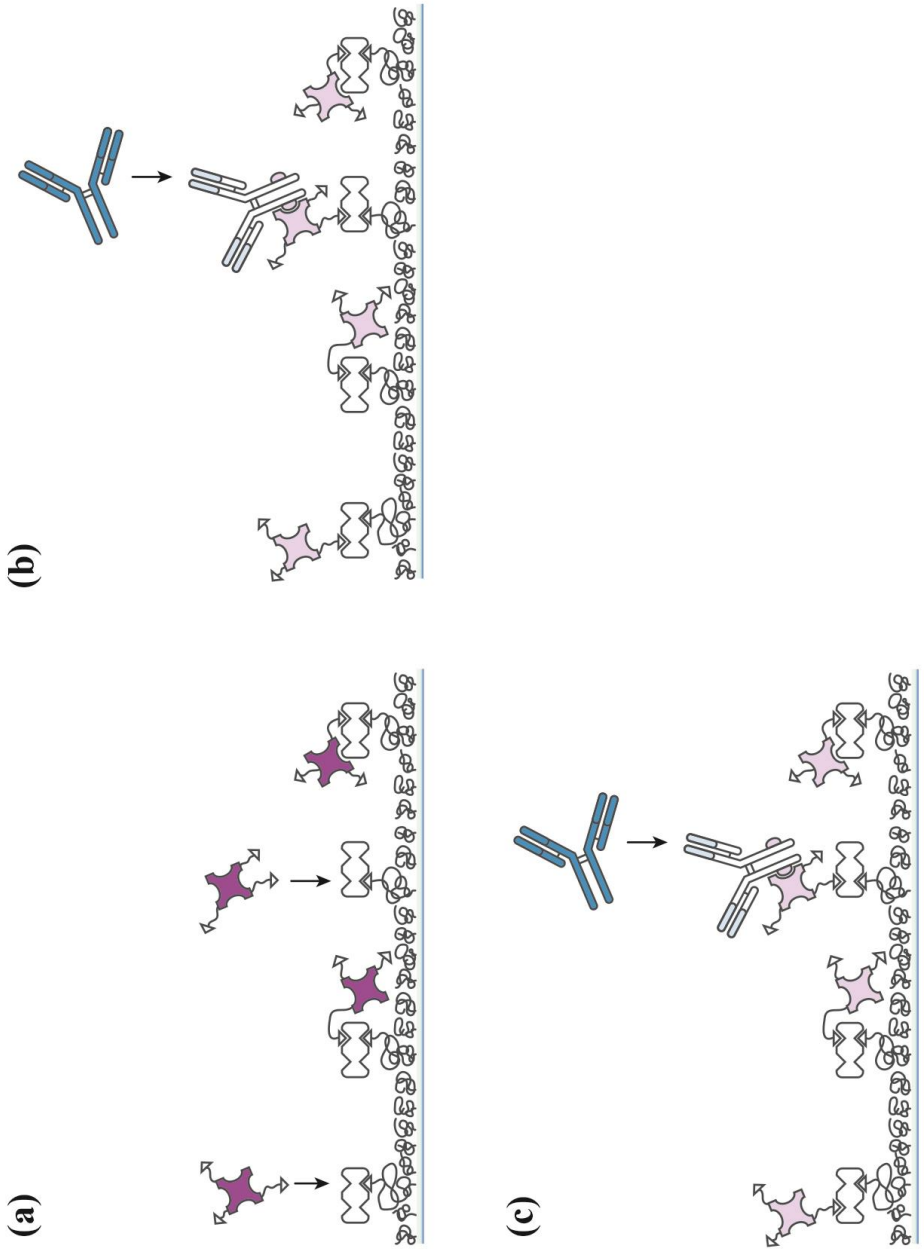
(a)
(b)
(c)

upper threshold (~2×10^{-12} mol/m^2) for resolving discrete fluorescent spots using optical based microscopy; therefore, the two-step immobilization of biotin-EpA-cy3 and anti-GtIgG-cy3 experiment was not colocalized with the initial streptavidin capture sites. The values reported for this experiment include the entire population of streptavidin-bound and passively adsorbed EpA population. However, the fraction of streptavidin-bound EpA should be higher than for the CAb results above because of the ~5-fold greater biotin capture site density.

The surface adsorbed population of biotin-EpA-cy3 had an average fluorescence intensity of $\mu_{\text{biotin-EpA-cy3}}$ = 378 photoelectron counts with a variation in spot-to-spot intensity of $\sigma_{\text{biotin-EpA-cy3}}$ = 25 photoelectrons. The fluorescent intensity and spot-to-spot intensity variation for the subsequently immobilized anti-GtIgG-cy3 and GtIgG-cy3 were consistent with results reported above (see Figure 4.4). On average, $3 \pm 1 \times 10^{-13}$ mol/m^2 of biotin-EpA-cy3 were bound to the streptavidin-modified surface after the accumulation/rinse cycle, which was well within the limits of resolving individual molecules using TIRF imaging techniques. Of the total immobilized biotin-EpA-cy3 population, 5.4 ± 0.5% was able to capture an Fc domain of anti-GtIgG-cy3 molecules, forming a surface immobilized biotin-EpA-RbAbGt-cy3 complex. The colocalization of these complexes with subsequently bound GtIgG-cy3 revealed that 33 ± 2% of the biotin-EpA-anti-GtIgG-cy3 complexes captures a GtIgG-cy3 molecule. By immobilizing a CAb through an EpA molecule to a surface using the two-step method, there was a small, but distinguishable, ≥ 8%, increase in the activity of protein A immobilized CAbs compared to biotinylated antibodies immobilized randomly to streptavidin. Despite this increase in activity for CAbs sequentially immobilized through EpA, the total apparent

surface activity exhibited by the two-step formation of the EpA-anti-GtIgG complex was extremely low (~0.1%) due to the poor efficiency exhibited by EpA (5.4%) for capturing the Fc domain of an IgG. The inefficient capture efficency could be the result of inaccessible Fc binding domains or deactivation of those binding domains upon immobilization.

In order to exercise better control over the orientation of CAbs and increase the antibody capture activity of a EpA, biotin-EpA and anti-GtIgG-cy3 were pre-associated as a (biotin-[EpA/anti-GtIgG]-cy3) chimeric complex in solution and then immobilized to a low density (~5×10^{-13} mol/m^2) streptavidin-modified surface, as illustrated in Figure 4.10. A solution containing 6 μg/ml (125 nM) biotin-EpA and 38 μg/ml (250 nM) anti-GtIgG-cy3 was pre-equilibrated for 1 hour. Anti-GtIgG-cy3 was present at a much higher concentration in solution to minimize the probability of an unconjugated EpA being immobilized to streptavidin capture sites. After the incubation period, the solution was diluted by a factor of 500 in PBS buffer and then injected onto the low-density streptavidin modified surface.

Because anti-GtIgG-cy3 was not biotinylated, all anti-GtIgG-cy3 locations that colocalized the original cy3-SA locations were assumed to be associated through a biotin-EpA intermediate. To test this assumption, the fraction of immobilized streptavidin that colocalized with anti-GtIgG-cy3 was measured and found to be 7.9 ± 0.2%, which agrees with the previously observed capture efficiency of streptavidin for biotinylated antibodies (8 ± 2%) and suggests that the anti-GtIgG-cy3 were indeed associated with biotinylated EpA. Following the immobilization of the chimeric complex, 75 ng/ml (500 pM) of GtIgG-cy3 in PBS was injected, accumulated/rinsed, and imaged. Colocalization

Figure 4.10: One-step chimeric protein A/capture-antibody immobilization: (a) Preassociation of 125 nM biotin-EpA and 250 nM antiGtIgG-cy3 *ex situ*. (b) The capture of biotinylated-chimeric complex by surface immobilized streptavidin. (c) The binding of solution GtIgG molecules to oriented surface immobilized anti-GtIgG capture molecules.

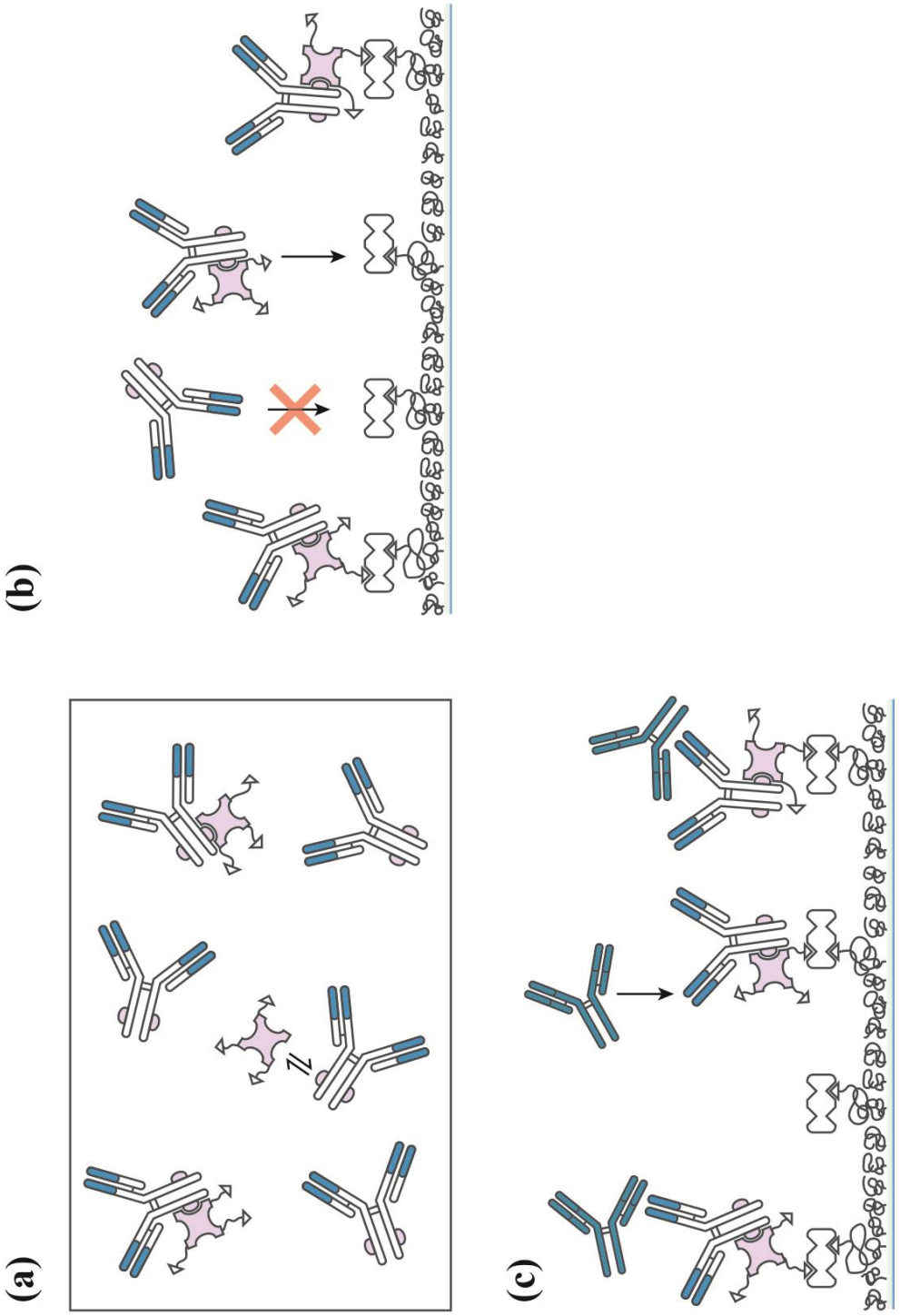
(a)
(b)
(c)

revealed that 54 ± 2% of the total SA-biotin-[EpA/anti-GtIgG]-cy3 conjugates captured GtIgG-cy3 molecules. The one-step chimeric EpA/Ab method was ~30 times more active at capturing Ag molecules compared to the two-step sequential surface immobilization of EpA and CAb due to the poor efficiency (5.4%) of the immobilized EpA binding to a CAb binding site. It is important to note that the EpA used in this experiment had four binding domains. It is possible that with the high concentration of anti-GtIgG present during the pre-association period for the chimeric complex, that each EpA could have been associated with multiple anti-GtIgG molecules. It may very well be that the size and multivalency of the formed complex was responsible for the 30% increase in observed antibody activity and not necessarily the orientation of an individual anti-GtIgG through the biotin-EpA intermediate. Regardless, this result clearly demonstrates the effectiveness of immobilizing a pre-associated Fc binding protein (A, G, A/G)-CAb complex to interfaces. The efficiency of the streptavidin for capturing the biotin-chimeric complex remains small (7.9 ± 0.2%), leading to an overall apparent capture efficiency of 4.2 ± 0.9% relative to the immobilized streptavidin population.

4.4 Discussion

The activity of solid phase immunoassays was characterized for a variety of CAb immobilization strategies commonly used in "sandwich-type" immunoassays using single-molecule TIRF imaging techniques, as summarized in Figure 4.11. The PABC method was employed as a generic means to immobilize any biotin-conjugated protein to PEG-modified surfaces. By using PEG-modified surfaces containing a low density (10^{-13} mol/m^2) of biotin conjugations sites, the concentration of immobilized streptavidin was

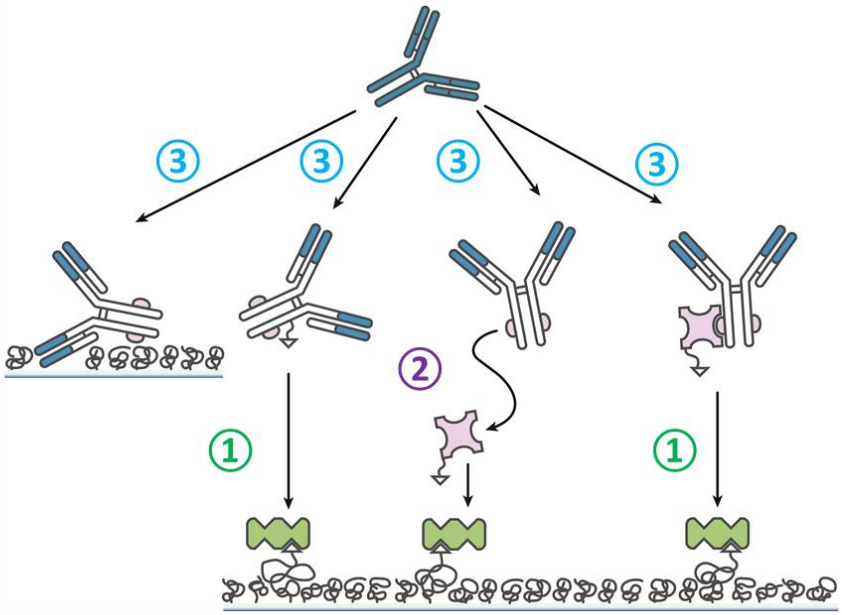

Activities (%)	*passive adsorption*	*random streptavidin*	*2-step protein A*	*1-step protein A*
③ *αIgG*	14 ± 4	26 ± 1	33 ± 2	54 ± 2
② *protein A*	—	—	5.4 ± 0.5	—
① *streptavidin*	—	8 ± 2	—	7.9 ± 0.2
Overall apparent activity (%)	14 ± 4	2.1 ± 0.4	< 0.1‡	4.2 ± 1

‡ This value assumes the efficiency of streptavidin capturing biotin-EpA is equivalent to biotin-[EpA/anti-GtIgG] (7.9 ± 0.2%).

Figure 4.11: Tabulated activity associated with each immobilization scheme.

controllable, while minimizing the nonspecific adsorption of subsequently added proteins. The activity of anti-GtIgG was measured and compared for four immobilization strategies: (i) passive adsorption to the mPEG surface, (ii) immobilization through biotinylation to streptavidin capture sites, (iii) a two-step oriented immobilization through streptavidin-EpA intermediate, and (iv) a one-step immobilization to streptavidin as a chimeric [EpA/anti-GtIgG] complex. In all cases, the bioaffinity tethering using the streptavidin intermediate resulted in 2- to nearly 4-fold increase in observed CAb activity compared to a passivly adsorbed antibody.

The one-step immobilization of the chimeric EpA-CAb complex, resulting in ~54 % antigen capture activity, maintained the highest activity of any immobilized anti-GtIgG. In all cases utilizing indirect immobilization through a streptavidin intermediate, the overall activity arising from the PABC-immobilized antibodies was less than half of the passively adsorbed antibodies. This was due to the poor efficency (~8 %) of surface immobilized streptavidin molecules capturing biotinylated-proteins (both antibodies and protein A), which resulted in low PABC-bound CAb surface concentrations. Although only ~14% of passively adsorbed CAbs remain active, the magnitude of this population dominates the observed activity. From these experiments, it becomes obvious that protein-protein interactions at interfaces can exhibit poor capture efficiencies; therefore, the compounded activity of multistep immobilization strategies can suffer from poor yields. As a result, the efficiency of the scaffolding that supports CAb for solid phase immunoassays should be carefully considered when preparing sensor surfaces.

4.5 References

(1) Engvall, E.; Jonsson, K.; Perlmann, P. *Biochim. Biophys. Acta, Protein Struct.* **1971**, *251*, 427.

(2) Carlsson, R.; Glad, C.; Borrebaeck, C. K. A. *Bio/Technology*. **1989**, *7*, 567.

(3) McNeil, C. J.; Athey, D.; Renneberg, R. *EXS.* **1997**, *81*, 17.

(4) Stefan-van Staden, R.-I.; Bokretsion, R. G.; van Staden, J. F.; Aboul-Enein, H. Y. *Crit. Rev. Anal. Chem.* **2015**, *45*, 2.

(5) Butler, J. E.; Feldbush, T. L.; McGivern, P. L.; Stewart, N. *Immunochemistry*. **1978**, *15*, 131.

(6) Butler, J. E.; Spradling, J. E.; Suter, M.; Dierks, S. E.; Heyermann, H.; Peterman, J. H. *Mol. Immunol.* **1986**, *23*, 971.

(7) Joshi, K. S.; Hoffmann, L. G.; Butler, J. E. *Mol. Immunol.* **1992**, *29*, 971.

(8) Dierks, S. E.; Butler, J. E.; Richerson, H. B. *Mol. Immunol.* **1986**, *23*, 403.

(9) Ferretti, S.; Paynter, S.; Russell, D. A.; Sapsford, K. E.; Richardson, D. J. *TrAC, Trends Anal. Chem.* **2000**, *19*, 530.

(10) Tang, D.-Q.; Zhang, D.-J.; Tang, D.-Y.; Ai, H. *J. Immunol. Methods.* **2006**, *316*, 144.

(11) Butler, J. E.; Ni, L.; Brown, W. R.; Joshi, K. S.; Chang, J.; Rosenberg, B.; Voss, E. W., Jr. *Mol. Immunol.* **1993**, *30*, 1165.

(12) Kennel, S. J. *J. Immunol. Methods.* **1982**, *55*, 1.

(13) Kochwa, S.; Brownell, M.; Rosenfield, R. E.; Wasserman, L. R. *J. Immunol.* **1967**, *99*, 981.

(14) Bull, H. B. *Biochim. Biophys. Acta.* **1956**, *19*, 464.

(15) Oreskes, I.; Singer, J. M. *J. Immunol.* **1961**, *86*, 338.

(16) Nyilas, E.; Chiu, T. H.; Herzlinger, G. A. *Trans., Am. Soc. Artif. Intern. Organs.* **1974**, *20-B*, 480.

(17) Catt, K. J.; Tregear, G. W. *Science.* **1967**, *158*, 1570.

(18) Butler, J. E. *Immunochemistry of Solid-Phase Imunoassay*; CRC Press: Boca Raton, Florida, 1991, p 221.

(19) Wong, S. S. *Chemistry of Protein Conjugation and Cross-Linking*; CRC Press: Boca Raton, Florida, 1991.

(20) Guo, A.; Zhu, X. Y. *Drug Discovery Ser.* **2007**, *8*, 53.

(21) Peterman, J. H.; Tarcha, P. J.; Chu, V. P.; Butler, J. E. *J. Immunol. Methods.* **1988**, *111*, 271.

(22) Butler, J. E.; Ni, L.; Nessler, R.; Joshi, K. S.; Suter, M.; Rosenberg, B.; Chang, J.; Brown, W. R.; Cantarero, L. A. *J. Immunol. Methods.* **1992**, *150*, 77.

(23) Green, N. M. *Methods Enzymol.* **1990**, *184*, 51.

(24) Suter, M.; Butler, J. E. *Immunol. Lett.* **1986**, *13*, 313.

(25) Ruiz-Taylor, L. A.; Martin, T. L.; Zaugg, F. G.; Witte, K.; Indermuhle, P.; Nock, S.; Wagner, P. *Proc. Natl. Acad. Sci. U. S. A.* **2001**, *98*, 852.

(26) Huang, N.-P.; Voeroes, J.; De Paul, S. M.; Textor, M.; Spencer, N. D. *Langmuir.* **2002**, *18*, 220.

(27) Pollheimer, P.; Taskinen, B.; Scherfler, A.; Gusenkov, S.; Creus, M.; Wiesauer, P.; Zauner, D.; Schoefberger, W.; Schwarzinger, C.; Ebner, A.; Tampe, R.; Stutz, H.; Hytoenen, V. P.; Gruber, H. J. *Bioconjugate Chem.* **2013**, *24*, 1656.

(28) Vermette, P.; Gengenbach, T.; Divisekera, U.; Kambouris, P. A.; Griesser, H. J.; Meagher, L. *J. Colloid Interface Sci.* **2003**, *259*, 13.

(29) Chung, J. W.; Park, J. M.; Bernhardt, R.; Pyun, J. C. *J. Biotechnol.* **2006**, *126*, 325.

(30) Gretch, D. R.; Suter, M.; Stinski, M. F. *Anal. Biochem.* **1987**, *163*, 270.

(31) Hlady, V.; Buijs, J. *Curr. Opin. Biotechnol.* **1996**, *7*, 72.

(32) Stenberg, M.; Nygren, H. *J Immunol Methods.* **1988**, *113*, 3.

(33) Xu, H.; Lu, J. R.; Williams, D. E. *J. Phys. Chem. B.* **2006**, *110*, 1907.

(34) Suter, M.; Butler, J. E.; Peterman, J. H. *Mol. Immunol.* **1989**, *26*, 221.

(35) Hoffman, W. L.; O'Shannessy, D. J. *J. Immunol. Methods.* **1988**, *112*, 113.

(36) Abbas, A. K.; Lichtman, A. H.; Pillai, S. *Cellular and Molecular Immunology*; 7 ed.; Elsevier Saunders: Philadelphia, Pennsylvania, 2012.

(37) Lu, B.; Smyth, M. R.; O'Kennedy, R. *Analyst.* **1996**, *121*, 29R.

(38) Werner, S.; Machleidt, W. *Eur. J. Biochem.* **1978**, *90*, 99.

(39) Gersten, D. M.; Marchalonis, J. J. *J. Immunol. Methods.* **1978**, *24*, 305.

(40) Anderson, G. P.; Jacoby, M. A.; Ligler, F. S.; King, K. D. *Biosens. Bioelectron.* **1997**, *12*, 329.

(41) Bae, Y. M.; Oh, B.-K.; Lee, W.; Lee, W. H.; Choi, J.-W. *Biosens. Bioelectron.* **2005**, *21*, 103.

(42) Owaku, K.; Goto, M.; Ikariyama, Y.; Aizawa, M. *Anal. Chem.* **1995**, *67*, 1613.

(43) Forsgren, A.; Sjoquist, J. *J. Immunol.* **1966**, *97*, 822.

(44) Cantarero, L. A.; Butler, J. E.; Osborne, J. W. *Anal. Biochem.* **1980**, *105*, 375.

(45) Vareiro, M. M. L. M.; Liu, J.; Knoll, W.; Zak, K.; Williams, D.; Jenkins, A. T. A. *Anal. Chem.* **2005**, *77*, 2426.

(46) Nygren, H.; Czerkinsky, C.; Stenberg, M. *J. Immunol. Methods.* **1985**, *85*, 87.

(47) Ikawa-Yoshida, A.; Yoshii, K.; Kuwahara, K.; Obara, M.; Kariwa, H.; Takashima, I. *Microbiol. Immunol.* **2011**, *55*, 100.

(48) Procaccia, S.; Gasparini, A.; Colucci, A.; Lanzanova, D.; Bianchi, M.; Forcellini, P. *Boll Ist Sieroter Milan.* **1987**, *66*, 124.

(49) Broom, A. K.; Charlick, J.; Richards, S. J.; Mackenzie, J. S. *J Virol Methods.* **1987**, *15*, 1.

(50) Guo, X.; Lin, C.-S.; Chen, S.-H.; Ye, R.; Wu, V. C. H. *Biosens. Bioelectron.* **2012**, *38*, 177.

(51) Kanno, S.; Yanagida, Y.; Haruyama, T.; Kobatake, E.; Aizawa, M. *J. Biotechnol.* **2000**, *76*, 207.

(52) Hahn, C. D.; Riener, C. K.; Gruber, H. J. *Single Molecules.* **2001**, *2*, 149.

(53) Wikstroem, P.; Mandenius, C. F.; Larsson, P.-O. *J. Chromatogr.* **1988**, *455*, 105.

(54) Schneider, C. A.; Rasband, W. S.; Eliceiri, K. W. *Nat. Methods.* **2012**, *9*, 671.

(55) Harris, J. M.; Yoshinaga, K. *J. Bioact. Compat. Polym.* **1989**, *4*, 281.

(56) Merrill, E. W.; Salzman, E. W. *ASAIO J.* **1983**, *6*, 60.

(57) Holmberg, K.; Bergstroem, K.; Stark, M. B. *Immobilzation of Proteins via PEG Chains*; Plenum Press: New York, New York, 1992, p 303.

(58) Li, Y.-J.; Bi, L.-J.; Zhang, X.-E.; Zhou, Y.-F.; Zhang, J.-B.; Chen, Y.-Y.; Li, W.; Zhang, Z.-P. *Anal. Bioanal. Chem.* **2006**, *386*, 1321.

(59) Nygren, H.; Stenberg, M. *J. Colloid Interface Sci.* **1985**, *107*, 560.

(60) Harris, J. M.; Zalipsky, S. *Polyethylene Glycol: Chemistry and Biological Applications*; Plenum Press: New York, New York, 1992.

(61) Hjelm, H.; Hjelm, K.; Sjoquist, J. *FEBS (Fed. Eur. Biochem. Soc.) Lett.* **1972**, *28*, 73.

(62) Hjelm, H.; Sjodahl, J.; Sjoquist, J. *Eur. J. Biochem.* **1975**, *57*, 395.

CHAPTER 5

CONCLUSION

5.1 Future Perspectives

The goal of this research was to develop a method capable of overcoming the limitations, discussed in Chapter 1, associated with high-density capture assays. Transport-limited binding rates, nonreversible interfacial kinetics, and poor capture efficiencies for surface immobilized protein-receptor molecules, in theory, can be overcome with decreased capture site densities on a measurement surface. In this work single-molecule total internal refection fluorescence (TIRF) imaging was employed to monitor discrete protein-surface, protein-hapten, and protein-protein interactions at a glass-water interface. While decreasing the density of receptor sites reduced transport limitations and prevented bivalent interactions between adjacent receptor sites, many new challenges were revealed and required attention in order to accurately characterize the interfacial processes governing protein recognition at surfaces.

The primary challenge associated with imaging individual ligand-receptor interactions at glass-water interfaces is the ability to discern specific (ligand-receptor) from nonspecific (ligand-surface) interactions. Although this task can be addressed in multiples ways, preventing the nonspecific adsorption of proteins to the capture surface is

the most ideal method. Discussed in Chapter 3, the optimal surface density of immobilized receptor molecules spans the range of ~60 to 100 amol/cm^2. This density corresponds to a large enough surface population of receptor sites to obtain statistically valid observations, while the binding sites are well resolvable within the diffraction limits of optical microscopy. Ideally, the surface passivation technique should prevent the nonspecific adsorption of proteins at much lower surface concentrations than specific interactions (<<60 amol/cm^2); however, in many cases, nonspecific interactions account for significant fractions (>50%) of the total observed interfacial events. This requires additional filtering techniques, such as colocalization, in order to discern specific from nonspecific interactions.

In this research, grafted poly(ethylene glycol) (PEG) monolayers were used to prevent the nonspecific adsorption of biomolecules to glass surfaces, while providing a means to control the surface density of biotin conjugation sites. In Chapter 2, the grafting of mPEG-amine molecules to epoxide-modified glass slides resulted in surfaces that were adequately resistant to the nonspecific adsorption of IgG. From a solution containing 1 nM anti-biotin, ~20 amol/cm^2 of IgG remained strongly bound to the 750 g/mol mPEG monolayer after a 4 hour accumulation/wash period, whereas only ~1 amol/cm^2 remained adsorbed to the 2000 g/mol mPEG monolayer. In both cases, these surfaces are highly resistant to the adsorption of IgG at the macroscopic level, where the nonspecifically adsorbed IgG is less than 10^{-6} of a monolayer for the 750 g/mol mPEG surface; however, this coverage corresponds to high background signals (>50 molecules/frame) with respect to imaging individual molecules on a surface. From the work conducted in Chapter 2, it was determined that defect sites within the deposited PEG monolayers are always present

at the molecular level (>1 amol/cm^2), and all of the mPEG surface modifications prepared in this work were insufficient at eliminating all nonspecific protein-surface adsorption.

In Chapter 3, the density of biotin conjugation sites was shown to be controllable by diluting in a low concentration biotin-PEG into a 750 g/mol mPEG monolayer. The concentration of tetrameric streptavidin molecules that strongly bound to these surfaces increased linearly with respect to the dilution ratio of mPEG to biotin-PEG composing the reaction solutions. Although the 2000 g/mol mPEG monolayers produced in Chapter 2 exhibited a much higher resistance to the nonspecific adsorption of IgG, a mixed monolayer of 2000 g/mol biotin-PEG and 2000 g/mol mPEG resulted in uncontrollable conjugation site densities and poor streptavidin surface conjugation. It is believed that this outcome was the result of the biotin conjugation sites being inaccessibly buried/hindered by the equivalently sized diluent mPEG layer. In contrast, streptavidin bound at a controllable density to a longer chain (2000 g/mol) biotin-PEG, diluted into a shorter chain (750 g/mol) mPEG monolayer. It was demonstrated that the density of biotin sites was controllable over a range of ~40 to 140 amol/cm^2, where the optimal site density for single-molecule imaging is within ~60 to 100 amol/cm^2. While this "optimal density" of surface sites for imaging could be achieved, the population of nonspecifically adsorbed IgG molecules, resulting from a 1 nM solution of antibody, accounts for >20% of the total observed surface events at such densities. Thus, the receptor-modified surfaces can only support measurement of analyte (IgG) concentrations that are much lower than 1 nM or otherwise require additional image processing in order to discern nonspecific from specific interactions.

Because the zero-binding site 750 g/mol mPEG slides showed negligible (0.3

amol/cm^2) nonspecific adsorption of streptavidin, this intermediate protein linker could be used to quantify the surface biotin-PEG density as described above. Beyond this step, colocalization was used in Chapter 4 as a means to overcome all nonspecific protein-surface interactions. By exploiting the ability to permanently photobleach the fluorescent cy3 molecule, cy3-labeled protein-ligands were sequentially captured and colocalized to each previously located receptor molecule. In Chapter 4, capture antibodies (anti-IgG) were immobilized using four techniques and then exposed to antigen (IgG): (i) passive immobilization, (ii) directed immobilization to streptavidin, (iii) oriented two-step sequential immobilization to protein A, and (iv) a one-step immobilization as a CAb-protein A chimeric complex. The activities of each capture step were calculated through colocalization of bound proteins and then compared.

The work presented within this dissertation resulted in two important conclusions. In Chapter 4, it is evident that the capture efficiency of proteins directly immobilized to a PEG modified surface is extremely low. Although it is possible to increase the capture efficiency of a protein-receptor molecule by immobilizing the receptor molecule in a more oriented manner through the sequential build up of complex protein scaffolding, the capture activities of each additional layer are compounded and often result in total apparent observed activities that are <5%. In many cases, it is not uncommon for nonspecific interactions to account for >90% of the total observed events. The PEG-modified surfaces developed in this dissertation were unable to completely overcome nonspecific adsorption at the molecular level, which made resolving specific interactions from nonspecific interactions a difficult task. In addition, the low capture activities associated with surface immobilized receptor sites resulted in convoluted and statistically

limited information about the measured surface interactions. The high backgrounds and low sensitivity associated with single-molecule fluorescence imaging of discrete ligand-receptor interactions suggests that the single-molecule TIRF methodology presented within this dissertation is an impractical tool for immunodiagnostic measurements.

Although this research did not produce a selective and highly sensitive single-molecule immunoassay method, a better understanding of the fundamental interactions that govern immunoassays at the molecular level was achieved. All of the interfacial protein-protein and protein-hapten interactions observed in this research revealed little-to-no measureable reversibility over the timescale of days. The strong ligand-receptor interactions measured were not the consequence of bivalent interactions or recapture processes, but the result of a single-ligand bound to a single-receptor. Although little kinetic information can be gained from such interactions, the signal measured in "sandwich" assays is likely not influenced by the dissociation of subsequently deposited protein layers.

In addition, all of the surface immobilized proteins studied within this research exhibited much lower capture activities than theoretically achievable. Although larger IgG receptor-molecules appeared to be more robust once immobilized to a surface in comparison to the smaller streptavidin and protein A receptor-molecules used in these experiments, the deposition method and orientation of the immobilized receptor-protein was the most influential factors in maintaining high surface activity. Depending on the capture protein being immobilized, the immobilization method should carefully be considered in order to maximize the sensitivity of the measurement surface. For example, a surface-immobilized protein A will potentially capture an IgG molecule

through the Fc fragment with one or both Fab fragments oriented away from the surface, as discussed in Chapter 4. The capture of an IgG by a surface immobilized protein A is an inefficient process; however, the apparent capture efficiency of a receptor surface can be increased by nearly 30-times when the capture antibody is deposited as a one-step protein A-IgG chimeric complex. It is clear that the sensitivity of the immunodiagnostic measurement is greatly influenced by the method in which the CAbs are deposited, and small differences in methodology can result in large changes in sensitivity. The protein scaffolding used and means of deposition for each protein layer needs to be carefully considered in order to achieve maximum signal and high sensitivity from a capture surface.